NUMERICAL MODEL DEVELOPMENT FOR GÜZELYURT AQUIFER, NORTHERN CYPRUS

A THESIS SUBMITTED TO
THE GRADUATE SCHOOL OF NATURAL AND APPLIED SCIENCES
OF
MIDDLE EAST TECHNICAL UNIVERSITY

BY

CANSU DEMIR

IN PARTIAL FULFILLMENT OF THE REQUIREMENTS
FOR
THE DEGREE OF MASTER OF SCIENCE
IN
ENVIRONMENTAL ENGINEERING

JULY 2018

Approval of the thesis:

NUMERICAL MODEL DEVELOPMENT FOR GÜZELYURT AQUIFER, NORTHERN CYPRUS

Submitted by **CANSU DEMİR** in partial fulfillment of the requirements for the degree of **Master of Science in Environmental Engineering Department, Middle East Technical University** by,

Prof. Dr. Halil Kalıpçılar
Dean, Graduate School of **Natural and Applied Sciences** ____________________

Prof. Dr. Kahraman Ünlü
Head of Department, **Environmental Engineering** ____________________

Prof. Dr. Kahraman Ünlü
Supervisor, **Environmental Engineering Dept., METU** ____________________

Assist. Prof. Dr. Bertuğ Akıntuğ
Co-Supervisor, **Civil Engineering Program, METU-NCC** ____________________

Examining Committee Members:

Prof. Dr. Erdal Çokça
Civil Engineering Dept., METU ____________________

Prof. Dr. Kahraman Ünlü
Environmental Engineering Dept., METU ____________________

Assoc. Prof. Dr. Orhan Gündüz
Environmental Engineering Dept., DEU ____________________

Assist. Prof. Dr. Bertuğ Akıntuğ
Civil Engineering Program, METU-NCC ____________________

Assist. Prof. Dr. Zöhre Kurt
Environmental Engineering Dept., METU ____________________

Date: 03.07.2018

I hereby declare that all information in this document has been obtained and presented in accordance with academic rules and ethical conduct. I also declare that, as required by these rules and conduct, I have fully cited and referenced all materials and results that are not original to this work.

Name, Last name: Cansu Demir

Signature :

ABSTRACT

NUMERICAL MODEL DEVELOPMENT FOR GÜZELYURT AQUIFER, NORTH CYPRUS

Demir, Cansu

M.Sc., Department of Environmental Engineering

Supervisor: Prof. Dr. Kahraman Ünlü

Co-Supervisor: Assist. Prof. Dr. Bertuğ Akıntuğ

July 2018, 144 pages

Güzelyurt, coastal aquifer, which is an unconfined, is the most important, at the same time the largest drinking, municipal, and irrigational water resource in Turkish Republic of Northern Cyprus (TRNC). However, the aquifer has exceeded its safe yield capacity due to excessive and uncontrolled pumping over the years and the water quality has been seriously degraded due to seawater intrusion. The "TRNC Water Supply Project", completed in June 2016, will annually supply about 75 MCM of water via pipeline under Mediterranean Sea from Alaköprü Dam in Anamur by Turkish Republic to solve the water shortage problem in TRNC. About 38 MCM/year of water out of the total transfer has been allocated to domestic water demand. The remaining 37 MCM/year planned to be used for irrigation can potentially be used to artificially recharge the aquifer and in turn, the deteriorated water budget of the aquifer can be reestablished in the mid- and long-term. The objective of this study is to predict the hydraulic behavior of the aquifer under predefined stress and recharge scenarios regarding the water usage. For this purpose, the 3-D detailed conceptual and numerical simulation models of Güzelyurt Aquifer have been developed using system modeling approach integrated with today's modern technologies of Geographical Information Systems (GIS) and numerical simulation techniques. The available geologic, hydrologic and hydrogeological data provided by Geology and Mining Department (G&MD) of TRNC and collected from previously published field reports have been used in model development process. The developed numerical model has been first calibrated under steady-state and transient conditions. The calibrated model has been then run for simulations of three different scenarios involving rehabilitation of the deteriorated water balance of the aquifer. In the initial scenario, the aquifer has been simulated under the conditions of no pumping for irrigation. In the second and the last scenarios, in addition to no-pumping conditions of the first scenario, 28 MCM/year of the water from the project was artificially fed to the aquifer from the Güzelyurt Dam and the Dam and injection wells combined, respectively. In all three scenarios, the depression zone has disappeared and the "zero" head contour has approximated to the coast after average of 12 years, in all three cases. Moreover, it has been found that at least 76% of the water allocated for irrigation should be used for artificial recharge to obtain an effective aquifer recovery. However, although more than half of the water coming for irrigation is used for this purpose, the aquifer has not returned to its natural conditions in the near future based on the simulated years. The earliest natural state was achieved in 48 years by the recharge method with the combination of injection wells and dam. Therefore, this option has been the most effective method.

Keywords: Numerical model, Simulation, Aquifer, Groundwater, Güzelyurt

ÖZ

KUZEY KIBRIS TÜRK CUMHURİYETİ (KKTC) GÜZELYURT AKİFERİ İÇİN SAYISAL MODEL GELİŞTİRİLMESİ

Demir, Cansu

Yüksek Lisans, Çevre Mühendisliği Bölümü

Tez Yöneticisi: Prof. Dr. Kahraman Ünlü

Yardımcı Tez Yöneticisi: Yrd. Doç Dr. Bertuğ Akıntuğ

Temmuz 2018, 144 sayfa

Basınçlı bir kıyı akiferi olan Güzelyurt, Kuzey Kıbrıs Türk Cumhuriyeti'nde (KKTC) yer alan en önemli ve aynı zamanda en büyük içme, kullanma ve sulama suyu kaynağıdır. Fakat, akifer yıllar içinde aşırı ve kontrolsüz çekim nedeniyle güvenli verim kapasitesini aşmış ve deniz suyu girişimi nedeniyle su kalitesi ciddi şekilde bozulmuştur. Haziran 2016'da tamamlanan "KKTC Su Temini Projesi" ile, KKTC'deki su sıkıntısı sorununun çözümü için Türkiye Cumhuriyeti Anamur Alaköprü Barajı'ndan Akdeniz'e döşenen boru hattıyla yılda yaklaşık 75 milyon m^3 su Kuzey Kıbrıs'ta ki Geçitköy Barajı'na temin edilecektir. Toplam transferden yıllık yaklaşık 38 milyon m^3 su, evsel su ihtiyacına tahsis edilmiştir. Sulama için kullanılması planlanan kalan 37 milyon m^3 su akifere suni besleme yapmak için kullanılabilir ve buna karşılık akiferdeki bozulmuş su bütçesi orta ve uzun vadede yeniden kurulabilir. Bu çalışmanın amacı, su kullanımına ilişkin olarak önceden tanımlanmış beslenim/boşalım senaryoları altında akiferin hidrolik davranışını tahmin etmektir. Bu amaçla, Güzelyurt Akiferi'nin 3 boyutlu detaylı kavramsal ve sayısal simülasyon modelleri, günümüzün modern Coğrafi Bilgi Sistemleri (GIS) teknolojileri ve sayısal simülasyon teknikleriyle entegre edilen sistem modelleme yaklaşımı kullanılarak geliştirilmiştir. KKTC'nin Jeoloji ve Maden Dairesi (G & MD) tarafından temin edilen ve daha önce yayınlanmış saha raporlarından derlenen mevcut jeolojik, hidrolojik ve hidrojeolojik veriler model geliştirme sürecinde kullanılmıştır. Geliştirilen sayısal model ilk olarak kararlı durum ve zamana bağlı koşullar altında kalibre edilmiştir. Kalibre edilmiş model daha sonra akiferdeki bozulan su dengesinin rehabilitasyonunu içeren üç farklı senaryodan oluşan simülasyonlar için çalıştırılmıştır. İlk senaryoda, akifer sulama amaçlı pompaj olmadan simüle edilmiştir. İkinci ve son senaryoda, birinci senaryodaki pompalama koşullarına ek olarak, Türkiye'den sağlanan suyun 28 milyon m^3'lük miktarı, sırasıyla Güzelyurt barajından, ve hem baraj hem enjeksiyon kuyuları aynı anda kullanılarak akifere suni olarak beslenimi sağlanmıştır. Her üç senaryoda da, ortalama 12 yıldan sonra, "sıfır" konturunun deniz seviyesine ulaşarak ve depresyon bölgesinin ortadan kaybolduğu bir toparlanma sağlanmıştır. Ayrıca, akiferdeki su seviyesinin etkin bir şekilde yükselmesini sağlamak için, sulamaya tahsis edilen suyun en az % 76'sının suni besleme için kullanılması gerektiği bulunmuştur. Sulama için gelen suyun yarısından fazlasının bu amaçla kullanılmasına rağmen, akifer, simüle edilen yıllara dayanarak yakın bir gelecekte doğal koşullarına geri dönmemiştir. Enjeksiyon kuyularının ve barajın birleşimi ile yapılan besleme yöntemiyle en erken doğal duruma, 48 yılda ulaşılabilmiştir. Bu nedenle, bu seçenek en etkili yöntem olmuştur.

Anahtar Kelimeler: Sayısal model, Simülasyon, Akifer, Yeraltısuyu, Güzelyurt

To my beloved parents and brother

ACKNOWLEDGEMENT

The author would like to express her deepest gratitude to her supervisor Prof. Dr. Kahraman Ünlü for providing the opportunity to work on this valuable research subject under his guidance. His endless support, encouragement, positive and constructive attitude have always been great sources of inspiration and hope for the author to complete her study. With his great knowledge, he has been a role model for the author on how students should be supervised, and how to make proper judgments in scientific studies.

The author expresses her sincere thanks to her co-advisor Assist. Prof. Dr. Bertuğ Akıntuğ for his advice, critical comments, and beneficial guidance. Valuable information provided by him to understand the Northern Cyprus in every aspect have greatly contributed to the judgments made during the study and to the cultural sharing between the author and the professor.

Sincere appreciation and thanks are expressed to the dear examining committee members, Prof. Dr. Erdal Çokça, Assoc. Prof. Dr. Orhan Gündüz and Assist. Prof. Dr. Zöhre Kurt for their worthful suggestions and contributions.

The author would also like to thank the Geology and Mining Department of North Cyprus, Hydraulic Works of North Cyprus and The Turkish Republic State Hydraulic Works (DSİ) for their providing raw data and expert comments.

The author dedicates her study to her mother Müjgan Demir, father Hasan Demir and brother Burak Demir for their patience, understanding and endless support. Also, the author expresses her thanks to beloved friends Ezgi Çınar, Elif Bal, Ulaş Can, Miray Mazlumoğlu, Hale Demirtepe, Ruken Dilara Zaf, Zeynep Özcan, Kumru Kocaman, Özge Yücel, Sena Uzunpınar, Mert Erkanlı and Ozan Cem Yalçın for always being by her side and showing patience.

TABLE OF CONTENTS

ABSTRACT V
ÖZ VII
ACKNOWLEDGEMENT XI
TABLE OF CONTENTS XIII
LIST OF TABLES XVI
LIST OF FIGURES XVII

CHAPTERS

1. INTRODUCTION 1
  1.1. Definition of the Problem 1
  1.2. Project Area Overview 2
    1.2.1. Water Resources of TRNC 3
    1.2.2. Groundwater Management in TRNC 7
    1.2.3. TRNC Water Supply Project 8
    1.2.4. Previous Studies: Güzelyurt Aquifer 11
  1.3. Scope and Objectives of the Study 13
  1.4. Importance of Numerical Modeling in Groundwater Management 14
  1.5. Similar Numerical Modeling Studies from Literature 15
  1.6. Modeling with Limited Data 18
  1.7. Organization of the Thesis 19
2. MATERIALS AND METHODS 21

2.1. Description of the Study Area: Güzelyurt Aquifer 21
2.1.1. Location and Areal Coverage 21
2.1.2. Precipitation 22
2.1.3. Temperature and Evaporation 23
2.1.4. Land Use 23
2.1.5. Surface Water Conditions in the Güzelyurt Aquifer Basin 24
2.1.6. Hydrogeology of the Aquifer 26
2.2. Groundwater Model Development 29
2.2.1. Available Field Data 31
2.2.2. Conceptual Model Development 32
2.2.2.1. Material Distribution: Solid Model and the Cross-sections 34
2.2.2.2. External Boundary Conditions 45
2.2.2.3. Sources and Sinks 47
2.2.2.4. Transmissivity Field Data 52
2.2.3. Numerical Model Development 55
2.2.3.1. A Tool for Numerical Groundwater Modeling: MODFLOW 56
2.2.3.2. Unstructured Grid with MODFLOW-USG 57
2.2.3.3. Mathematical Descriptions 59
2.2.3.4. Numerical Modules/Packages Used 63
2.2.3.5. Numerical Grid Design 67
3. RESULTS AND DISCUSSIONS 71
3.1. Pumping Test Data Analysis 71
3.2. Numerical Model Calibration 79
3.2.1. Steady-State Calibration 80

3.2.2. Transient Calibration and Validation 88

3.3. Simulations for Güzelyurt Aquifer Response 98

3.3.1. Steady-state Natural Conditions Simulation 104

3.3.2. SCENARIO 1: Minimum Stress 106

3.3.3. SCENARIO 2: Artificial Recharge by Güzelyurt Dam 109

3.3.4. SCENARIO 3: Artificial Recharge by the Combination of Güzelyurt Dam and Injection Wells 112

4. CONCLUSIONS AND RECOMMENDATIONS 117

4.1. Summary and Conclusions 117

4.2. Recommendations for Future Work 122

4.2.1. Future Data Need 125

REFERENCES 129

APPENDIX A 137

APPENDIX B 143

LIST OF TABLES

TABLES

Table 1.1. Main aquifers of Northern Cyprus (DSI, 2003; Türker et al., 2013) *5*

Table 2.1. Water budget of the Güzelyurt Aquifer *50*

Table 3.1. Transmissivity values calculated from pumping test data *75*

Table 3.2. Ranges of transmissivity and hydraulic conductivity values estimated in Master Plan (MP) wells (DSI, 2003) *76*

Table 3.3. Specific capacity values determined in MTA's gzg wells and the calculated transmissivity data *77*

Table 3.4. Hydraulic conductivity values for Güzelyurt Aquifer *78*

Table 3.5. Observed and predicted head values in 10 sample wells *83*

Table 3.6. Transient Calibration Stress Periods *89*

Table 3.7. Observed and predicted head values in 8 sample wells *95*

Table 3.8. Observed and predicted head values in 8 sample wells *97*

Table 3.9. The stress periods dialog for the future prediction simulations *103*

Table 4.2. Descriptions of the legend of hydrogeological map of Northern Cyprus given in Figure 2.4 (Grouping by Fanta (2015)) *137*

LIST OF FIGURES

FIGURES

Figure 1.1. Physical map of The Island Cyprus 3
Figure 1.2. Distribution of the three main aquifers in Northern Cyprus 6
Figure 1.3. Water transfer line from Turkey to Northern Cyprus (Cinar et al., n.d.) 10
Figure 2.1. Aerial distribution of Güzelyurt Aquifer (the north and the south parts) and its associated watershed 22
Figure 2.2. The agricultural land distribution within the boundaries of Güzelyurt Aquifer... 24
Figure 2.3. The six watershed basins where precipitation turns into a direct runoff flowing through the given 6 streams (Fanta, 2015).. 25
Figure 2.4. Hydrogeological map of the study area (The material descriptions are explained in Appendix A) Data source: Geology and Mining Department of TRNC. 28
Figure 2.5. Regrouped lithological descriptions (For the formation of southern part, the hydrogeological map developed by British Geological Survey was incorporated with the map of North (Fanta, 2015).)... 29
Figure 2.6. Stages of model development followed in this study............................... 31
Figure 2.7. The available borehole data and their locations 35
Figure 2.8. The clone boreholes to represent the areas where no log information exists.. 36
Figure 2.9. The lithological data view of the available boreholes............................ 37
Figure 2.10. The lithological data view of the clone boreholes 37
Figure 2.11. The contour map for the bottom elevation of Güzelyurt Aquifer (Ergil, 2000) 38
Figure 2.12. The topographic map of the Güzelyurt Aquifer 39
Figure 2.13. The digitized base map of Güzelyurt Aquifer.. 39
Figure 2.14. Solid model of the Güzelyurt Aquifer (Top View) 41

Figure 2.15. Solid model of the Güzelyurt Aquifer (Front View) *42*
Figure 2.16. Solid model of the Güzelyurt Aquifer (Side View) *43*
Figure 2.17. Cross-sectional representation of the material distribution (a) created with auto-filled borehole cross-section command and manual edit (b) solid model cuts *44*
Figure 2.18. Boundary conditions suggested by Fanta (2015) *46*
Figure 2.19. Boundary Conditions *46*
Figure 2.20. Distribution of pumping wells used for different purposes (This data is not showing the up-to-date distribution of the all wells and there is no information about which wells are actively used.) *48*
Figure 2.21. Monthly rainfall data recorded at Güzelyurt Station between 1992-2015 .... *51*
Figure 2.22. A sample curve matching by Theis type curve method *53*
Figure 2.23. Structured finite difference MODFLOW-2005 grid (left), and an UnStructured grid with Voronoi cells for MODFLOW-USG grid (right) (Waterloo Hydrogeologic, 2013) *58*
Figure 2.24. The unstructured grid configuration of an aquifer with continuous and discontinuous confining units (Panday et al., 2013)... *59*
Figure 2.25. Illustration of the cell connection (Panday et al., 2013) *62*
Figure 2.26. The active numerical grid cells for the Güzelyurt Aquifer Model. The constant head cells along the coast and the general head boundary cells are shown with pink and orange, respectively. The proposed pumping wells are colored with green. *69*
Figure 3.1. Locations of wells used for pumping test.. *72*
Figure 3.2. Locations of observation wells where the heads were measured during the tests *72*
Figure 3.3. Sample data fit using "Theis with Jacob Correction" method in Aquifer Test Pro software... *74*
Figure 3.4. Additional observation wells investigated by DSI and MTA *76*

Figure 3.5. The sample observation wells *81*
Figure 3.6. Groundwater head level change in a sample set of observation wells *81*
Figure 3.7. The predicted head contours (in meters) of the Güzelyurt Aquifer at the end of the steady-state calibration process & the observation wells of 2013 .... *83*
Figure 3.8. Hydraulic conductivity (m/d) distribution determined by steady-state automated PEST and hand calibration *84*
Figure 3.9. The groundwater level contour map indicating the status of 2013, dry season (March) (Fanta, 2015) *86*
Figure 3.10. Comparison of predicted head values with the corresponding measured head values for steady-state calibration *87*
Figure 3.11. The location of the observation wells used in the transient runs (measurements between 2009-2013) *91*
Figure 3.12. Recharge Rate changing with time (showing the dataset for both calibration and validation periods) *93*
Figure 3.13. Groundwater head contours drawn after the completion of calibration (a) April 2009, (b) December 2009, (c) April 2010, (d) December 2010 .... *94*
Figure 3.14. Groundwater head contours drawn for validation (a) April, (b) March 2013 .... *96*
Figure 3.15. The computed versus observed head values covering both results of calibration and the validation *97*
Figure 3.16. The location of the Güzelyurt Dam, modeled injection wells and the existing streams *101*
Figure 3.17. The water table contours in 1950 (M. Ergil et al., 1993) *105*
Figure 3.18. The modeled natural state of the Güzelyurt Aquifer *105*
Figure 3.19. The groundwater head contours changing with time (Scenario 1) *107*
Figure 3.20. The groundwater head contours changing with time (Scenario 1, continued) *108*
Figure 3.21. The groundwater head contours changing with time (Scenario 2) *110*

Figure 3.22. The groundwater head contours changing with time (Scenario 2, continued) ... 111
Figure 3.23. The groundwater head contours changing with time (Scenario 3)...... 113
Figure 3.24. The groundwater head contours changing with time (Scenario 3, continued) ... 114
Figure 4.1. The areas where borehole log information is not available. ... 125
Figure 4.2. The areas suggested for new pumping test. ... 126
Figure 4.3. Water level observation wells of 2013 and the areas of no data ... 127
Figure 4.4. Theis with Jacob Correction type curve fit for observation wells numbered with 833 and 846... 143
Figure 4.5. Neuman method type curve fit for observation wells numbered with 833 and 846... 144
Figure 4.6. Theis with Jacob Correction type curve fit for observation wells numbered with 1864 and Laleland-1 ... 144
Figure 4.7. Neuman method type curve fit for observation wells numbered with 1864 and Laleland-1 ... 145
Figure 4.8. Theis with Jacob Correction type curve fit for observation wells numbered with 1861 and 1887... 145
Figure 4.9. Neuman method type curve fit for observation wells numbered with 1861 and 1887... 146
Figure 4.10. Theis with Jacob Correction type curve fit for observation wells numbered with 2405 and 4043... 146
Figure 4.11. Neuman method type curve fit for observation wells numbered with 2405 and 4043... 147

CHAPTER 1

INTRODUCTION

1.1. Definition of the Problem

Among the existing and limited amount of water resources, Güzelyurt Aquifer is the most important, at the same time the largest drinking, municipal, and irrigational water resource in Turkish Republic of Northern Cyprus (TRNC). Agricultural activities are the backbone of the Northern Cyprus's economy. Especially the citrus fruit which is the main crop in the Güzelyurt Region has the greatest percent in the total agricultural production and it returns much as an income to the country. However, the excessive and uncontrolled water extractions from the aquifer, to satisfy the high demand of citrus irrigation water has resulted in significant reduction in the amounts of extractable groundwater over the years. Moreover, due to the serious depression of the water table at the center part of the aquifer, saltwater intrusion in turn degradation of water quality near the coastal areas is another critical problem of the region. Both the quantity and the quality of water do not allow the expected amounts of agricultural product yields (Gozen et al., 2008). This is a serious threat for the economy.

The Güzelyurt Aquifer lacks proper water management strategies. The absence of water management law has hindered the complete control of groundwater extractions. In the past, several management strategies have been applied to remediate the water scarcity problem in the region. But non of them have been sufficient to solve the issue in the long run. However, a recently implemented project called TRNC Water Supply Project aiming to transfer 75 MCM of water annually from Turkey to TRNC has raised hopes in terms of continuous drinking water supply and the long-term rehabilitation of the water balance in the Güzelyurt Aquifer. With this initiation, if the water coming is managed efficiently, the aquifer will be ameliorated seriously. A more detailed information on the water management in TRNC is given in Section 1.2.3.

In developing proper management plans, the role of numerical modeling is proved to be very promising. The proposed study with this thesis is aimed to predict the aquifer's hydraulic behavior by numerical simulations. Therefore, the eventual findings can set light to the steps of decision making for the Güzelyurt Aquifer's water management.

1.2. Project Area Overview

Cyprus is the third largest island located in the Mediterranean Region (Iacovides, 2011). TRNC covers the area from the tip of the Karpass Peninsula in the northeast to Güzelyurt (Morphou) Bay (Figure 1.1.). In the south, the country border is drawn with the United Nation buffer zone. Northern Cyprus consists of 5 main administrative divisions; Güzelyurt (Morphou), Girne (Kyrenia), Gazimağusa (Famagusta), İskele (Trikomo), Lefke (Léfkes) and Lefkoşa (Nicosia) and have a population of above 300,000 (TRNC State Planning Organization, 2017).

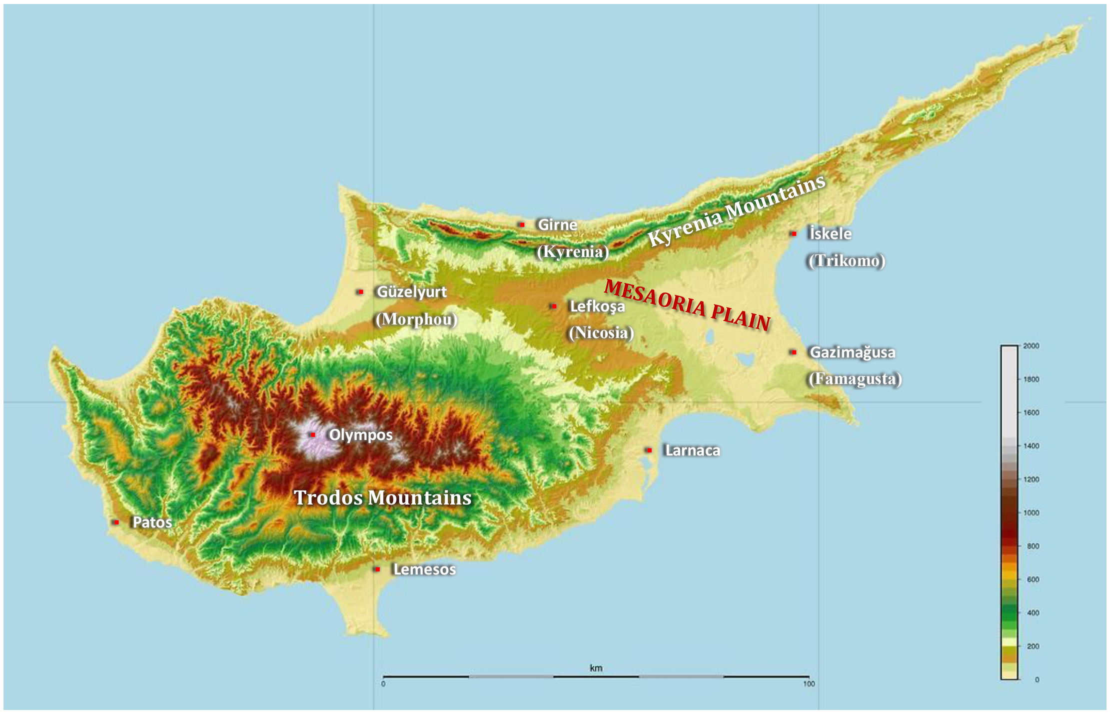

Figure 1.1. *Physical map of The Island Cyprus*

In the Island, two mountain ranges lie along the east-west line. Trodos Mountains located in the middle of the island covers approximately 3,500 km^2 and the Kyrenia (Beşparmak) Mountains run parallel to the northern coast line. The formed lowland lying in between the two mountain ranges is the central plane named as Mesaoria where the Güzelyurt Aquifer located. The plane is good for agriculture (Iacovides, 2011).

1.2.1. Water Resources of TRNC

In the island of Cyprus, from the ancient times to today, the water has always been an important issue for the governments and the nations ever lived. The remains of Roman aqueducts, rain collecting cisterns, Turkish chains of wells, concrete dams, irrigation ditches, and wells of modern era clearly explains the significance of water on the island (Thorp, 1961).

The active water pumping applications have started by the end of 19^{th} century. These were put one step further with the establishment of borehole drilling in the island in 1920. During 1950s, this practice was considerably increased the number of boreholes drilled around the island which in turn resulted in intensified exploitation of groundwater resources (Cyprus Geological Survey Department, 2016).

Cyprus's water resources are limited with the precipitation occurring and therefore depends on the surface runoff, springs, and the groundwater. In Northern Cyprus, the aquifers are the main water resources since there are no perennial streams flowing on the land (Elkiran et al., 2006). In the country, there are 38 seasonal surface runoff streams carrying approximately 70 MCM of water annually. Approximately 38 MCM of this amount of water feeds the aquifers in the West of TRNC (Agboola et al., 2011). Among the all streams, 10 are born in the Trodos mountains in the Southern Cyprus and carry 43 MCM of water annually. When there is flow, these streams are the richest in terms of water amount compared to the others. However, the dams constructed during the last 70 years in the Southern part block the water flowing through the Northern Cyprus (Agboola et al., 2011; Water Development Department, 2009).

To satisfy water requirements and to prevent uncontrolled stream flow through Mediterranean Sea, 41 small dams, mostly ponds, were built in the Northern Cyprus (Elkiran et al., 2006). They were mostly used to provide water to the agricultural sector and to feed the aquifers in the regions that they are constructed (DSI, 2003). However, according to the information gathered in 2004, only 18 of them with a total capacity of 19 MCM are in use. And the sediment accumulation transported by ephemeral streams is the problem of two of these dams. Moreover, because of management deficiencies and high evaporation, the water stored in the dams are mostly depleted (Elkiran et al., 2006; Elkiran et al., 2008).

There are 15 aquifers located within the boundaries of Northern Cyprus (Table 1.1.). Each groundwater body has different water storage capacity and are encountered in different hydrological regions. Among them, 3 aquifers are the main water resources from which most of the domestic and irrigational water demand of the Northern Cyprus is obtained (Figure 1.2.). Güzelyurt Coastal Aquifer is located on Maseoria Plain; Girne Limestone Mountains host the Girne Range Aquifer; and Yeşilköy Aquifer lies beneath the Karpass peninsula (Türker et al., 2013).

Table 1.1. Main aquifers of Northern Cyprus (DSI, 2003; Türker et al., 2013)

No	Name of the Aquifer
1	Güzelyurt/Morphou Aquifer
2	Girne/Kyrenia range aquifer
3	Girne/Kyrenia coastal aquifer
4	Yeşilkoy/Agios Andronikos aquifer
5	Yeni Erenköy/Yalusa-Sipahi/Agia Triada aquifer
6	Dikarpaz/Rizokarpazo aquifer
7	Büyükkonuk/Komikebir aquifer
8	Lefkoşa-Serdarli Aquifer
9	Lefke-Gemikonağı-Yedidalga Akiferi
10	Doğu Maserya/East Mesaoria-Bogazici/Lapithos aquifer
11	Gazimagusa/Famagusta coastal aquifer
12	Orta Maserya/Central Mesaoria aquifer
13	Akdeniz/Agia Irini-Koruçam/Kormakiti aquifer
14	Güneydoğu Maserya/Southeastern Mesaoria aquifer
15	Batı Maserya/Western Mesaoria aquifer

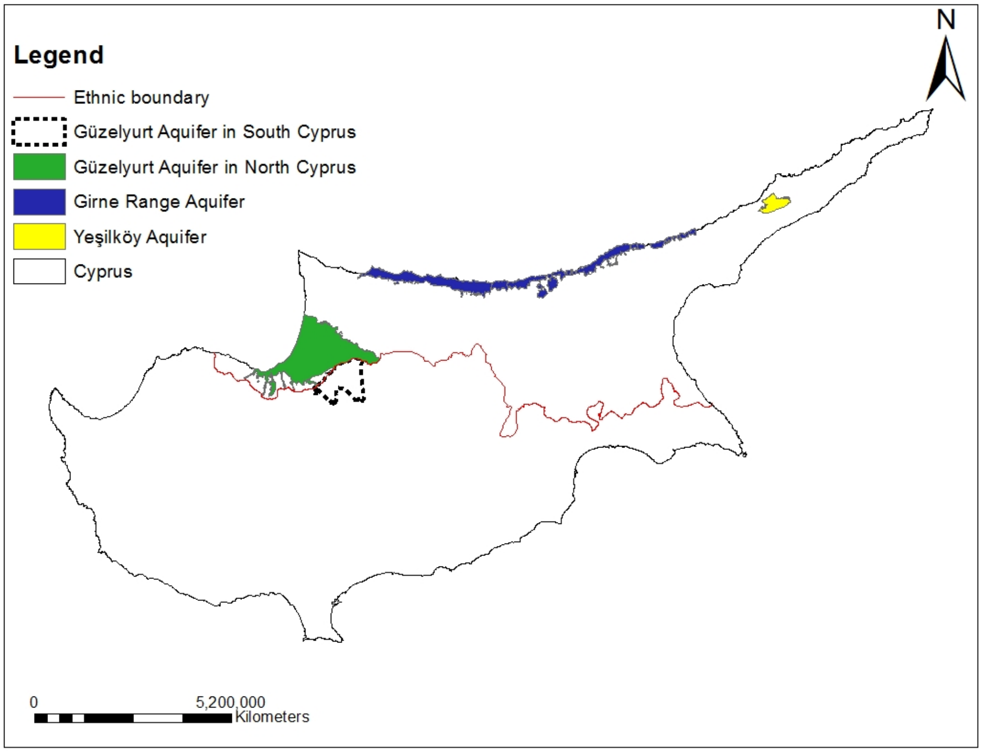

Figure 1.2. Distribution of the three main aquifers in Northern Cyprus

In 1960's, the main groundwater supply was the Gazimağusa/Famagusta Aquifer. However, excessive pumping from this aquifer resulted in sea water intrusion in whole of the area. Therefore, the aquifer is no longer in active use (Gozen et al., 2008).

Yesilköy Aquifer is the third major groundwater resource in North Cyprus. It has been in use since late 1960's for agricultural and domestic water supply. The main product grown in the field was Colocasia esculenta (Taro) starting from 1970's. However, the depletion of water stored in the aquifer due to water scarcity and excessive pumping, Taro was replaced with Solanum tuberosum (potato). Unfortunately, this action did not prevent the continuously increasing depth to the water table in the aquifer (Türker et al., 2013).

Most of the aquifers in Northern Cyprus are unconfined and consists of alluvial deposits which are mainly silt, sand and gravel. However, the Girne Range Aquifer which is the second main aquifer, is a limestone aquifer (Turker, 2012). The Karstic region (Elkiran et al., 2006) enables spring discharges; and 30 springs were used to be flowing actively. However, the water depletion has affected the Girne Range Aquifer, too. Today, most of the springs are dry (Türker et al., 2013).

Güzelyurt Aquifer is the most important and the largest of the aquifers in Northern Cyprus. After the depletion of Gazimağusa Aquifer, most of the stress has been carried to Güzelyurt (Gozen et al., 2008). It has been used not only for irrigational activities of Güzelyurt alone but also for the municipal water demands of Lefkoşa and Gazimağusa (Elkiran, 2004). However, the water level in the aquifer has been dropping at a high rate, since 1950s. Since it is the water supply of most prosperous irrigation areas, Güzelyurt Aquifer has always been the focus of most researchers (Thorp, 1961).

1.2.2. Groundwater Management in TRNC

Northern Cyprus is suffering from water resources management problems because still there is no water management law implemented and published. The law was aimed to be published in December 2017 (TDKB, 2016) but today, it is still in preparation process. With the release of the law, integrated water management committee will be established which will coordinate the law to achieve good quality/quantity surface and groundwater status (Gökçekuş, 2014).

Gozen et al. (2008) has summarized the management strategies that have been evaluated by the authorities. In 1998, huge water containing bags were transported form Turkey to Kumköy pumping station in Northern Cyprus. The project allowed transfer of 4.1 MCM water in 5 years. However, due to the inevitable high transportation costs, the project has stopped in 2002. In the beginning of 2000s, desalination plants were started to be implemented in order to downshift the salinated water problem (Elkiran et al., 2006). But, this application is costly and not feasible in large scale. The salination problem should be solved with another alternative strategy. Moreover, in the Northern Cyprus there has been an irrigational development such that about 80% of the irrigated lands use drip irrigation method. This method is very beneficial in terms of crop yield and water use efficiency. Additionally, rather than discharging to the sea, reuse of treated wastewater to irrigate the agricultural lands has been proposed as another strategy. Finally, the TRNC Water Supply Project which is started to be implemented in June 2016 has promised a hope, regarding the worrisome water status of the country.

It is critical to implement detailed investigations on the aquifers of TRNC, in order to allow the further possible management strategies to be implemented. Especially, the critical water resources of the country should be examined, conceptual and numerical models of the aquifers must be built to understand the hydraulic behavior of the aquifer and spread of salt water intrusion. With this proposed study, the developed numerical model of Güzelyurt Aquifer, the most important water reserve of TRNC, will help authorities to develop alternative management strategies that will rehabilitate the aquifer's stress and water quality.

1.2.3. TRNC Water Supply Project

The limited water resources, the excessive exploitation of the aquifers and the seawater intrusion in the coastal aquifers of Northern Cyprus have caused serious water scarcity which risks the country's water demand and eventually, results in food security problems. In the past 30 years, the average annual precipitation has shown a declining trend. This has a great effect on water resources because they depend mostly on the precipitation, there are no perennial flows or stable surface water bodies on the northern part of the island. Moreover, since 2004, the water demand has been increasing due to population rise caused by foreigners moving to Cyprus and the tourists (Gungor, 2016). The increasing stress on the aquifers is a thread for the sustainability of the water resources and so, the socio-economic future of the Northern Cyprus.

In order to solve the water quantity and quality problem in North Cyprus, some efforts have been practiced, however, non of them could serve for the purpose. For instance, regarding the aim, a few low capacity desalination plants were built in TRNC to treat the salinated groundwater. Although, these plants can offer local solutions, it is not satisfactory for long term water management in coastal aquifers where salt intrusion problem exists (Yildiz et al., 2014). However, Turkish Republic of Northern Cyprus (TRNC) Water Supply Project seemed as a very promising solution. The project aimed to transfer a total of 75 MCM water annually from Alaköprü Dam in Turkey to Geçitköy Dam in TRNC via 80 km pipeline under Mediterranean Sea (Figure 1.3.). Of the total water planned to be transferred, 38 MCM has been allocated to domestic purposes while the remaining 37 MCM was for irrigational water demand. The project has been approved in 1998 and started with the construction of Alaköprü Dam in the Turkey side in 2011. All of the dams and the submerged pipeline, except the inland distribution lines were completed in 2015 (Gungor, 2016). With the finalization of the project in June 2016, the water was successfully transported from Turkey to the TRNC (TDKB, 2017).

Figure 1.3. Water transfer line from Turkey to Northern Cyprus (Cinar et al., n.d.)

Güzelyurt Aquifer is the country's main source for drinking and the irrigational water supply since Güzelyurt region is the most important agricultural land where citrus production is carried out. However, it is also one of the aquifers that are in danger of complete water quality degradation by saline water. With TRNC Water Supply Project, the amount of water reserved for the irrigation can be a remedy for the existing stress on the aquifer by decreasing the need of water extraction or by its direct artificial recharge to compensate the water deficit in the aquifer.

1.2.4. Previous Studies: Güzelyurt Aquifer

Starting from late 1960s, considerable number of field investigations have been made on Güzelyurt Aquifer. In 1970, UNDP has released a report on Cyprus's water and mineral resources (UNDP, 1970). Afterwards, in 1975 and 1976, Turkish Republic State Hydraulic Works (DSI) has prepared reports on hydrology of the Güzelyurt Region and the aquifer (DSI, 1975) (DSI, 1976). In these studies, the geology and hydraulic features of the region have been mostly revealed. In late 1990s, Turkish Republic General Directorate of Mineral Research and Exploration (MTA) has also conducted hydrogeological field investigations on Güzelyurt Aquifer. MTA has drilled approximately 20 boreholes in the area, in order to find new water resources to meet additional water demand with the depletion and salination of Güzelyurt Aquifer. As a result of this study, it was evident that the seawater had been intruded about 8.5 km from the coast to the inland, thus it was necessary to stop additional pumping well drillings in the area and to keep the level of water use way below the estimated replenishment amounts (MTA, 1997).

Unfortunately, there are not many published research papers specifically on Güzelyurt Aquifer. It can be said that the research competed by Ergil (2000) is the only study on salination of the Güzelyurt Aquifer. In this study, the aquifer's water budget was estimated by incorporating a reverse approach which approximates the water balance from salt concentration in groundwater and the head distribution. The author needed to use this kind of general approach due to the data uncertainties in temporal and spatial basis. To determine the continuous water utilization from the aquifer, a volumetric water balance approach which is combined with the salt balance equations has been followed. Additionally, the water level and salinity concentration data gathered during the 20 years period between 1977-1997 have been used to draw contour maps of groundwater head and salt concentration by kriging technique. As a result of these, the groundwater extraction in the Güzelyurt Aquifer by the Southern Part was estimated as 8.5 MCM/year. And, it was found that between 1977 and 1997, approximately 24 MCM of seawater has intruded inland by 12 km from the coast. Moreover, by considering the plantation type on the Aquifer, the total annual irrigational water demand of the Güzelyurt were calculated as 60 MCM.

The study conducted by Ergil, 2000 has been a benchmark for the future academic research attempts. Hence, it carries a great importance for the sake of Güzelyurt Aquifer, since it emphasizes the need for sustainable water management to stop further degradation of the aquifer. However, the approach used in this study is way different from the numerical modeling method that is extensively employed to predict groundwater elevation and water budget. Numerical techniques help to understand and predict the behavior of the aquifer system by means of simulations. Therefore, the need for such fundamental modeling tools triggered a set of modeling projects by the Geology and Mining Department of Northern Cyprus and the Middle East Technical University. As a first project along this line, Fanta (2015) has developed a conceptual model of Güzelyurt Aquifer which lighted the road towards a numerical model development. This study aimed to analyze the current state of the aquifer by compiling and analyzing existing geological, hydrological and hydrogeological data related to Güzelyurt Aquifer and to investigate the potential use of the existing data in the future stages of numerical aquifer simulation model. In the light of the evaluations made with this study, it is understood that the existing data together with the new ones have a potential to be used in the development of the numerical simulation model of the aquifer.

1.3. Scope and Objectives of the Study

The primary objective of this study is, based on the available data, to develop a numerical model of the Güzelyurt Aquifer to simulate the hydraulic behavior of the aquifer system. The simulation results can ultimately be used for the purposes of contributing to the development of sustainable groundwater management plans since the simulation runs are analyzed with respect to the groundwater level changes and water budget impacts associated with groundwater pumping scenarios, artificial and natural recharge schemes that will stop saltwater intrusion and shrink the salted areas. In order to achieve this aim, there are several steps that were completed:

- Analysis of the aquifer pumping test data and to determine hydraulic conductivity distribution in the aquifer.
- Development of the aquifer conceptual model through delineation of the 3-D lithological aquifer material distribution in the Güzelyurt Aquifer and with the identification of the internal and external boundary conditions.
- Design of a numerical grid system based on the developed conceptual model.
- Calibration to estimate the distribution of aquifer hydraulic properties (hydraulic conductivity distribution, specific yield and conductance) by comparing the distributions of measured and predicted hydraulic heads.
- Validation of the calibrated numerical model.
- Identification of simulation scenarios and conducting numerical model runs to predict the hydraulic behavior of the aquifer.

Groundwater modeling exercises require a systematic approach. For this reason, standard guidance documents on how to perform groundwater modeling work have been developed. For example, the Australian Government National Water Commission has published the Australian groundwater modeling guidance document (Barnett et al., 2012) to ensure a consistent and a healthy approach to the development of groundwater models in Australia. A similar document has been published by the American Society for Testing and Materials (ASTM) to describe a holistic approach and the required data types that must be followed step-by-step in the development of groundwater conceptual models that constitute the underlying structure of digital groundwater models (ASTM, 2014). In the modeling study carried out in this thesis, the mentioned and similar guidance documents were taken into account (Spitz et al., 1996; McMahon et al., 2001). Up to date, no attempts have been made so far to develop a numerical model for Güzelyurt Aquifer. This work is the first to shed some light on future research.

1.4. Importance of Numerical Modeling in Groundwater Management

The increasing pressure on global water resources requires proper groundwater management strategies to be applied by the authorities. The groundwater, among the other resources on Earth, carry the most strategic significance. They are fed by rain water after a process of infiltration through the subsurface geological layers, which in turn makes their quality better than that of surface waters. Aquifers, due to their concealed nature, are protected from atmospheric pollution and evaporation losses. Thus, they are the most reliable and preferable water resource of the Earth, unless they are poorly managed (Sen, 2015).

Numerical groundwater modeling is a powerful tool for water resources management. Rapid improvements in computational power and useful software interfaces enabled groundwater modeling concept to be a standard tool for hydrogeological analysis (Zhou et al., 2011). Models are used to predict the behavior of aquifer systems before making decisions. They simplify real systems and try to mimic the natural mechanisms. However, due to great uncertainties in data and the complexity of the natural aquifer systems, models can not be perfect. Therefore, it is a big challenge for the modeler to design a realistic system in the computer environment without sacrificing the preciseness of the model and having impractical assumptions. However, although the product is imperfect, numerical modeling is a very powerful tool for hydrogeological characteristics determination and deciding proper management strategies (Baalousha, 2008).

Groundwater models have three modes of action in water resources management. They can be used to interpret the system behavior, predict future conditions (e.g. head or concentration distribution) or analyze different water resources management or remediation scenarios. Although the outputs of the models are successful in giving a sight on what management applications, one should not rely only on software programs blindly. In management decision making processes, each region has its own local conditions and different strategies should be determined under the light of each circumstances (Sen, 2015).

1.5. Similar Numerical Modeling Studies from Literature

Many interpretive and predictive studies have been carried out to determine hydraulic properties, flow regimes, water budgets and specific behaviors of aquifer systems. Among the current technologies, Geographical Information Systems and integrated aquifer system modeling approach, are now widely used for proper and reasonably suitable planning of groundwater use. In engineering applications, multifunctional integrated software interfaces such as GMS (Groundwater Modeling System) and Visual MODFLOW are widely used with GIS. An up-to-date example of this is the modeling of the Helena Valley Aquifer in the North Hill region of the Montana in United States, to predict the effects of current groundwater pumping activities on groundwater and surface water levels (Waren et al., 2013). In this study, the water budget of the Helena Aquifer system was investigated by using GMS besides GIS and the approximate timing and the grade of effects of different water use activities on groundwater and surface water levels in the region were determined. The model has been run in both steady state and transient conditions. In steady state runs, pilot points parameter estimation tool (PEST) (Doherty, 1998) and manual calibration were used to determine the hydraulic conductivity distribution. In the transient case, temporal changes in the stresses such as seasonal irrigational activities were simulated and additional calibration for storativity parameter has been done. Similarly, Ünlü et al. (2004) has investigated the effects of drawdowns resulted due to water extraction from newly drilled wells in Usak Ulubey Aquifer to supply the process water need of a mining site on nearby drinking water wells by using GIS and GMS tools.

Hashemi et al., (2012) have investigated the best hydraulic parameters and boundary conditions of an unconfined aquifer located on the Gareh-Bygone Plain. For this purpose, ten different steady-state terms were analyzed with MODFLOW and calibrated with PEST tool against field observations. It is concluded that, steady state parameter estimation in unconfined aquifer models is a trustable method in determining high precision hydraulic parameters and boundary conditions.

Qiu et al., (2015) have applied numerical groundwater modeling approach to a River Valley Basin in China. GMS is the software employed in this study. In this investigation, the hydraulic conductivities and the specific yield values were estimated with the analysis of pumping test data. The model then was calibrated by applying trial and error approach. As a result, the water budget of the system has been determined.

In the study conducted by Barazzuoli et al. (2008), a coastal multi-aquifer system in southern Tuscany, Italy was mentioned to be deteriorated by over-pumping for irrigation and tourism and eventually, it caused seawater intrusion. The research aimed to model the aquifer system by a 3-D finite element model employing FEFLOW numerical engine, in order to make some conclusions on the causes of seawater intrusion. The hydrogeological structure of the aquifer has been delineated by the help of borehole data and the hydraulic conductivity values have been estimated by the help of pumping test analysis and the automated calibration method, PEST (Doherty, 1998). During the calibration stage of the study, hydraulic conductivity and the specific storage parameters were optimized for fitting the model to actual groundwater levels. After the forward runs, the estimated water budget showed that the difference between the inflow and the outflow along the coastal boundary represents the amount of seawater entering to the aquifer (Barazzuoli et al., 2008).

The saltwater intrusion is one of the most prevalent and significant processes that result in degradation of water quality which may be way worse than the drinking and irrigational water standards. Salt water intrusion is a great concern of coastal aquifer since it threatens the future water use (Alfarrah et al., 2018). The water budget analysis gives a rough estimate of the seawater front and the flow rate. But, determination of seawater intrusion and concentration distribution can be modelled in detail and more precisely with the SEAWAT model which employs finite difference approximation for variable density flow equation (Esca et al., 2006). An example for this concept has been studied by Mansour et al. (2017) on a coastal aquifer of Karaburun Peninsula located in the west of Turkey. In this study, with the development of a conceptual model of the aquifer and the use of SEAWAT numerical model, the saltwater movement through aquifer towards the inlands was simulated. As a conclusion, it was stated that the main reason of the intrusion is the seasonal overexploitation of the aquifer.

As summarized in the above, each referred research is a case study for numerical model development in different aquifers which are at risk in terms of groundwater level depletion and/or water quality degradation by salt water intrusion. The groundwater modeling is based on mostly a common approach, as seen in the other studies. In this framework, first, a detailed conceptual model is created by generally using Geographical Information Systems and collecting/interpreting field data. Then a numerical model is developed by designing a grid system and doing calibration for unknown parameters. Finally, model simulations are implemented in order to predict the behavior of the groundwater system. The mostly preferred, calibration analysis is

PEST, which is a code developed by Doherty (1998) to be used for automated parameter estimation.

The modeling study explained in this thesis is based on a regional groundwater flow modeling where the characteristic flow behavior of the Güzelyurt aquifer was tried to be predicted. In order to do this, the detailed conceptual model and then the numerical grid system was designed. After the calibration and validaiton, the model whose accuracy was proved by the statistical error estimations was used to simulate different water use activities and artificial recharge through Güzelyurt Dam and borehole injections. The resultant head contours of each scenario run were analyzed and accordingly, the behavior of the aquifer were tried to be predicted.

In this study, the salt water intrusion has not been modeled as done by Mansour et al. (2017). However, after analyzing the head contours, the areas with head values below sea level indicated the potential distance of salt water intrusion. In the further studies to be completed for the Güzelyurt Aquifer, SEAWAT tool can be used to appropriately simulate the intrusion in terms of determination of its net inflow and the concentration distribution.

1.6. Modeling with Limited Data

Groundwater flow models are the simple forms of complex natural systems. Therefore, it is normal to have some limits in precision in the model outputs. These limitations must be acknowledged while using the models and evaluating the model results. There are several roots of error and uncertainty in models (Gannett et al., 2012). In this study, the biggest challenge faced is the limitation of available data. For example, lithological descriptions and water level measurements are available only in the central part of the aquifer. Additionally, especially, there is a big uncertainty in the number, location and extraction amounts of active pumping wells within the area.

Gannett et al., (2012) were developed and simulated a regional groundwater model on the upper Klamath Basin. The actual system was simplified and did not represent the true complexity, due to the geological information limitations. However, this model was found to be helpful in simulation of the spatial distribution of hydraulic head and in predicting the response of the groundwater system to climatic and irrigational stress effects. Therefore, even the above limitations exist, a model can be a very informative tool for informing the groundwater management in the basin.

It is important to restrict the groundwater extractions to a level in order to protect the water resources and to be able to use them sustainably. Generally, the groundwater extractions are not measured well by well. Limited or lack of extraction data may greatly affect the diagnosis of the historical stress changes, future impact predictions, the correctness of the model calibration and eventually the determination of sustainable groundwater management strategies (Keir et al., 2018).

1.7. Organization of the Thesis

In this thesis, firstly, in an introductory chapter, the problems of the Güzelyurt Aquifer are summarized and the objectives of the study were given. Moreover, a general condition about the water resources and the management status of the TRNC, the previous studies conducted on Güzelyurt Aquifer and the importance of numerical modeling in achieving a good management strategies were concisely narrated and a literature review was presented.

Secondly, the area of focus has been introduced by giving its geographical, climatic, hydrologic and hydrogeological characteristics. Following that, the two main steps required before moving into the calibration and simulations period in groundwater modeling were elaborated. These are conceptual and numerical model development stages. In the conceptual model development part, the delineation process of the internal/external boundary conditions and lithological materials distribution have been presented. Moreover, the applied techniques for the transmissivity parameter distribution estimation were explained in detail. The findings about the transmissivity and the hydraulic conductivity values were given in the Results and Discussions chapter. In the numerical model development section, the employed numerical methods and techniques were first introduced and the information on the numerical grid design has been given.

Lastly, in the Results and Discussion section, all the analysis including the pumping test data evaluation by the use of a different software called Aquifer Test Pro, calibration studies for estimating the hydraulic parameters and the boundary conditions and the simulations of different scenarios considered to analyze the hydraulic behavior of the aquifer have been presented and the results have been discussed.

The chapter 4 covers the overall assessment of the whole study and the recommendations for future studies.

CHAPTER 2

MATERIALS AND METHODS

2.1. Description of the Study Area: Güzelyurt Aquifer

2.1.1. Location and Areal Coverage

The study area Güzelyurt Aquifer is located in Güzelyurt Plain next to the west coast of Northern Cyprus (Figure 2.1.). In a report prepared by Gokmenoglu et al. (2002), it is stated that Güzelyurt Plain has a total surface area of 415 km^2 and a drainage area of 900 km^2; about 2/3 of the aquifer area is within the boarders of the TRNC and the remaining one third is within the borders of the South Cyprus (SC); and a large majority of the drainage area is located in the SC borders in the south. According to DSI (2003), approximately 373 km^2 of the drainage area of Güzelyurt Plain, which is composed of 6 sub-basins, is within the borders of TRNC. For the aim of determination of the geographical distribution of the aquifers more precisely using the latest technology, hydrogeological maps and the topographic map converted to digital elevation model (DEM) were analyzed in the study carried out by Fanta (2015). As a result of this analysis, it is determined that the Güzelyurt Plain has a drainage (basin) area of approximately 880 km^2 where the runoff from both Trodos and Beşparmak Mountains drain and the alluvial-type coastal aquifer spreads within a total area of 255 km^2, where 180 km^2 is in the boundaries of TRNC and 75 km^2 is in the SC (Figure 2.1.).

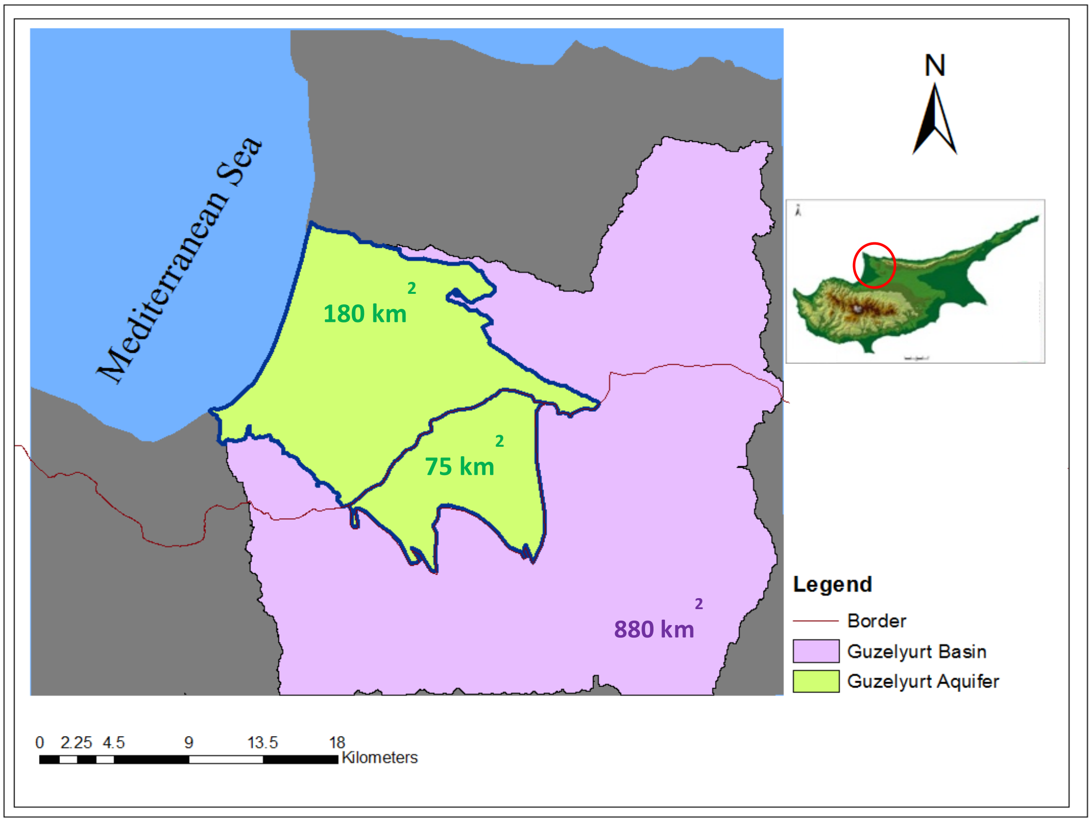

Figure 2.1. Aerial distribution of Güzelyurt Aquifer (the north and the south parts) and its associated watershed

2.1.2. Precipitation

The Güzelyurt region is in a semi-arid climatic zone, with hot and dry summers and cool and rainy winters. With this seasonal pattern it represents the typical Mediterranean climate (Ergil, 2000; Thorp, 1961). The precipitation pattern in the Island is generally in the form of heavy showers rather than persistent rains (Burdon, 1951). The average annual rainfall in the island is approximately 500 mm (Sofroniou et al., 2014), in the central plain it ranges between 300-400 mm and at the higher altitudes in Trodos Mountains it reaches up to 1200 mm (Elkiran et al., 2006). The available long term meteorological data has showed that Güzelyurt Aquifer has an annual average rainfall of approximately 285 mm. In the region, the rainfall generally falls during the period including the end of October and the beginning of April. It almost never rains in the summer. The yearly average throughout the North Cyprus was observed to be declining continuously (Ergil, 2000).

2.1.3. Temperature and Evaporation

In TRNC, the mean monthly temperature was estimated as 18.2°C. The minimum and maximum values were measured as 10.9 and 33.7°C, in January and August, respectively (Gokmenoglu et al., 2002).

Gokmenoglu et al. (2002) analyzed the evaporation data collected between 1984-1997 and they estimated the annual average evaporation as 2117 mm. They also reported that this value being very high when the conditions in the Mesaoria plain are considered. In another study reported by DSI (2003), the monthly evaporation data shows that the highest evaporation occurs during the months between May and September. In DSI (2003) report, the annual evaporation estimated as 2210, which approximately verifies the evaporation value reported by Gokmenoglu et al. (2002).

2.1.4. Land Use

Güzelyurt Aquifer is located in the agriculturally most productive region and therefore is the most important reservoir in TRNC (Gozen Elkiran et al., 2008). The land in the Güzelyurt Basin is used for three main activities; of the total land area, 65% is used for agricultural purposes, 2% is covered by forests, 12% is utilized for pasture ground and the rest 21% is an unused area (TDKB, 2017). The region's agricultural products consist of mainly citrus fruits. The parts looking green within the agricultural land boundary shown in the Figure 2.2. are the indicators of citrus tree gardens. In the remaining areas where the arable red soil can be seen, mostly fruits and vegetables are being produced. These areas can be seen in between the citrus trees and especially in the south of land located between Doğancı and Aydınköy.

Guzlyurt Aquifer’s physical boundary

Agricultural land boundary

Figure 2.2. The agricultural land distribution within the boundaries of Güzelyurt Aquifer

2.1.5. Surface Water Conditions in the Güzelyurt Aquifer Basin

The main sources for the recharge of Güzelyurt Aquifer are the precipitation and the infiltration of seasonal run off water which originate in the Trodos and Beşparmak

Mountains and flow through the ephemeral streams. The water stored as snow on Trodos mountains starts to melt in spring, however it is less in amount to persist in the summer. Most of the year, the rivers are dry. Most of the runoff which is formed by rainfall and the snow melt observed in winter. After March when the portion of the runoff from melted snow disappear, the flow rates of the streams decrease rapidly (Burdon, 1951; Ergil, 2000). The Figure 2.3. shows the location of the streams and their basins in the area. Their flow direction is through the sea. The drainage areas of these streams mostly remain in the southern part of the Cyprus. Due to the dams or ponds built on them in the South, they are almost dry.

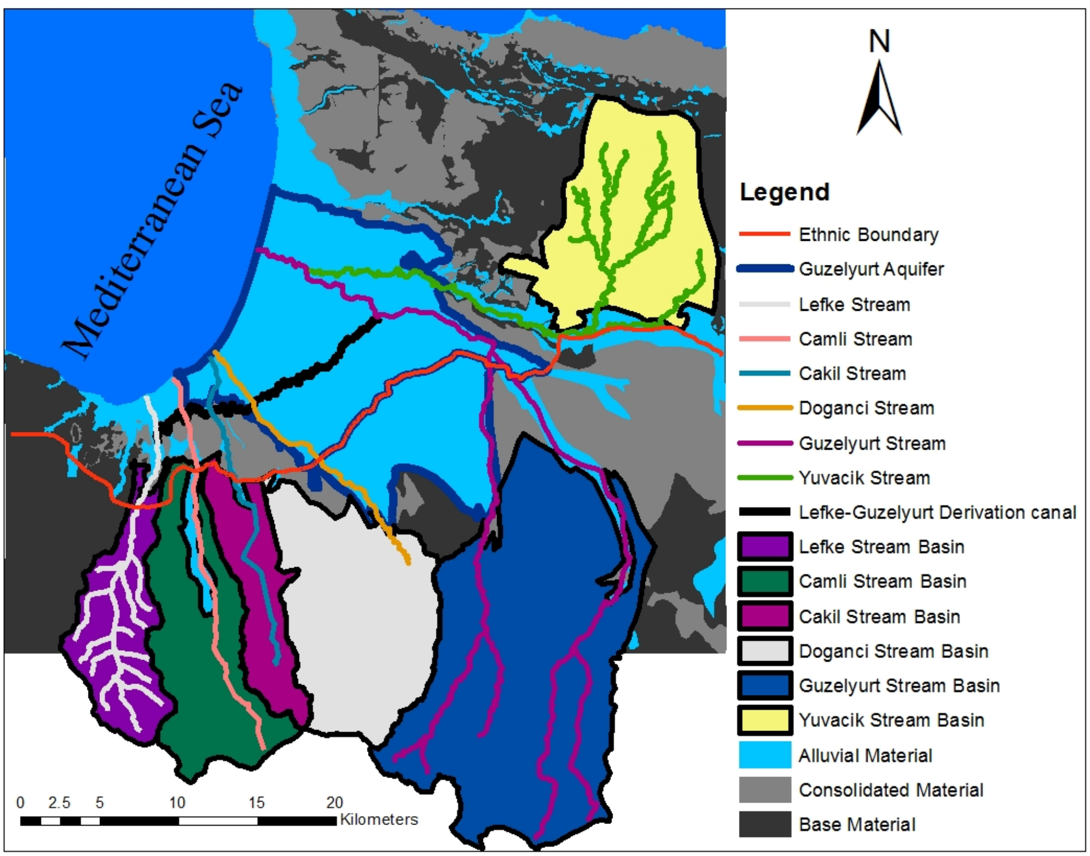

Figure 2.3. The six watershed basins where precipitation turns into a direct runoff flowing through the given 6 streams (Fanta, 2015)

In the study area, in order to replenish the groundwater in Güzelyurt, before 1974, Serhatköy Pond and Güzelyurt Dam on Güzelyurt Stream and Mevlevi (Ovgos) Dam on Dardere Stream were constructed. However, there is not enough water in these structures to feed the aquifer. In order to increase the amount of water stored in the Güzelyurt Dam, to prevent the streams losing their water to the sea and to infiltrate more water by increasing the residence time of water flowing on the aquifer, the Lefke-Güzelyurt Derivation Channel has been constructed between 1983-1994. In this structure, annually 8 MCM water from the winter flows of Lefke, Çamlık and Maden streams depots to Güzelyurt Dam. However, due to siltation in the channel, a large part of the water is evaporated during its journey to the Dam. Therefore, only a small amount of water reaches to the Dam Lake (DSI, 2003).

In the hydrological report prepared by DSI (2003), it was proposed that only 23% of the water in the watershed basins is available for runoff and approximately 77% of it is lost through evapotranspiration. Moreover, out of the 23% of water flowing as runoff, Doğanci, Güzelyurt, and Yuvacik streams, only infiltrates 25% of their water to the aquifer. On the other hand, in Lefke, Çamlı, and Çakıl steams, approximately 25% of the available total runoff (%23) infiltrates into secondary aquifer of consolidated material (shown in Figure 2.3.) before reaching the derivation channel.

2.1.6. Hydrogeology of the Aquifer

Güzelyurt aquifer is a coastal unconfined groundwater reservoir (M. E. Ergil, 2000). Güzelyurt alluvial basin as a whole mostly consist of permeable units which are sand and gravel and impermeable silt-clay lenses. Besides that, sandstone, limestone and conglomerate containing materials, which have large water holding feature; and partially impermeable/semi-permeable units, called base material, containing marl, lava pads and other volcanic rocks are contained in the subsurface of the aquifer (DSI, 2003; Gokmenoglu et al., 2002). Fanta (2015) has conducted hydrogeological grouping of various similar materials into three main categories (Figure 2.4 and 2.5) and suggested that the Güzelyurt alluvial coastal aquifer is mainly consist of sand and gravel, where silt and clay lenses are randomly distributed within the aquifer. The impermeable base of the unconfined aquifer is formed by Pliosen aged marl and thick clay layer. At higher altitudes, alluvial aquifer material contacts with calcareous sandstone. The major water holding formations in the Güzelyurt Aquifer are the old alluviums (Qal) and fanglomerates of Bostancı gravel (Qmb). Calcareous sandstone and calcarnite are in contact with alluvial sand and gravel aquifer (Güzelyurt) in the vicinity of Serhatköy; and it is considered to be a low-water yielding separate aquifer.

Since 1959, with the initiation of more lands for agriculture, the groundwater extraction exceeding the recharge caused sea water intrusion. The progress of the salt water intrusion from the shore to the inland in the horizontal direction is apparent along the stream beds. The saltwater intrusion is progressing 7 km along the Güzelyurt stream bed and 4 km along Doğancı-Çakıl streams. The seawater mixture in the aquifer reached up to 28% in the vicinity of Doğancı Stream. The recharge and discharge in the aquifer is offset by refilling of the depressed areas with the sea water (DSI, 2003).

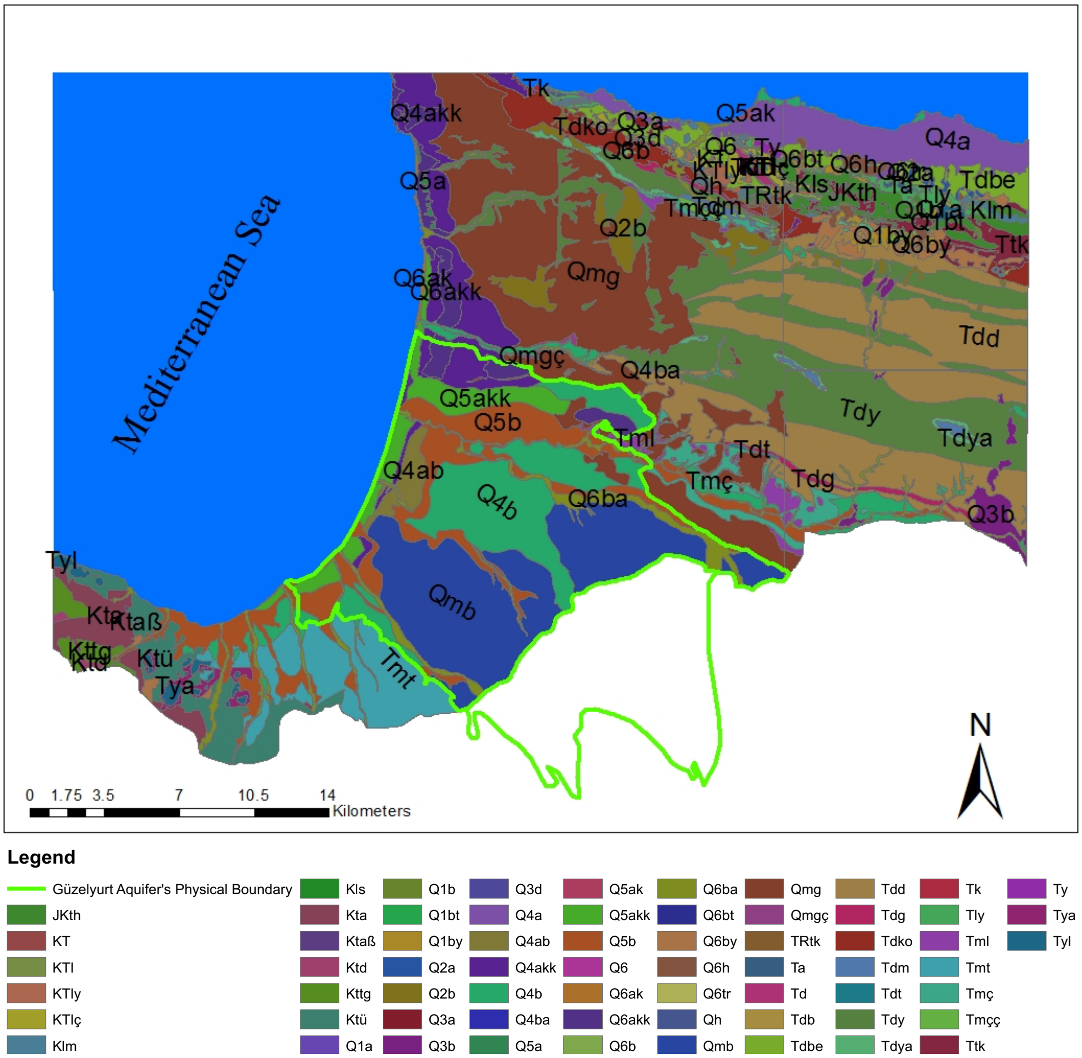

Figure 2.4. Hydrogeological map of the study area (The material descriptions are explained in Appendix A) Data source: Geology and Mining Department of TRNC

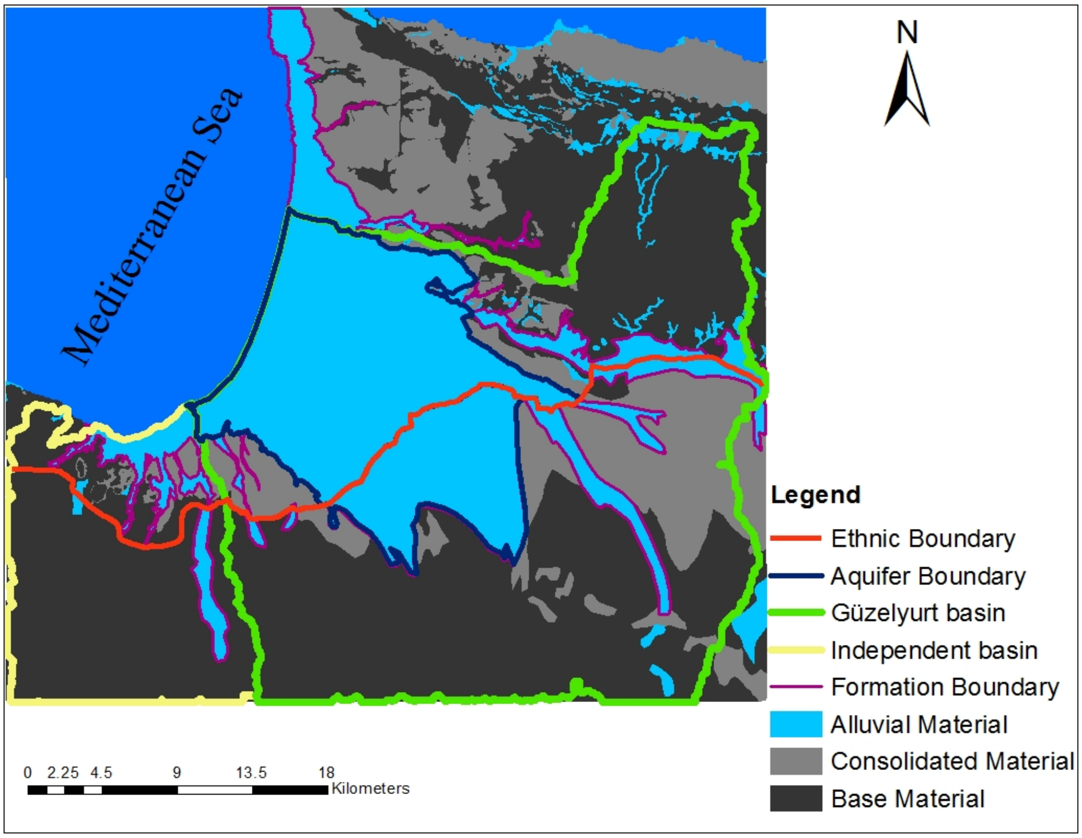

Figure 2.5. Regrouped lithological descriptions (For the formation of southern part, the hydrogeological map developed by British Geological Survey was incorporated with the map of North (Fanta, 2015).)

2.2. Groundwater Model Development

The first requirement for a numerical groundwater model design is the availability of an accurate conceptual model which defines the aquifer parameters, input parameter distributions and the boundary conditions. Within the scope of this study, at the first step, a detailed conceptual model of Güzelyurt Aquifer was developed using the available and data gathered from the field surveys. The flow domain characterized fully by the conceptual model is then descritized into a grid system using the Map to

MODFLOW command in GMS. All material property distributions and relevant boundary conditions are numerically assigned onto the grid system; by this way the conceptual model is efficiently converted to the numerical model in the software environment. Following this step, the numerical model becomes ready for the calibration studies. This process consisted of two steps; first the hydraulic conductivities were automatically calibrated with steady-state PEST (Doherty, 1998) runs and then, transient runs were applied to calibrate hydraulic conductance for the general head boundary and the specific yield parameter. The overall process scheme suggested by Zhou et al. (2011) was followed during the model development stage as given in Figure 2.6. As it can be seen from the figure, all the steps are actually dependent on each other. And most of the times, there is a need for completion of loops between steps to achieve accurate and meaningful results.

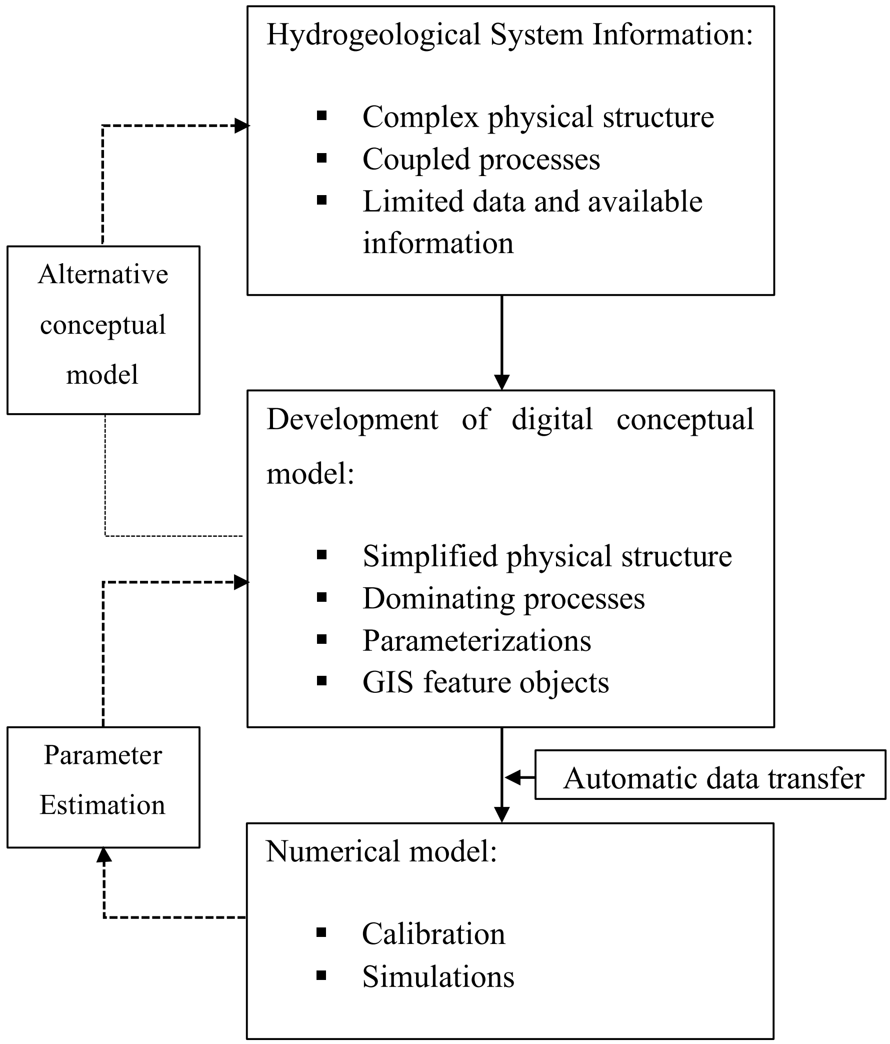

Figure 2.6. Stages of model development followed in this study

2.2.1. Available Field Data

In the first step of the groundwater modeling process, it is necessary to identify the modeling problem, and to collect the necessary data about the aquifer system to be modeled. It is an important requirement to have sufficient level of field data for a reliable modeling work. With a protocol signed between METU Northern Cyprus

Campus Rectorate and TRNC Ministry of Environment and Natural Resources, Geology and Mining Department (J&MD), a scientific research study has been carried out in 2013. In this study, it was aimed to examine the current situation of the aquifer. In this manner, existing geological, hydrological and hydrogeological data related to Güzelyurt Aquifer have been analyzed. The suitability of the existing data for numerical aquifer simulation model and during possible development of water management plans at later stages was evaluated. Additionally, the data requirements have been determined. As a result of the evaluations made, it was concluded that there is a potential in the available data to be used in the numerical model simulation model. In this context, the available data used in this study is given below:

- Monthly precipitation data of the years between 1978 – 2015 obtained from Güzelyurt, Zumrutkoy, Lefke, Gaziveren and Yesilirmak stations; of the years between 2002 – 2015 obtained from Bostanci and Kalkanli stations and years between 1984 – 2015 from Kozankoy station
- A total of 73 borehole logs (lithological data) and coordinates
- Coordinates of total 67 observation wells, depths and water level measurements made during the rainy and dry seasons of different years. Not all of them have the same dates of measurements
- Digitized topographic and hydrogeological maps of the basin where Güzelyurt Aquifer is located
- Pumping test results in total of 5 wells and their coordinates
- The water budget data given in Gokmenoglu et al. (2002) and DSI (2003) reports and the hydraulic parameter values measured in a total of 6 wells

2.2.2. Conceptual Model Development

Development of a suitable conceptual model of the aquifer system is a precondition for developing a successful modeling work and therefore a numerical simulation model. The conceptual model in general terms is a study tool which helps to identify the internal and external boundary conditions, hydraulic and material properties of the aquifer media, boundary of the subsurface water system, groundwater flow and operation mechanism of the hydrogeological system. For development of the conceptual hydrogeological model, there is no widely accepted standard method due to the fact that the approach may be very much dependent on the specific characteristics of the studied aquifer. A general framework proposed by ASTM (2008) and Fanta (2015)is used in this study.

The initial conceptual model of the Güzelyurt Aquifer was developed by Fanta (2015) using the available field data. In this study, a digital elevation model (DEM) of the study area was created by using the existing topographic maps. Then the ArcGIS 10.0 hydrological modeling extension “ArcHydro Tool” was used to define the 3-D physical boundaries of Güzelyurt basin and the sub-basins. Secondly, using the existing hydrogeological maps, a base map of the project area was formed by differentiating and grouping the different geological units having aquifer characteristics. Finally, in the GIS environment, the general boundary and areal extent of the Güzelyurt Aquifer was determined by overlaying the DEM and the base map of the project area. The boundary of the aquifer consists of hydraulic (artificial) boundaries defined by topographic heights and formation boundaries defined by real physical boundaries. In order to determine the aquifer thickness distribution, 3-D block diagram sections were created by inputting 73 borehole data into Borehole module of GMS. In these preliminary evaluations made in the GMS environment, it was concluded that the aquifer can be described as a relatively homogeneous, isotropic, single layer, unconfined aquifer. There are discontinuous silt-clay lenses in the sand-gravel mixture with relatively lesser volume.

The conceptual model of the Güzelyurt Aquifer has been developed by attributing the geometry, boundary conditions and sources - sinks to the MAP module in GMS. The steps explained below indicates the components of the conceptual model.

2.2.2.1. Material Distribution: Solid Model and the Cross-sections

Within the scope of this study, the initial conceptual model developed from the preliminary studies have been further developed. In this context, more detailed interpolation/extrapolation studies have been conducted using GMS 10.2.3. “Conceptual Model Tools” and “Subsurface Analyst” modules, and the results have been checked with correlation analyzes of these extrapolations with the existing borehole log information.

The existing borehole data have been found inadequate to obtain the complete solid model of the aquifer. Because, in the areas where log information is missing, the interpolation applied to predict the material, resulted in inaccurate material distributions. Thus, some of the existing boreholes near the empty areas are cloned to represent the missing information. The actual and the copied boreholes are given in the Figures 2.7 and 2.8, respectively. The materials information along the mentioned boreholes’ depths are shown with the Figures 2.9 and 2.10.

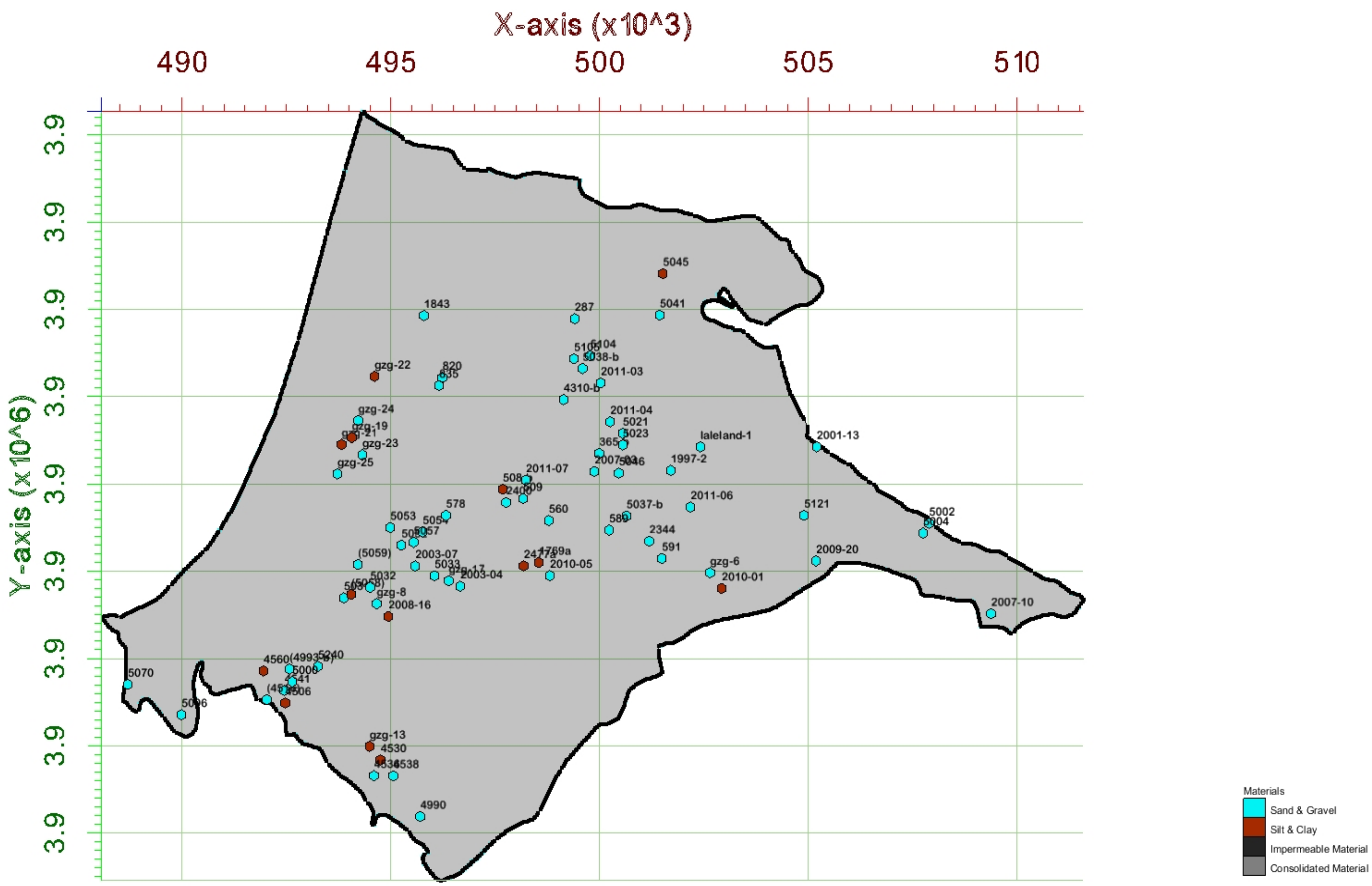

Figure 2.7. The available borehole data and their locations

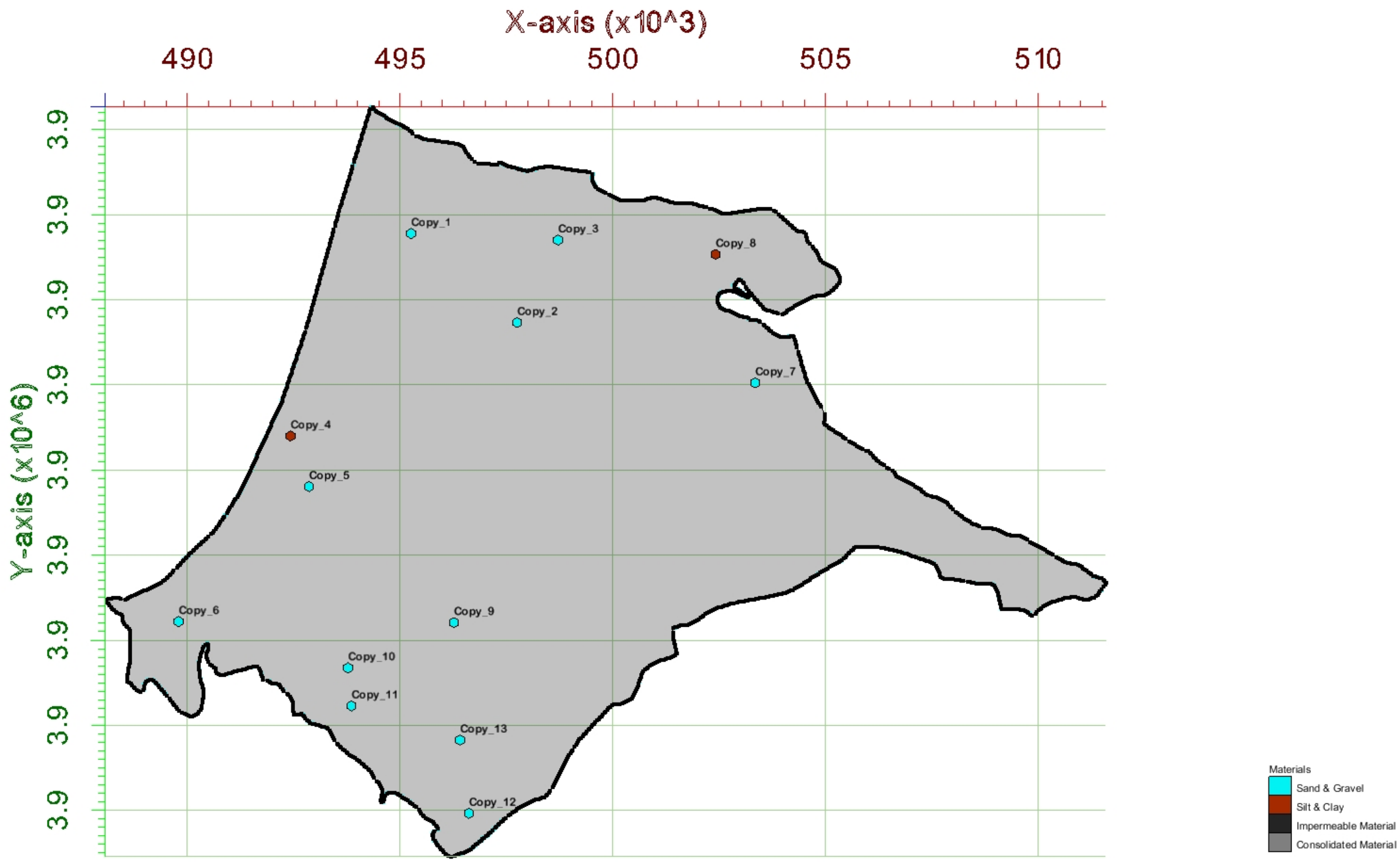

Figure 2.8. The clone boreholes to represent the areas where no log information exists

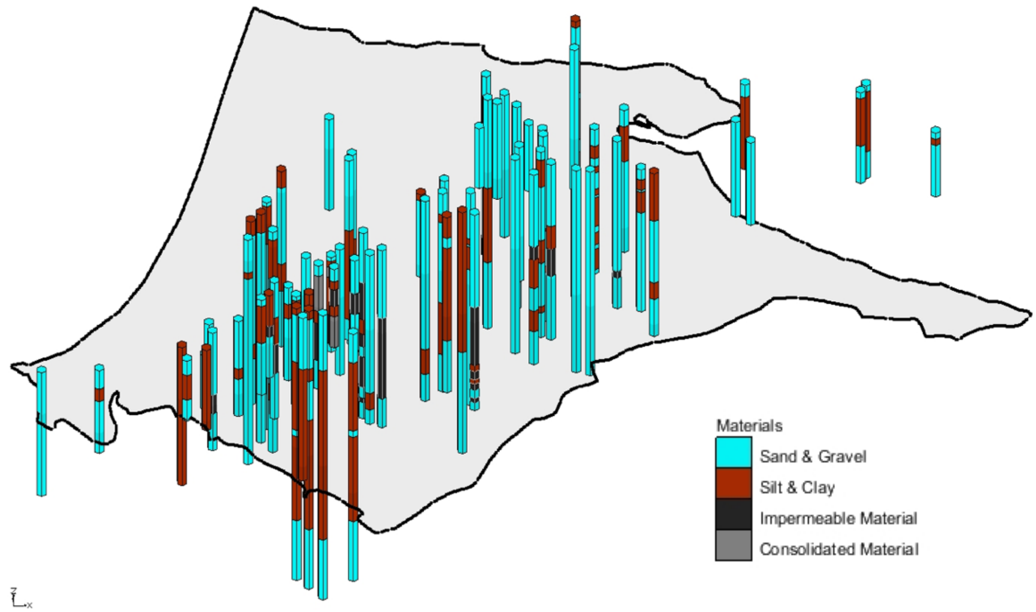

Figure 2.9. The lithological data view of the available boreholes

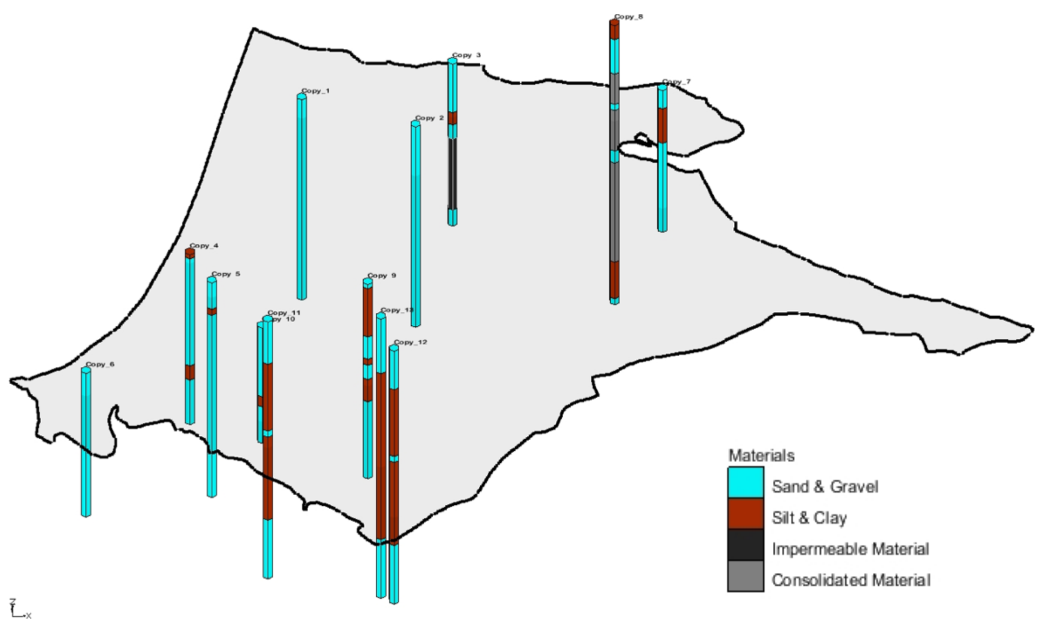

Figure 2.10. The lithological data view of the clone boreholes

In GMS, under the “Horizons to Solid” command in “Boreholes Module”, there comes several ways to create the solid model from borehole data. These are for example, creating solids with;

- the use of borehole cross-sections
- choosing the option “represent missing horizons implicitly”
- using different interpolation (inverse distance weighted and natural neighbor) and nodal function options (constant, gradient plane and quadratic)

Among the above options, the best result fitting the available borehole data was found with applying “represent missing horizons implicitly” option and using inverse distance weighted interpolation method with constant nodal functions. For the bottom elevation of the aquifer, the bottom of the boreholes would not give accurate results. Because, most of the wells have data finished at some depth which may not be the actual bottom. Therefore, the contour map shown in Figure 2.11 suggested by Ergil (2000) was digitized and converted into TIN format (Figure 2.13) to be able to use it in solid model construction. On the other hand, for the top elevation of the aquifer, the topographic data provided in “shape file” format was converted to TIN map (Figure 2.12) in GMS, and it was attributed during solid creation step.

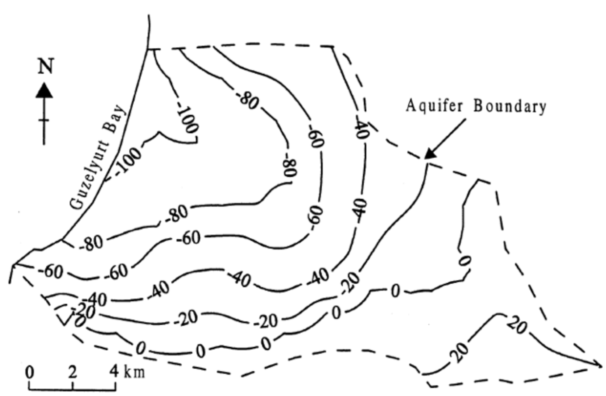

Figure 2.11. The contour map for the bottom elevation of Güzelyurt Aquifer (Ergil, 2000)

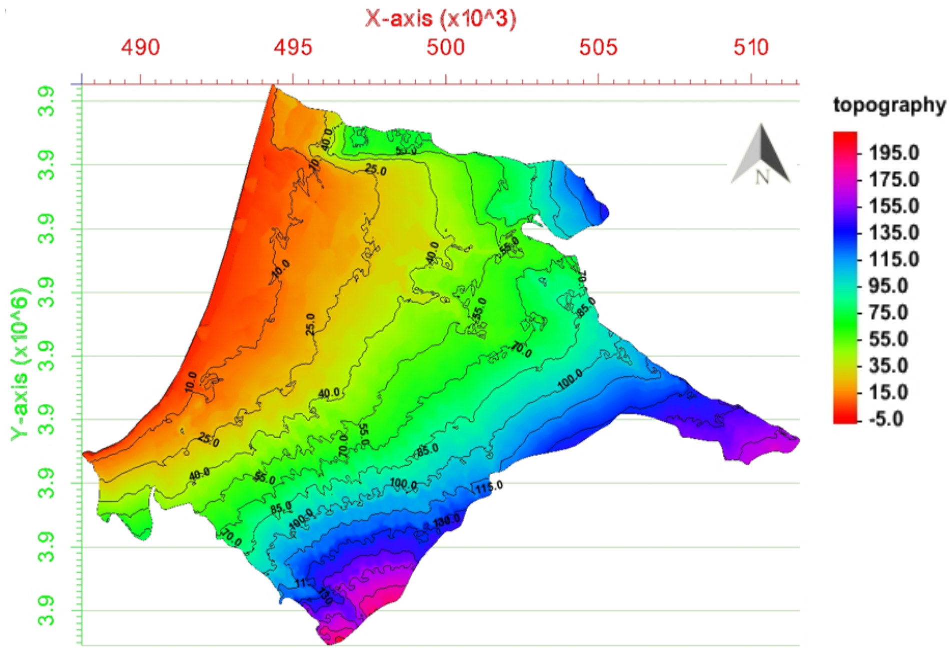

Figure 2.12. The topographic map of the Güzelyurt Aquifer

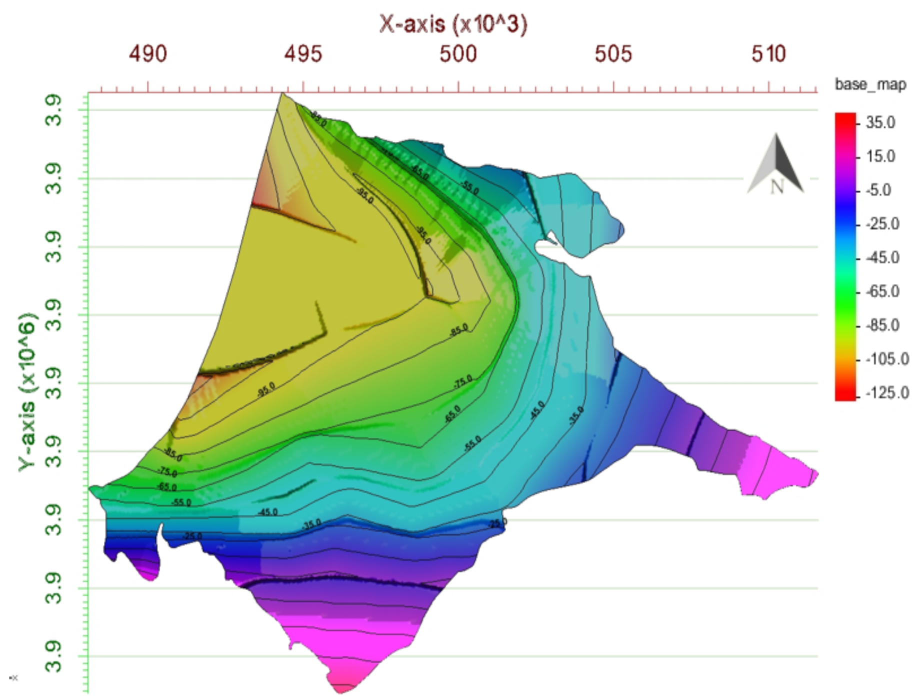

Figure 2.13. The digitized base map of Güzelyurt Aquifer

According to this, the improved 3-D block diagram's top, front and side views are depicted in Figures 2.14, 2.15 and 2.16, respectively.

The way of interpreting the developed solid model accurately is creating cross-sections. The cross-sections can be formed from the solid model itself by cutting it into intersects or form the borehole horizons by using Auto-filled borehole cross-sections allowing hand modifications. Both of the options were used to identify the material distribution that is closest to the reality. In Figure 2.17 (a), the views of borehole cross-sections and in Figure 2.17 (b) the solid model based sections are given.

As a result of this part of the study, it was seen that the localized silt-clay lenses are distributed in the subsurface. These lenses get closer to the surface near the coast. Since they are not continuous, the aquifer can be modeled as single layer. In the solid model created by Fanta (2015), the material diversities were simplified. In the present model, we see that there is silt-clay intensity through the south of the aquifer and in in the center very small amount of impermeable material in the center.

The aquifer material thickness varies between 60 m and 165 m from the east to the coast and between 110 m and 175 m from the south to the north.

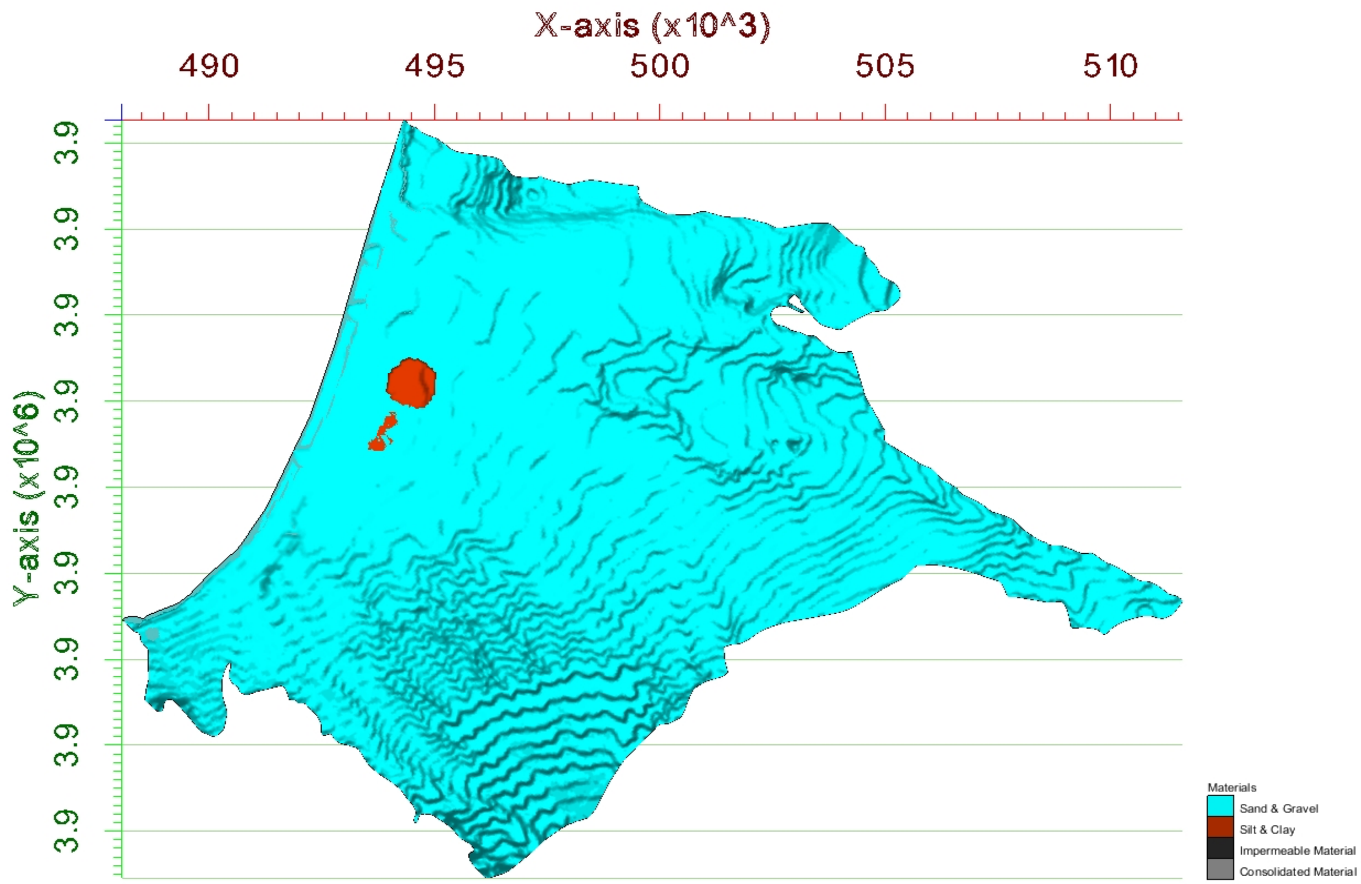

Figure 2.14. Solid model of the Güzelyurt Aquifer (Top View)

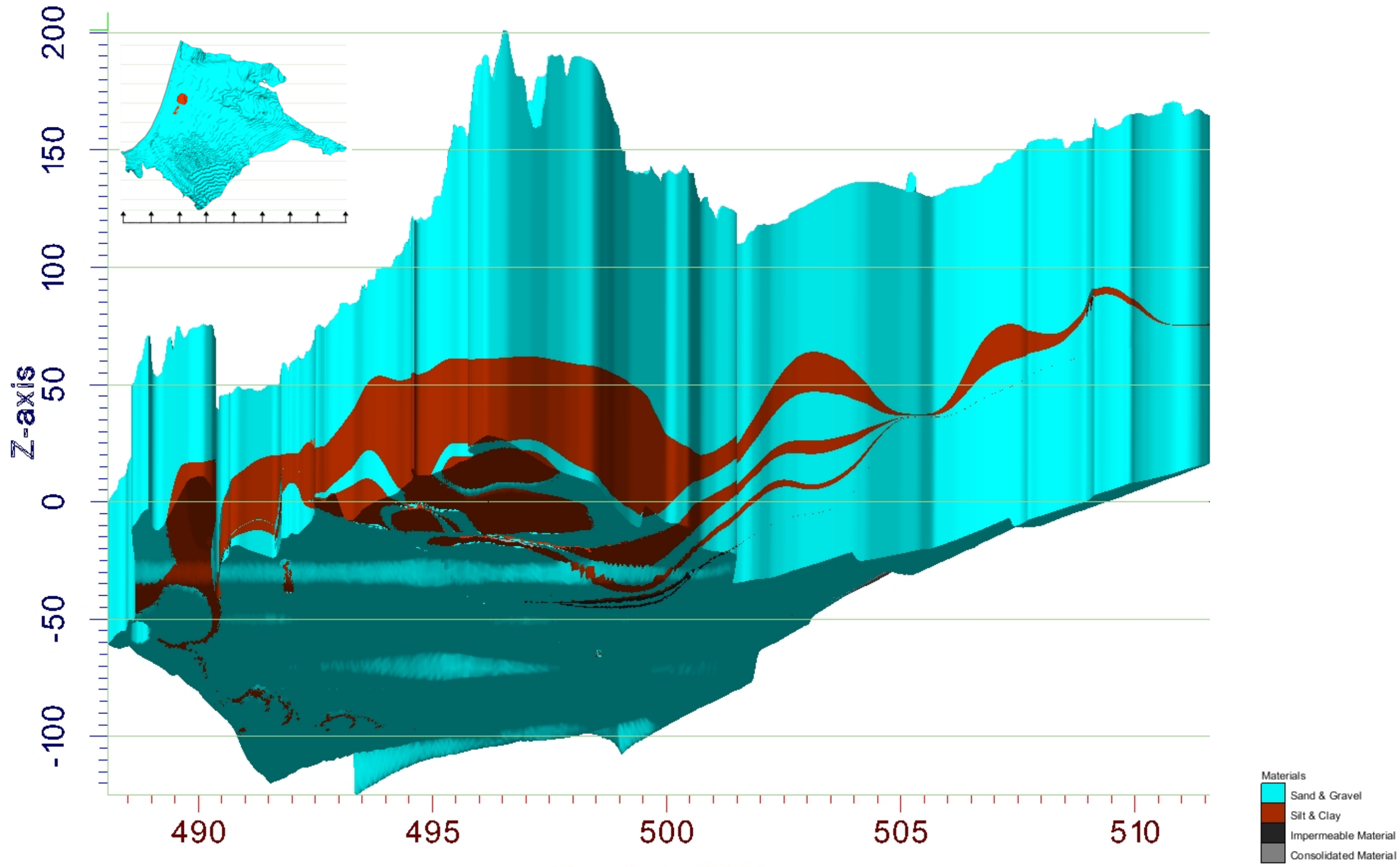

Figure 2.15. Solid model of the Güzelyurt Aquifer (Front View)

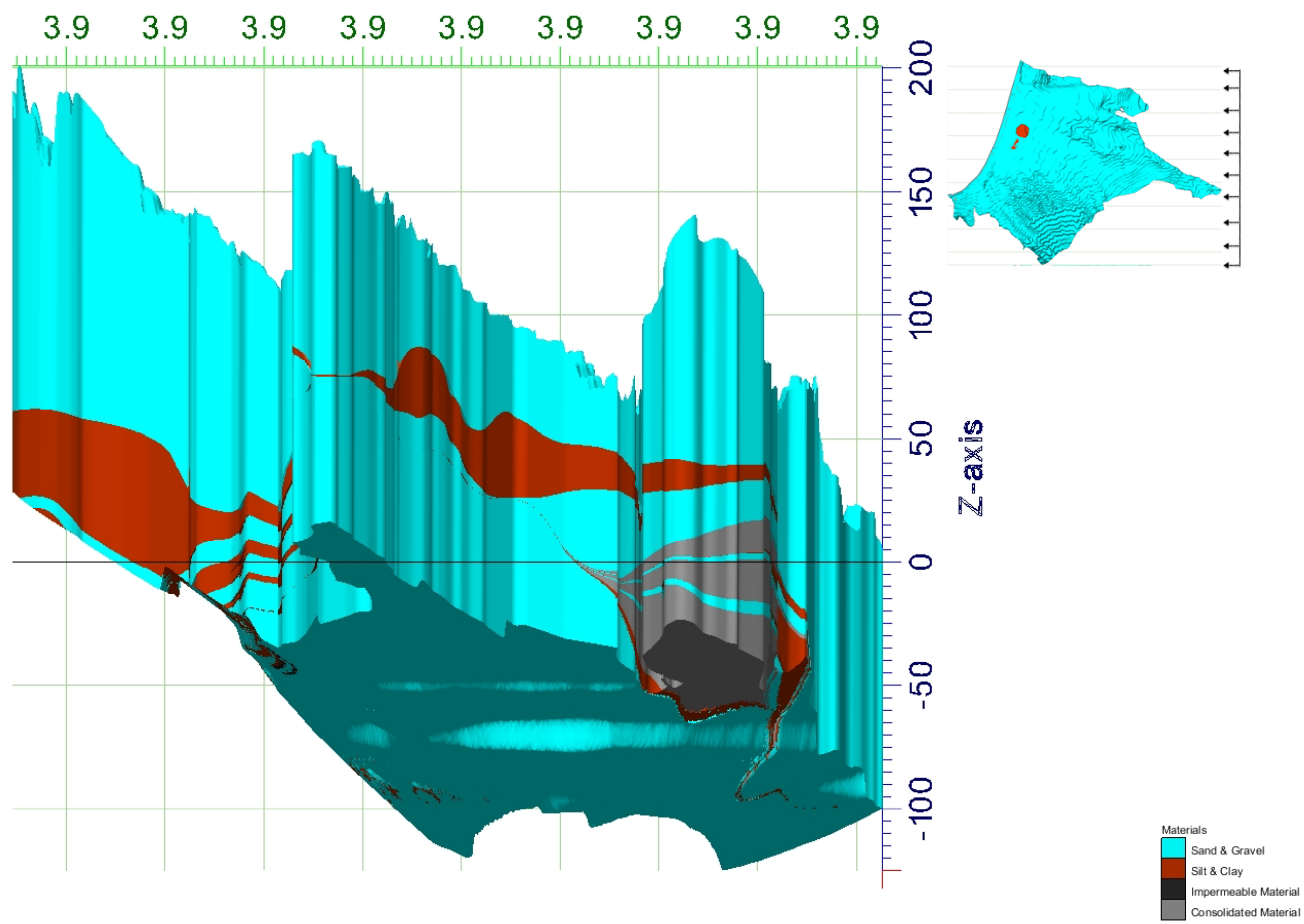

Figure 2.16. Solid model of the Güzelyurt Aquifer (Side View)

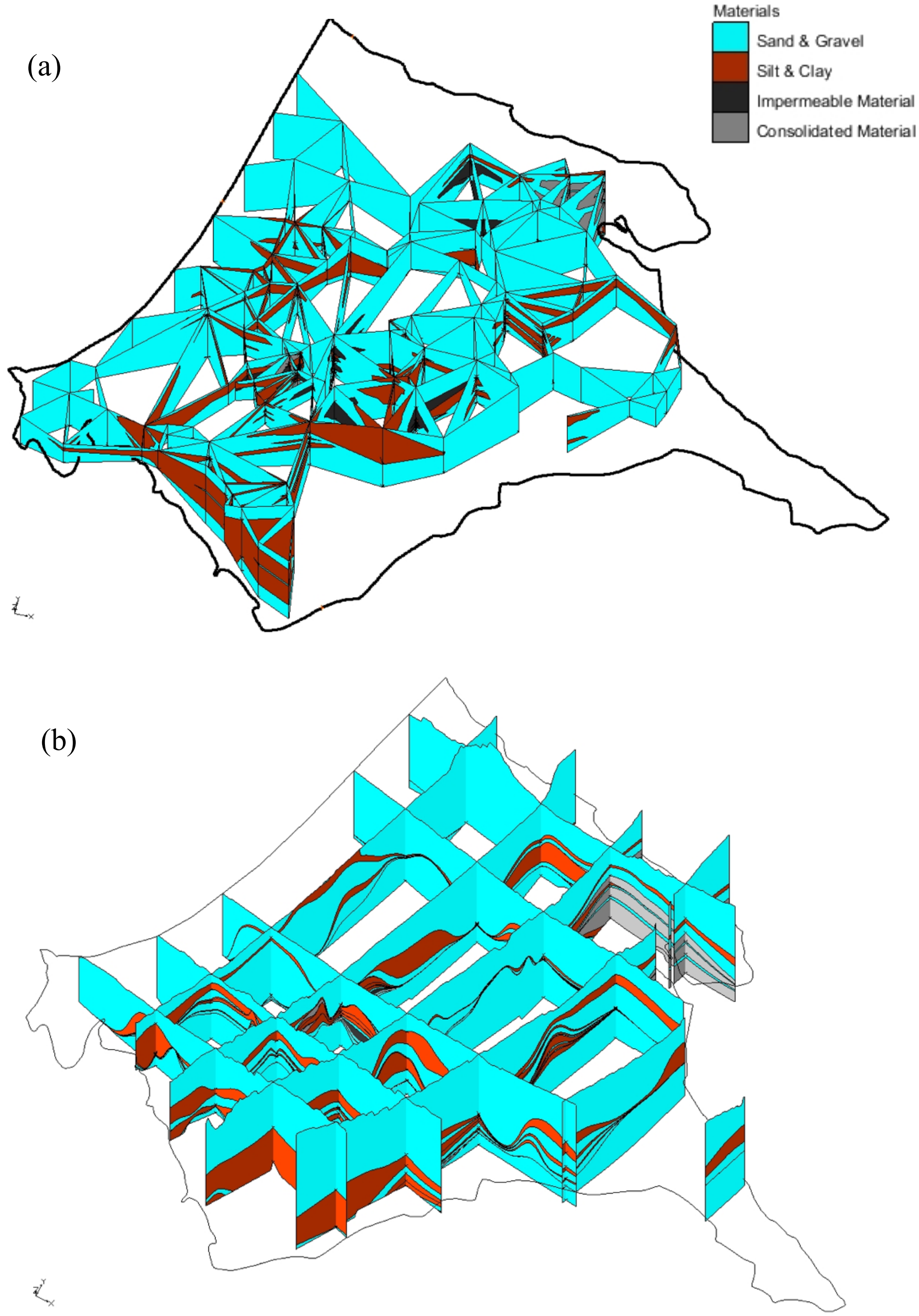

Figure 2.17. Cross-sectional representation of the material distribution
(a) created with auto-filled borehole cross-section command and manual edit
(b) solid model cuts

2.2.2.2. External Boundary Conditions

As another part of the conceptual model studies, the set of boundary conditions shown in Figure 2.18. suggested by Fanta (2015) was re-evaluated during the model development process and it was updated. In Figure 2.18, it can be seen that there are two groundwater divides due to topography. As shown in Figure 2.19, along the coastline, constant head boundary condition where zero "0" head was assigned.

In the southern part of the aquifer there is no data on such as lithology, groundwater head measurements and pumping activities. Therefore, considering the uncertainty in the incoming flow from the southern part of the aquifer, the country boarder was fixed as a General Head Boundary.

Although in Figure 2.18. the southwest and a part of the northeast boundaries were initially suggested as lateral flow boundary due to nearby formations, it was decided that only a small portion in the southwest line is receiving negligible flow. Therefore, this boundary was also assigned with General Head Boundary condition. This assumption has been made by evaluating the water level maps of different years. This analysis showed that the head contour lines becomes parallel to the boundary only in the mentioned part of the aquifer boundary. Thus, the remaining boundary lines (shown with black) where head contours are perpendicular to the boundary are assigned as no-flow boundaries. The working principles of boundary conditions used in our model were explained in section 2.2.3.4.

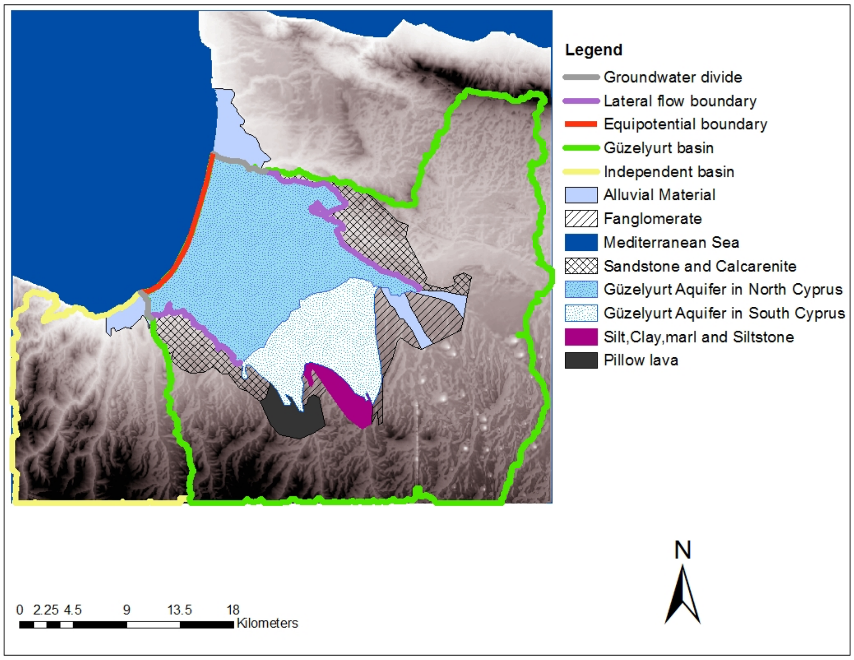

Figure 2.18. Boundary conditions suggested by Fanta (2015)

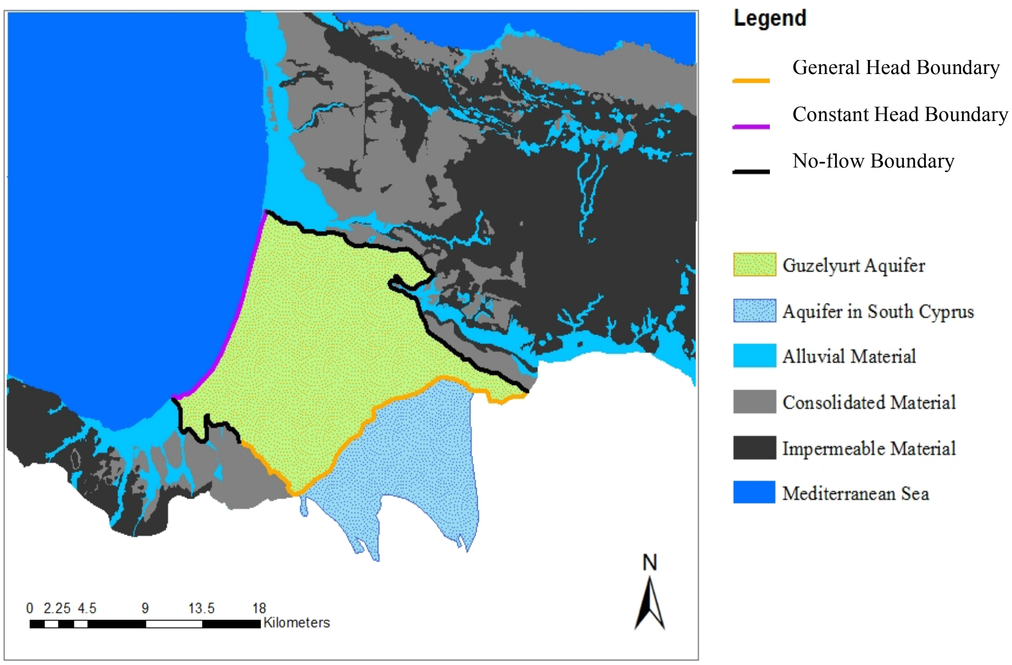

Figure 2.19. Boundary Conditions

2.2.2.3. Sources and Sinks

In addition to the the external boundary conditions, the recharge and discharge parameters were identified and attributed to the conceptual model which is to be transformed into numerical model.

According to the recent oral interviews with the responsible people in the departments, there are 53 drinking water wells of which 26 are in Kumköy, 2 are in Serhatköy and 25 are in Güzelyurt residential area. However, the Figure 2.20 is not showing all the up-to-date drinking well numbers. A part of them was abandoned due to salt water intrusion. And some of them were left because of pump failures caused by silt withdrawal since no graveling has been done. In addition to that, unfortunately, there is no data on which wells were being actively used and how much water was being extracted well by well. This limitation in data is the biggest problem of the model which affects the reliability of the results.

DSI (2003) states that the annual discharge from the aquifer due to the irrigational water extraction in the area is about 52 MCM. This number was an estimated value and its accuracy is doubtful.

Again according to DSI (2003), the drinking water extraction from Kumköy and Serhatköy pumping station is 8.7 MCM and from Güzelyurt residential areas is 4.6 MCM.

The limited data problem was tried to be overcome by dividing the total extraction amounts to an assumed number of wells (Figure 2.26) whose locations are approximated by considering all well locations and the agricultural lands given in Figure 2.20.

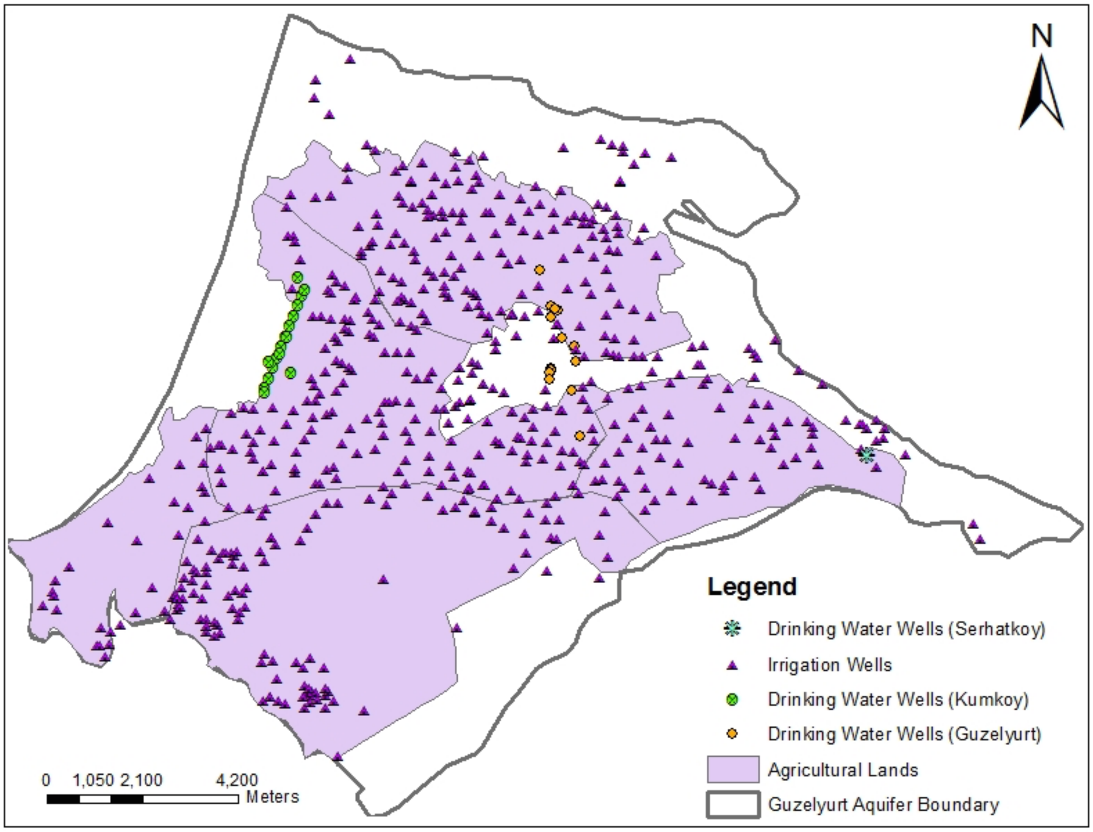

Figure 2.20. Distribution of pumping wells used for different purposes (This data is not showing the up-to-date distribution of the all wells and there is no information about which wells are actively used.)

Most of the recharge of the aquifer comes from precipitation. However, due to evapotranspiration 75% is lost and only 25% is available for infiltration (DSI, 2003). The monthly precipitation data collected in Güzelyurt station between the years 1978 and 2015 was used to create transient recharge data sets in our model. Figure 2.21. shows a sample annual rainfall data collected between 1992-2015. According to that, it can be referred that years are composed of dry and wet seasons, which are generally wet between October-April and dry from March to September. According to the statistical analysis conducted between 1992-2015, it was found that the average monthly rainfall is about 5 mm in a dry month and 39 mm in a wet month (Figure 2.21). The precipitation values are entered to the conceptual model, which is transformed to a numerical model, by multiplying them with the infiltration factor of 0.25.

The annual average rainfall was found to be 285 mm. The infiltration rate was calculated as given below and estimated as 12.8 MCM.

$$Rainfall \times Surface\ Area \times Infiltration\ ratio$$

$$= 285\ \frac{mm}{year} \times 180\ km^2 \times 10^6 \frac{m^2}{km^2} \times 10^{-3} \frac{m}{mm} \times 0.25$$

$$= 12.8 \times 10^6 \frac{m^3}{year}$$

Another source term is the recharge from streams, derivation channels and the southern part of the aquifer. According to the information given by DSI (2003), Fanta (2015) has given that approximately 17.4 MCM, 4.4 MCM and 5.2 MCM of water infiltrates through the aquifer annually form streams, derivation channel and the southern part of the aquifer, respectively. All the recharge and discharge data gathered can be summarized as in Table 2.1.

Table 2.1. Water budget of the Güzelyurt Aquifer

Recharge (MCM/year)		Discharge (MCM/year)	
Rainfall	12.8[a]	Irrigational Extractions	51.7[b]
Streams	17.4[a]	Drinking Water Extractions	13.3[b]
Lefke-Güzelyurt Derivation Channel	4.4[a]		
Southern Part of the Aquifer	5.2[a]		
TOTAL	**39.8**	**TOTAL**	**65**

[a] (Fanta, 2015)

[b] values of DSI (2003), updated by TRNC Geology and Mining Department

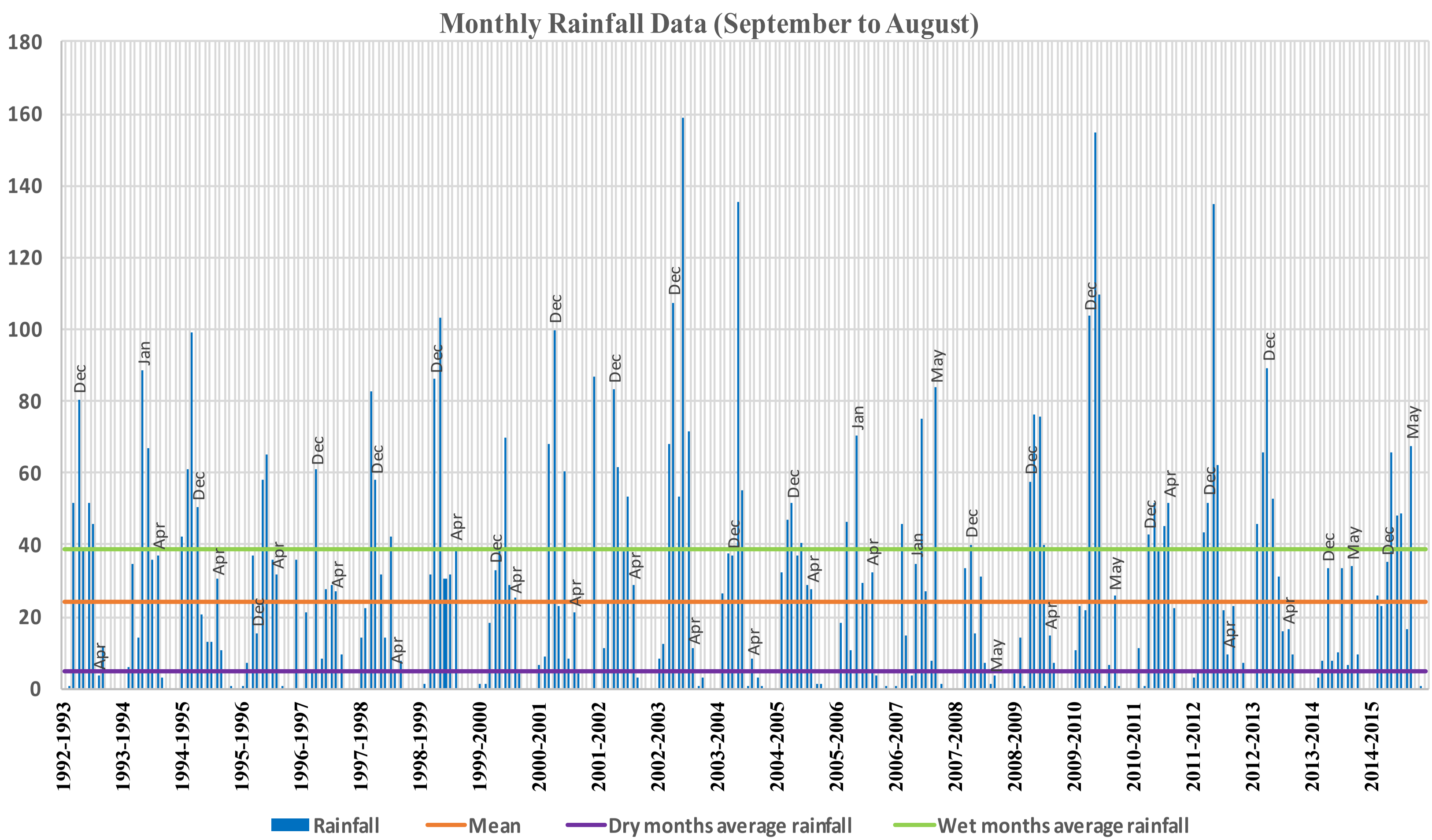

Figure 2.21. Monthly rainfall data recorded at Güzelyurt Station between 1992-2015

2.2.2.4. Transmissivity Field Data

Gathering and defining the required parameter values to set up an accurate groundwater model is not an easy task. Some data can be obtained in between the lines written in existing reports, but generally an additional on-site field work for data collection is needed. The transmissivity and storage coefficient values are typically obtained from pumping test results. If a vertically averaged hydraulic conductivity values will be used to model a local scale aquifer system, these values can be estimated with the pumping tests. The specific yield coefficients measured in the pumping test analysis are subjected to error (Anderson et al., 2002). Therefore, it is better to determine them in the calibration analysis by paying attention to value ranges given in literature for unconfined alluvial aquifers.

The pumping test is done by recording the hydraulic head changes (well drawdown) in a monitoring well in response to extracting water from a pumping well which is located nearby. With this approach, a relationship between the stress and the hydraulic head changes can be set. This relationship can be expressed by several analytical equations which enable an indirect calculation of the hydrogeological parameters such as transmissivity and storage properties (Kresic, 2007).

There are to main approaches for the analysis of the monitored drawdown data: (1) type curve matching (2) inverse modeling. The former is the most commonly used method in determining the hydrogeological properties. There are several curve matching methods developed for different cases, but all in a way based on the pioneering study conducted by Theis (1935). Because the Theis equation has no explicit solution, a graphical method (Figure 2.22) which estimates T and S values for each monitoring well drawdown data for a confined homogenous isotropic aquifer system was introduced by Theis (Kresic, 2007). Theis equation giving the drawdown at any time after the start of pumping is:

$$s = \frac{Q}{4\pi T} W(u) \quad \textbf{\textit{(Eqn. 2.1)}}$$

$$u = \frac{r^2 S}{4Tt} \quad \textbf{\textit{(Eqn. 2.2)}}$$

where

Q : pumping rate kept constant during the test (L^3/T)

T : transmissivity (L^2/T))

$W(u)$: well function of u

r : distance from the pumping well

S : storage coefficient

t : time since the beginning of pumping

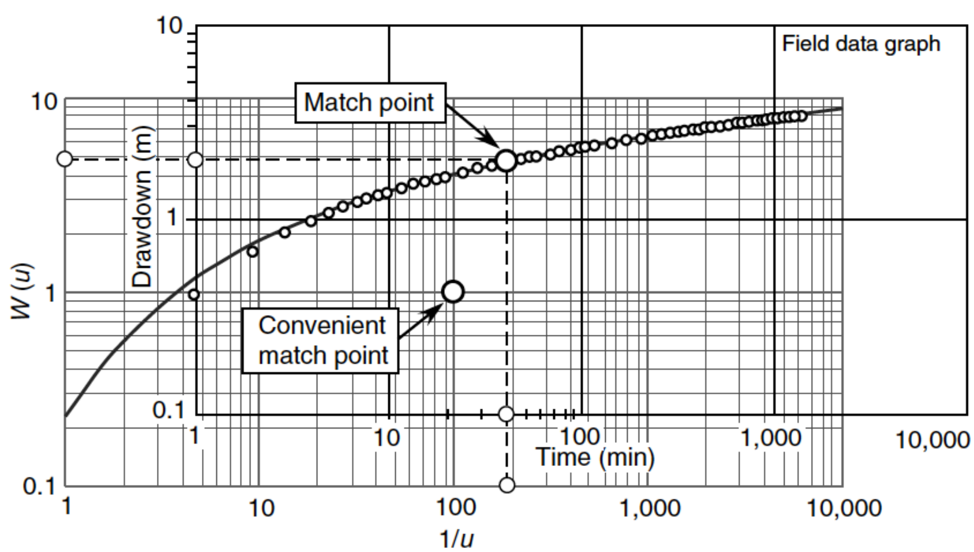

Figure 2.22. A sample curve matching by Theis type curve method

With some small modifications the Theis equation can also be used to determine parameters for unconfined aquifers. Various analytical methods have been continuously developed to serve for different situations such as leaky aquitards, aquifer anisotropy etc.

For drawdowns that are in between 10% and 25% of the aquifer's pre-pumping thickness, the measured data can be corrected using the equation (Eqn. 2.3) derived by Jacob (1963). For drawdowns which are less tan 10% of the saturated thickness, it is not necessary to correct the monitored drawdown data, because the resultant error by using the Theis equation is small (Kresic, 2007). In this study, even if the measured drawdown values are way below 10% criteria, the parameter results found by applying Theis with Jacob Correction method was preferred. However, both analysis (with and without corrections) gave almost the same numbers.

$$s' = s - \frac{s^2}{2h} \qquad \textbf{\textit{(Eqn. 2.3)}}$$

where

s' : corrected drawdown (L)

s : measured drawdown in a monitoring well (L)

h : saturated thickness of the unconfined aqufer before pumping started (L)

In this study, in addition to the Theis with Jacob Correction, the Neuman (1975) method was also applied. This method allows the estimation of the hydrogeologic parameters in anisotropic unconfined aquifers when drawdown response fails to follow the typical Theis solution. When drawdown versus time graph plotted on logarithmic paper, if the curve shows a steep section during early stages, a flat section during intermediate stages and steeper section at later stages, then one can say that there is a delay in drawdown response. (Kresic, 2007) However, in this study, the plots did not show any of these situations. Therefore, at the end it was decided that the Theis with Jacob Correction is the best suited method for the Güzelyurt aquifer case.

Both methods are included in Aquifer Test Pro software. The application of these methods to the Güzelyurt aquifer system and the results were presented and analyzed in section 3.1.

2.2.3. Numerical Model Development

Numerical aquifer simulation model generally consists of three major components namely, mathematical equations that define water flow processes, computer software that performs the solution of these equations, and application of this software on a defined tangible groundwater problem. In this study, the numerical simulation model was created using the MODFLOW-USG module in GMS 10.2.3.

In order to make the model ready for the simulations in GMS, first, an appropriate grid system must be designed. Then, the conceptual model is transformed into MODFLOW-USG.

Upon creation of the numeric grid with all boundary conditions and input values assigned, of the unknown/uncertain parameters or boundary conditions can be estimated by calibration process which can be implemented through trial and error or by automatic parameter estimation tools. Then, the model can simulate the system behavior and can be used to predict future scenarios.

The boundary condition packages used in the model are General Head Boundary Package (GHB), Constant Head Boundary Package, Well (WEL) Package and

Recharge Package (RCH1). For the flow package Layer Property Flow (LPF) was employed.

2.2.3.1. A Tool for Numerical Groundwater Modeling: MODFLOW

The regional groundwater flow system investigations are widely done by the utilization of 3-D models. Before the development of MODFLOW, the 2-D and 3-D finite difference models were used by the US Geological Survey (USGS). MODFLOW modular finite difference flow model was first developed in 1984 by USGS. After the first update released in 1988, in the early 1990s, it had already received a great attention not only by the US, but also from the rest of the World, and it eventually became the most extensively used groundwater flow model because of its flexible modular structure, comprisal of all natural hydrogeological processes and the most importantly its being an open source model (Harbaugh, 2005). Developers have created several interfaces for the commercial use of this code. The most extensively used ones are Processing Modflow, Visual Modflow, Groundwater Modeling System (GMS) and Groundwater Vista. The interfaces developed made the modeling work easier and faster. Especially, with the integration of Geographical Information System platform, interpretation and the representation of the results were improved (Zhou et al., 2011).

The model has the capability to simulate 2D areal / cross-sectional, and quasi- or fully 3D flow in anisotropic, heterogeneous, layered aquifer-systems. The spatial discretization within the model structure is done by the block centered finite difference approach. There are several solver types that are available within the body of the model; Direct Solution (DE45), the Preconditioned Conjugate Gradient 2 (PCG2), the Strongly Implicit Procedure (SIP) and the Slice Successive Over Relaxation (SSOR) (Mederer, 2009).

The MODFLOW structure contains a main program and a series of independent subroutines which are called packages. There are different packages within the modular structure solving for various specific hydrologic/hydrogeological system components, such as rivers, lakes, boundary conditions etc. (Harbaugh, 2005).

2.2.3.2. Unstructured Grid with MODFLOW-USG

The standard MODFLOW versions (Modflow-88, Modflow-96, Modflow-2000 and Modflow-2005) all depend on the rectangular finite-difference grid technique. However, there are two important limitations of this approach. Firstly, the use of rectangular grid system does not allow to fit the grid within irregular sharped model boundaries (See Figure 2.23). An unstructured grid can be a typical MODFLOW rectangular shaped grid, a set of nested rectangular grids, or in the shape of triangles, hexagons, irregular shapes or combination of all. This offers a great flexibility. Secondly, it is impossible in standard Modflow structured grid system to refine the grid resolution only in the areas where more detailed and accurate solutions are expected (wells, external boundary conditions etc.). The users are supposed to apply the refinements manually on the grid and most probably it will result in the refinement of unwanted areas. This will increase the computational time. But in unstructured grid (UGrid) concept used with Modflow-USG, the specific areas can be pre-defined in the coverage and when it is converted to UGrid, only the specified regions will be refined. In addition to this, in unstructured grid system approach, it is possible that different layers can be sub-discretized differently in the vertical direction. For instance, as in the case of Güzelyurt Aquifer, an aquifer within which distributions of random discontinuous non-aquifer material occurs can be represented by a grid structure as shown in the Figure 2.24 (Panday et al., 2013).

In the finite difference formulation of structured grid system with standard MODFLOW, a set of matrix formulations showing a fixed pattern of non-zero attributes are created. For example, for a given cell (i,j), the neighbors (i+1, j), (i-1, j), (i, j+1), (i, j-1), (i-1, j-1), (i+1, j+1) and so on are automatically defined. The unstructured approach does not depend on a fixed pattern and this allows to set random number of connections between cells which are identified through an explicit connectivity table. The key advantage of the UGrid design is that a single matrix for all of the grids is solved to determine the groundwater flow. This ability helps, especially in complex problems, to achieve convergence with less number of iterations (Liu et al., 1998) (Panday et al., 2013).

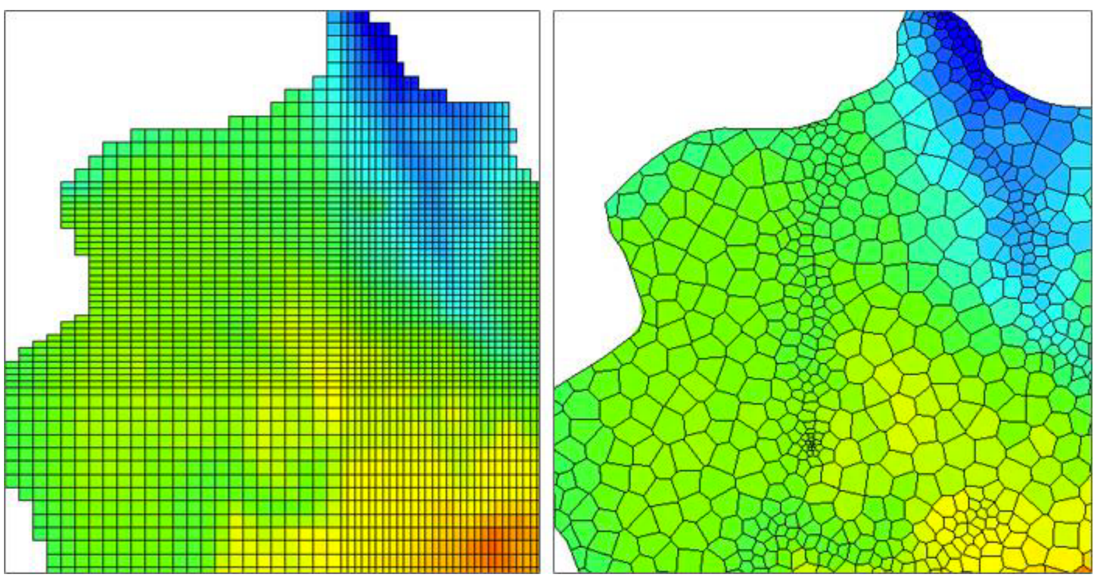

Figure 2.23. Structured finite difference MODFLOW-2005 grid (left), and an UnStructured grid with Voronoi cells for MODFLOW-USG grid (right) (Waterloo Hydrogeologic, 2013)

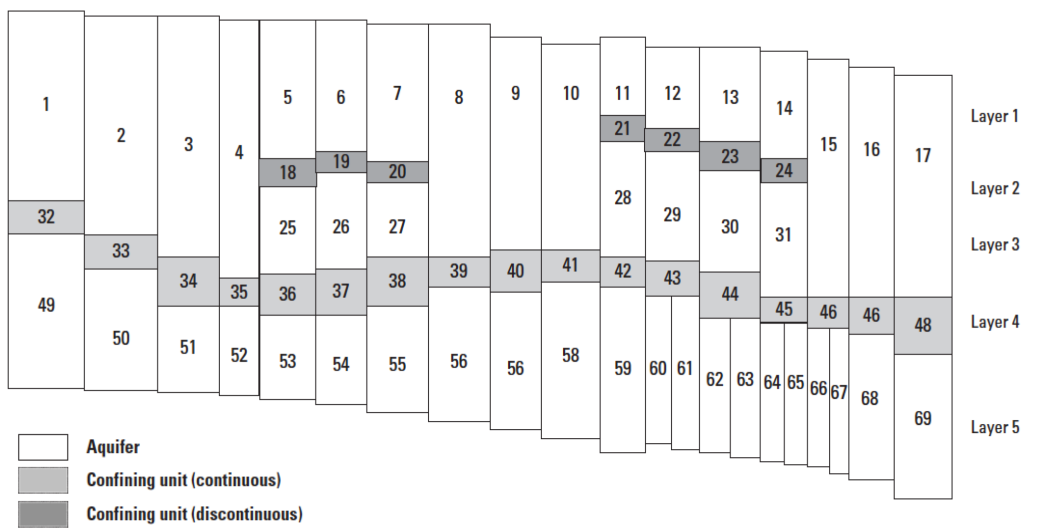

Figure 2.24. The unstructured grid configuration of an aquifer with continuous and discontinuous confining units (Panday et al., 2013)

In the study explained in this thesis, a Modflow interface of GMS version 10.2.3 have been used to develop both conceptual and numerical model. For the grid system, unstructured grid approach has been employed.

2.2.3.3. Mathematical Descriptions

Transient flow of groundwater in a heterogeneous anisotropic 3-D aquifer can be described by the following partial differential equation:

$$\frac{\partial}{\partial x}\left(K_{\mathrm{xx}}\frac{\partial h}{\partial x}\right)+\frac{\partial}{\partial y}\left(K_{\mathrm{yy}}\frac{\partial h}{\partial y}\right)+\frac{\partial}{\partial z}\left(K_{\mathrm{zz}}\frac{\partial h}{\partial z}\right)+W=S_{\mathrm{s}}\frac{\partial h}{\partial t} \qquad \textit{(Eqn. 2.4)}$$

where

K_{xx}, K_{yy} and K_{zz}	: Hydraulic conductivity values in the x, y and z directions (L/T)
h	: Potentiometric head (L)
W	: volumetric flux / unit volume representing sources and/or sinks of water (1/T)
S_s	: Specific Storage of the porous material (L^{-1})

The unstructured grids can be solved by finite element or finite differences methods. MODFLOW-USG offers a numerical scheme for tightly coupling multiple hydrologic processes. The concept of tight coupling is indicated with a formulation of global conductance matrix which can be symmetric or asymmetric. In MODFLOW-USG, the global conductance matrix is unstructured which means that each individual cell can have an arbitrary number of connections with other surrounding cells. A formulation called CVFD is used to define this unstructured numerical scheme (Panday et al., 2013). The general form of the CVFD balance equation, which is a rearranged form of Equation 1, for a cell numbered with "n" is given as follows:

$$\sum_{m\in\eta_n} C_{nm}(h_m - h_n) + HCOF_n(h_n) = RHS_n \qquad \textbf{\textit{(Eqn. 2.5)}}$$

where

C_{nm} : Inter-cell conductance between cells n and m

h_n & h_m : Hydraulic heads at cells n and m

$HCOF_n$: sum of all terms that are coefficients of h_n in the balance equation for cell n

RHS_n : The right-hand-side value of the balance equation

$\sum_{m \in \eta_n} C_{nm}(h_m - h_n)$: summation over all cells (m) that are an element of the set of cells that are connected to cell n (η_n)

In unconfined aquifers as in our case, for the groundwater flow between two cells, C_{nm} is dependent on the hydraulic head values in both cells n and m. The term $HCOF_n$ indicates the changes in storage and boundary fluxes which are relied on h_n. Moreover, the terms related to storage and/or boundary conditions form the term RHS_n (Panday et al., 2013). The C_{nm}, $HCOF_n$ and RHS_n terms are expressed as;

$$C_{nm} = \frac{a_{nm} K_{nm}}{[L_{nm} + L_{mn}]} \quad \textbf{\textit{(Eqn 2.6)}}$$

$$RHS_n = \frac{-SS_n V_n h_n^{t-1}}{\Delta t} \quad \textbf{\textit{(Eqn.2.7)}}$$

$$HCOF_n = \frac{-SS_n V_n}{\Delta t} \quad \textbf{\textit{(Eqn. 2.8)}}$$

where

$a_{nm}(= a_{mn})$: perpendicular saturated flow area between cells n and m (Figure 2.25)

K_{nm} : inter-cell hydraulic conductivity between cells n and m

L_{nm} and L_{mn} : the perpendicular distances between the shared n-m interface (Figure 2.25)

$t - 1$: previous time step

Δt : time step size

SS_n : specific storage of the cell. It means the volume of water that can be injected per unit volume of aquifer material per unit change in head

V_n : volume of cell n

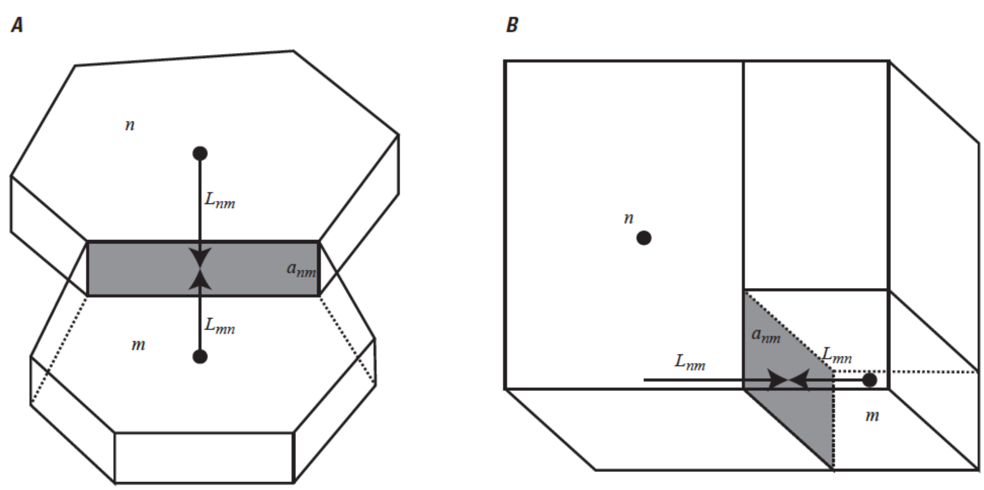

Figure 2.25. Illustration of the cell connection (Panday et al., 2013)

Equation 2.5 is solved in the model in the form of a matrix $Ah = b$ where, A is the global conductance matrix, h is the vector of hydraulic heads and b is the RHS vector. In unconfined aquifer solutions, the matrix becomes non-linear. Therefore, Picard iterative solution technique, where in each iteration the global conductance matrix is changed using previous iteration's head values, is used recurrently to solve the matrix until the convergence criteria is met. In MODFLOW-USG, other than Picard approach, Newton-Raphson solution approach is also provided to enhance the solution of the unconfined problems (Panday et al., 2013).

2.2.3.4. Numerical Modules/Packages Used

In this study, in order to simulate the internal and external conditions explained in part 2.2.2.2. and part 2.2.2.3., head-dependent flux (formation and country boarder), constant head (coast line), recharge and well packages were used. Their working principles are explained below.

General Head Boundary Package

General head boundary (GHB) package in MODFLOW is used to simulate head-dependent flux boundaries. In this type of boundary, the flow is always proportional to the change in the head (Winston, 2018).

The modular structure uses a parameter called "conductance", which is represented based on the hydraulic conductivity values and the geometrical features, to calculate the amount of water flowing through the model units in general head, river, stream and drain type time dependent variable head/flow conditions (Mederer, 2009).

General head conditions are defined by assigning head values and a conductance to a selected set of cells. If the groundwater level rises above the specified head, water flows out of the aquifer. If the water table elevation falls below the specified head, water flows into the aquifer. In both cases, the flow rate is proportional to the head difference and the constant of proportionality is the conductance.

Darcy's law states that:

$$Q = kiA = K\frac{\Delta H}{L}A \qquad \textbf{\textit{(Eqn. 2.9)}}$$

where

Q : Flow rate (L^3 / T)

K : Hydraulic conductivity (L / T)

i : Hydraulic gradient (L / L)

A : Gross cross-sectional area of flow (L^2)

ΔH : The head loss (L)

L : The length of the flow (L)

When the parameters besides the unknown "head" are grouped in the right hand side of the Eqn. 2.9:

$$Q = C\Delta H \qquad \textbf{\textit{(Eqn. 2.10)}}$$

where

C : Conductance (L^2 / T)

The Eqn. 2.10 results in the following general definition for the conductance term:

$$C = \frac{K}{L}A = \frac{K}{t}lw \qquad \textbf{\textit{(Eqn. 2.11)}}$$

where

t : The thickness of the material in the direction of flow (L)

lw : The cross-sectional area perpendicular to the flow direction (L^2)

In GMS, the lengths of the arcs and areas of polygons are calculated automatically. Hence, the conductance value defined in the conceptual model step is entered in terms of conductance per unit length. As the GMS converts the defined conceptual model to a grid cell, it automatically multiplies the entered value of conductance with the lengths/areas of the arc/polygon. The following equations (Eqn. 2.12 & Eqn. 2.13) show the conductance parameter calculation for arcs and and polygons.

$$C_{\text{arc}} = \frac{\frac{K}{t} lw}{L} = \frac{K}{t} w \qquad \textbf{\textit{(Eqn. 2.12)}}$$

$$C_{\text{poly}} = \frac{\frac{K}{t} lw}{A} = \frac{K}{t} \qquad \textbf{\textit{(Eqn. 2.13)}}$$

where

C_{arc} : conductance per unit length [(L^2/T) / L] or (L / T)

C_{poly} : conductance per unit area [(L^2/T) / L^2] or (1 / T)

t : the thickness of the material (L)

w : The width of the material along the length of the arc (L)

Constant Head Boundary:

This type of boundary condition occurs where a part of the boundary come across with a surface of which the head is uniform at all the points throughout the surface and also through time. Reservoir, lake, sea and ocean boundaries formed with the aquifers can be modeled with this type of boundary condition (Franke et al., 1987). The Constant Head boundary condition fixes the head values in defined grid cells paying little respect to the system conditions in the encompassing grid cells, consequently acting as an infinite source of water flowing into the system, or as an infinite sink for water leaving the system (Schlumber Water Services, 2011).

In GMS, the constant head cells are defined with the use of IBOUND arrays. In order to do this, the Specified Head (IBOUND) package is used, for the constant head cells a negative value (-1) is assigned in the IBOUND array. The values of constant head are defined in the starting heads array. In our model, the cells along the sea boundary were assigned with constant head value of zero "0" meter.

Recharge (RCH) Package:

The recharge package is utilized to simulate a specified flux to an aquifer due to rainfall and infiltration. The recharge value indicates the amount of water going through the aquifer system, not the amount of precipitation. Therefore, it has to be multiplied by an infiltration ratio. The recharge values assigned to the model have a unit of length/time.

The recharge package can be also used to include flow into the aquifer from streams, rivers and lakes if they can not be assigned with another package (Winston, 2018). In this study, the infiltration due to the streams and surface water structures were added on top of the recharge value which is due to precipitation.

Well (WEL) Package:

This package is used to simulate a specified flux (length^3/time) to the cells covered by the wells. The wells can be either extraction or injection wells. In the extraction case, the flow rate entered has to be a negative value while in the injection case, it should be positive.

Layer Property Flow Package

LPF package is one of the two packages in MODFLOW-USG that can be used to simulate flow in saturated zone. In this package there are two layer types: confined and convertible. The convertible layer can be either confined or unconfined depending on the elevation of the computed water table. In this study, due to the unconfined characteristic of the aquifer system, convertible layer type has been preferred.

2.2.3.5. Numerical Grid Design

In numerical models, the domain of the defined hydrological/hydrogeological problem is represented with a discretized system, called grid. There are two commonly used grid types: structured and unstructured grids (Oude Essink, 2000). In this study, due to its flexibility (explained in section 2.2.3.2) in designing the domain, the unstructured grid system has been used.

In the light of the judgments made according to the material distribution in section 2.2.2.1., Güzelyurt aquifer was modeled with 1 layer where the system behaves as a 2-D problem and hydraulic conductivity values are vertically averaged.

The Güzelyurt Aquifer’s grid system is projected at UTM, Zone: 36 (30°E - 36°E - Northern Hemisphere) in European Datum 50 (ED50). The length unit used in the whole system is in meters. The 1-Layer Unstructured QuadTree type grid system was created in GMS with an X origin of 488066.0 m, a Y origin of 3884914.4 m and a Z origin of -125.4 m. The total number of 3-D grids in the X, Y and Z dimensions is 39658. The width of the cells is 100 m in the X and Y direction while it can decrease up to 10 m in the refined areas such as boundary conditions and pumping wells (Figure 2.26). The height of the cells changes with the thickness of the aquifer.

In this study, as an interpolation technique, the inverse distance method has been used when needed such as in solid model creation and in assigning parameter values to the grids.

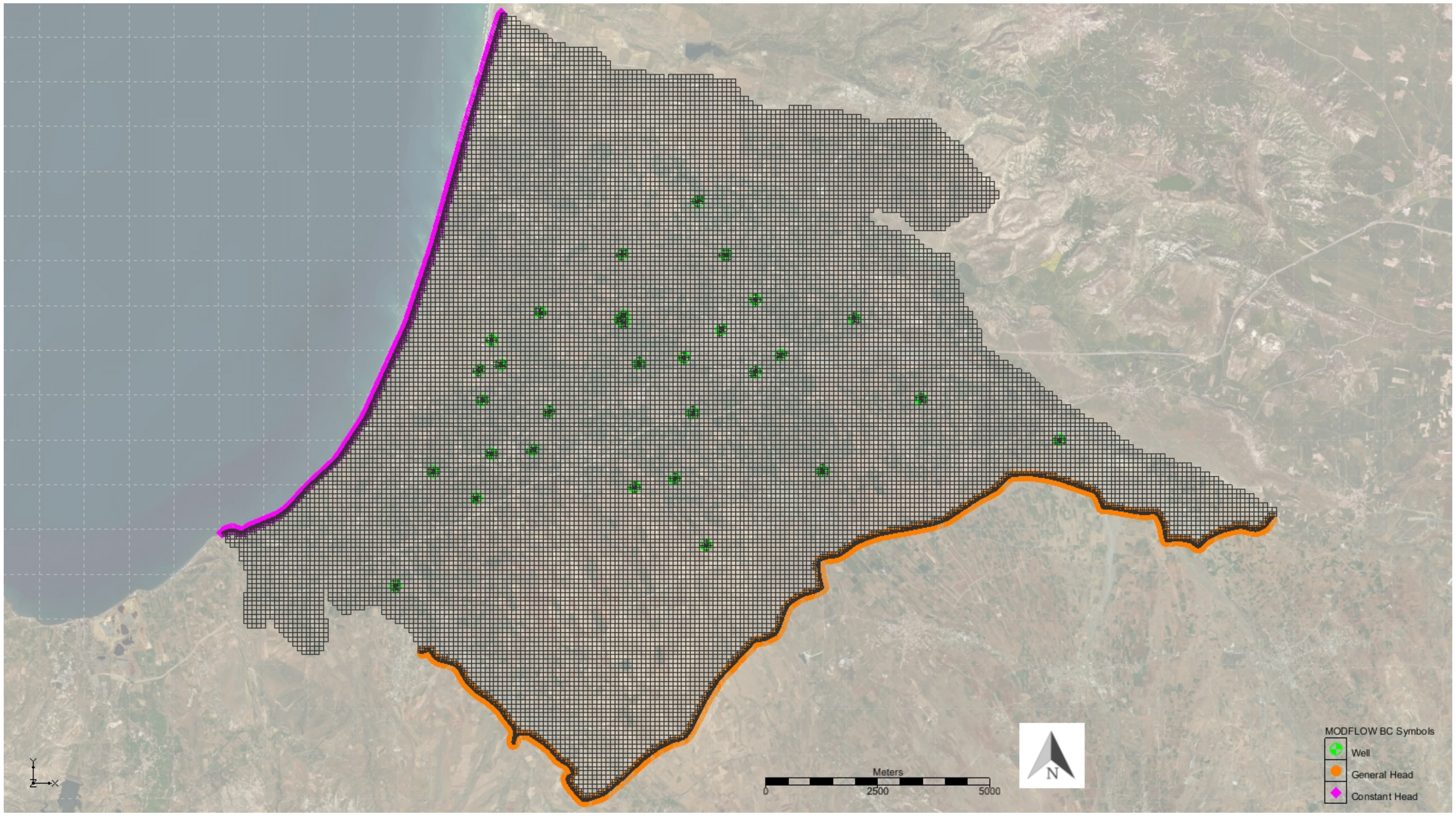

Figure 2.26. The active numerical grid cells for the Güzelyurt Aquifer Model. The constant head cells along the coast and the general head boundary cells are shown with pink and orange, respectively. The proposed pumping wells are colored with green.

CHAPTER 3

RESULTS AND DISCUSSIONS

3.1. Pumping Test Data Analysis

Hydraulic parameters constitute important input data for numerical model applicaitos. Hydraulic conductivity values of Güzelyurt Aquifer have been estimated using pumping test data of 5 pumping wells, which are provided by TRNC Geology and Mining Department. The analyses of pumping test data have been carried out using the Aquifer Test Pro software to estimate the transmissivity values and in turn, hydraulic conductivity values by dividing the transmissivity with aquifer thickness. The locations of the five pumping wells and their observation wells in the aquifer are given in Figures 3.1 and 3.2, respectively.

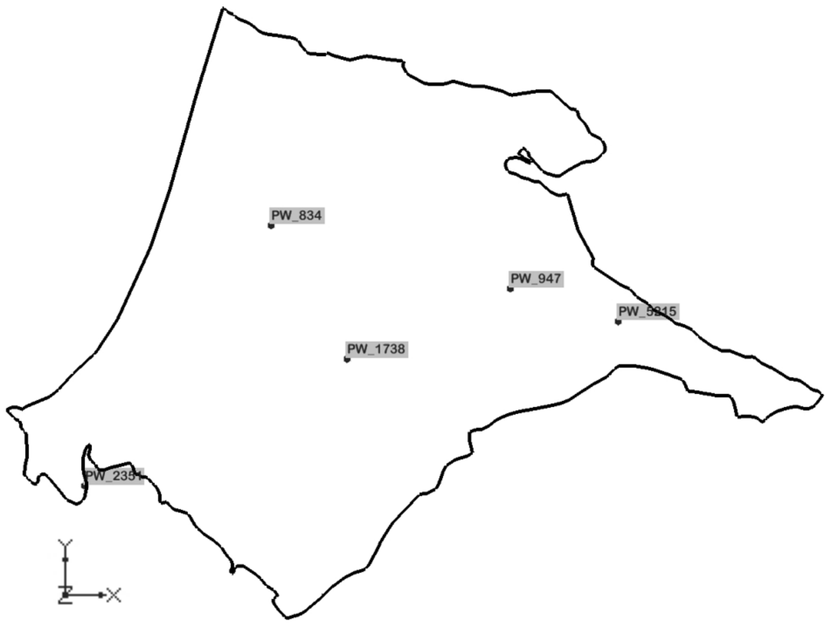

Figure 3.1. Locations of wells used for pumping test

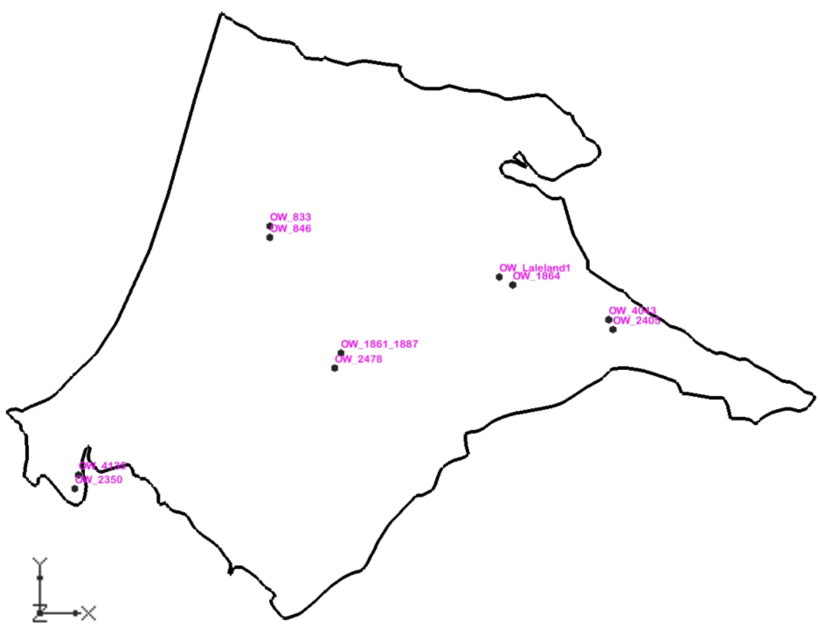

Figure 3.2. Locations of observation wells where the heads were measured during the tests

For Güzelyurt unconfined aquifer, pumping test data have been analyzed in Aquifer Test Pro software by using the Neuman (1975) and “Theis with Jacob Correction” methods. Both methods are developed for estimating hydraulic parameters for unconfined aquifers (explained in section 2.2.2.4.). It was seen that there was no delay in the response of the monitoring wells to the pumping application. Therefore, the Neuman method was found inappropriate for this study. Moreover, since Güzelyurt Aquifer was found to have isotropic characteristics (Fanta, 2015), the transmissivity results gathered from “Theis with Jacob Correction” method, which assumes isotropic conditions, were preferably used in this study.

The required saturated thickness values of the aquifer at the location of each pumping well have been determined using the water level data measured at the corresponding test dates. A sample program analysis output for the observation wells 846 and 833 is shown in Figure 3.3 (The type curve fit analysis of both Neuman (1975) and Theis with Jacob Correction methods for each observation well are given in Appendix B). As seen in the figure, firstly the type curve was drawn for the “Theis with Jacob Correction” method and the measured dimensionless drawdown data was fitted to them. As a result, the transmissivity values calculated for each well were given in the right column. The transmissivity values estimated with both methods for all observation wells are given in Table 3.1.

Only 4 out of 5of the pumping test data sets were suitable for the analyses; one set of the data set associated with the well numbered as 2351 and the water level data in its observation pits 2350-4135 has not provided meaningful results.

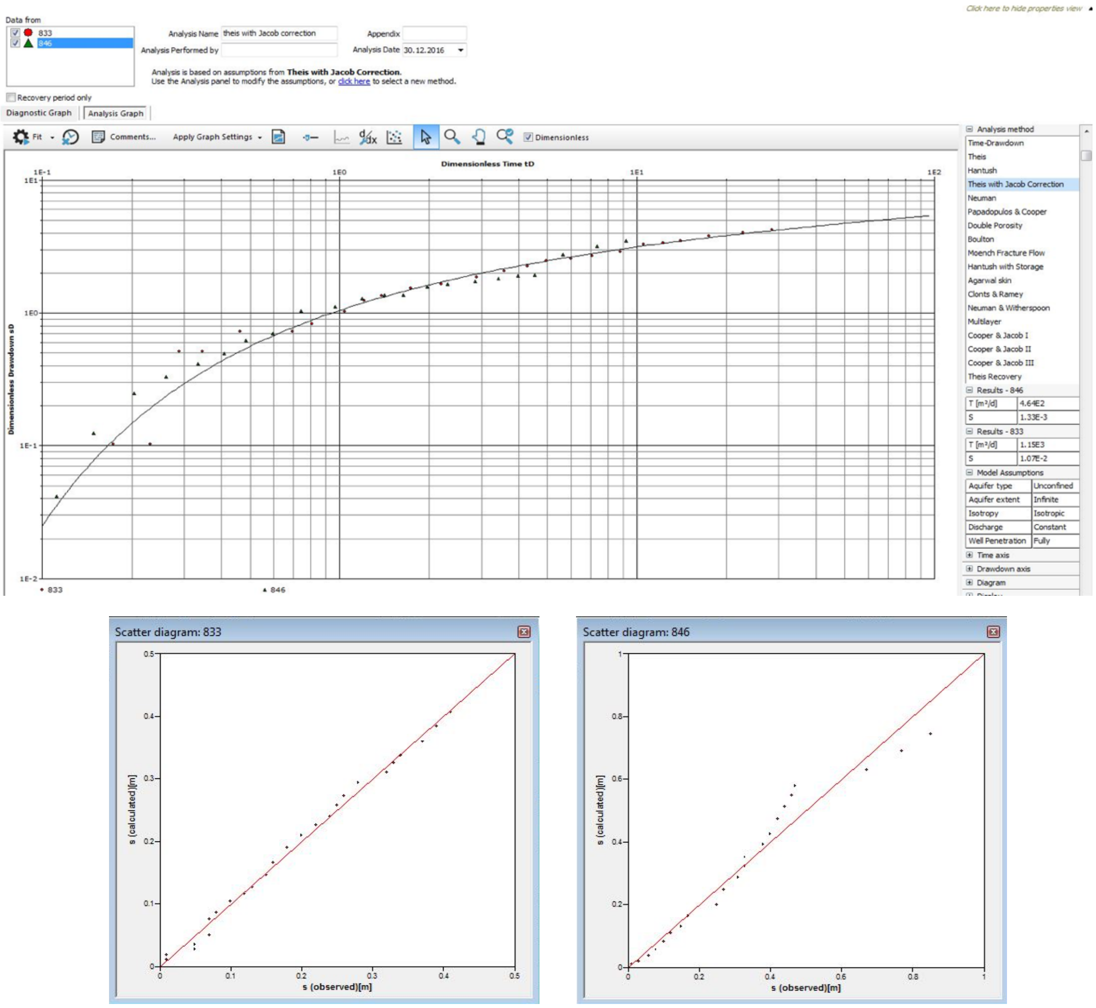

Figure 3.3. Sample data fit using “Theis with Jacob Correction” method in Aquifer Test Pro software

Table 3.1. Transmissivity values calculated from pumping test data

Pumping Wells	Observation Wells	T (transmissivity) (m^2/d)	
		Neuman	Theis with Jacob Correction
834	833	1110	1150
	846	667	464
947	1864	156	293
	Laleland-1	503	735
1738	1887	174	387
	1861	293	356
5215	2405	515	626
	4043	401	696

Apart from the transmissivity values obtained from the pumping test data mentioned above, 4 additional tests in the scope of MTA's "TRNC Natural Resources Research and Development Project" have been conducted. In addition, 3 more tests have been implemented by DSI, (2003) for the "TRNC Water Master Plan (MP) Studies". The data obtained in these studies have been published in the related reports (Gokmenoglu et al., 2002; DSI, 2003). The distribution of these wells in the aquifer area are shown in Figure 3.4. The transmissivity and hydraulic conductivity values recorded during the MP studies are given in Table 3.2.

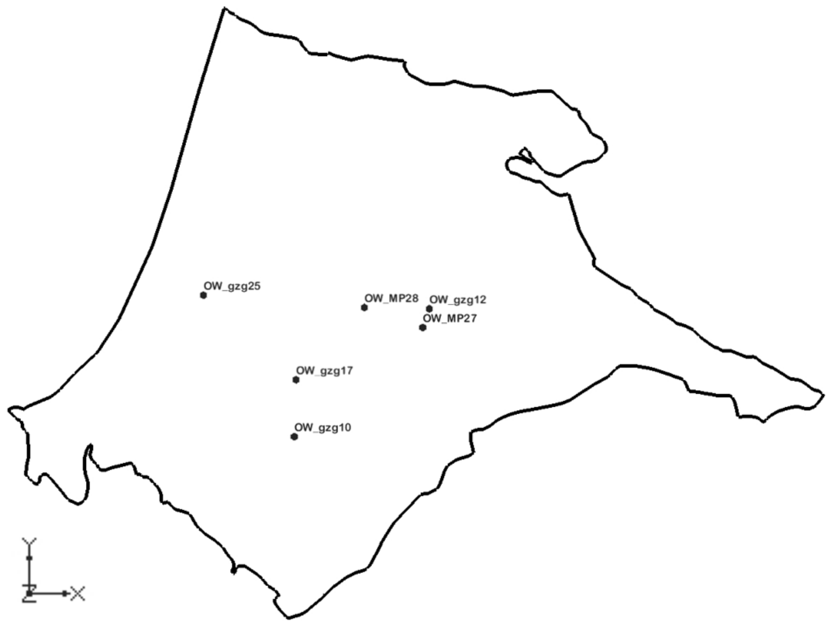

Figure 3.4. Additional observation wells investigated by DSI and MTA

Table 3.2. Ranges of transmissivity and hydraulic conductivity values estimated in Master Plan (MP) wells (DSI, 2003)

Observation Wells	**T (transmissivity) (m^2/d)**	**Average K (Hydraulic Conductivity) (m/day)**
MP-27	3873-5990	45.6
MP-28	307-360	4.4

The specific capacity values obtained from the pumping tests performed at the MTA's "Gzg" wells are given in Table 3.3. The following equations were used to calculate the transmissivity values from specific capacity data provided by using the method suggested by Weight (2008).

$$S_c = \frac{Q}{s} \qquad \textbf{\textit{(Eqn. 3.1)}}$$

For unconfined aquifers: $T = S_c * 90$ ***(Eqn. 3.2)*** whe re

S_c : specific capacity [L/sec / m]

Q : flowrate (L/sec)

s : the drawdown measured after 24 hours (m)

T : transmissivity (m^2/d)

Using Equations 3.1 and 3.2, the transmissivity values calculated for the mentioned wells and given in the Table 3.3.

Table 3.3. Specific capacity values determined in MTA's gzg wells and the calculated transmissivity data

Well ID	**Specific Capacity (L/sec/m)**	**T (transmissivity) (m^2/d)**
gzg-10	0.08	7.2
gzg-12	0.5	45
gzg-17	0.4	36
gzg-25	2.1	189

By applying the transmissivity formula (Eqn. 3.3) for unconfined aquifers, hydraulic conductivity values of all wells were calculated.

For unconfined aquifers: $T = K * b$ ***(Eqn. 3.3)***

where

b : saturated thickness (m)

To find the saturated thickness values, the aquifer bottom elevations at the well locations were subtracted from 2012's water level elevations. The resulting hydraulic conductivity data are given in Table 3.4 below. It can be concluded that the estimated hydraulic conductivity parameter values based on the available data, type curve analysis and the evaluations, range between 0.5 - 46 m/d.

Table 3.4. Hydraulic conductivity values for Güzelyurt Aquifer

Observation Wells	**K (hydraulic conductivity) (m/d)**
833	15.13
846	6.54
1864	5.52
Laleland-1	15.00
1887	9.92
1861	9.13
2405	7.54
4043	8.70
MP-27	45.6
MP-28	4.4
gzg-10	0.51
gzg-12	0.78
gzg-17	2.40
gzg-25	2.42

These point wise hydraulic conductivity values have been then used in the calibration study to estimate the hydraulic conductivity distribution throughout the aquifer for locations where measured data available. The value at each location was fixed at a pilot point. The rest of the area where data is missing is filled with more pilot points with an initial value. The tool called PEST (Parameter Estimation) (Doherty, 1998) was used to find the missing values by optimizing the output head data by matching it with observed head distribution. This application will be explained in detail in the following parts.

3.2. Numerical Model Calibration

Groundwater head data measured at various locations at randomly selected months during the years 2009 to 2013 were used as calibration targets (Not the all wells have the same measurement dates). Two methods were applied in parameter estimation: (1) hydraulic conductivity parameter estimation by PEST with pilot points approach under steady-state conditions, (2) specific yield and general head boundary conductance parameters calibration by trial-and-error approach under transient conditions between years 2009 to 2011. From 2011 to 2013, the remaining measured head data have been used to validate the model.

In this study, hundreds of calibration runs for both steady-state and transient conditions have been made, in order to achieve the most reasonable estimates. The estimated hydraulic conductivity distribution in steady state calibration, have been then used to run transient conditions. In transient case, the conductivity distribution has been kept constant and other uncertain/unknown parameters have been calibrated. However, one should keep in mind that numerical models can not represent the real conditions perfectly and there will be always some points whose reliability should be judged and re-analyzed.

3.2.1. Steady-State Calibration

In steady-state model, the time variable is set to infinity and therefore the partial derivatives of parameters based on time become equal to zero (Oude Essink, 2000). Thus, it can be said that inflows and outflows across model boundaries are constant in a steady-state groundwater flow model. Additionally, at steady-state conditions, the hydraulic head change in the observation wells from time to time is at minimum (Hashemi et al., 2012). In the Güzelyurt groundwater system which has been subjected to excessive pumping since 1950s, steady-state is likely to be achieved in time due to the sea water intrusion which may partially compensate the water deficit. Additionally, due to the excessive water extraction for so long, the depression in the aquifer has reached steady-state where it is almost no more impossible to pump sufficient and good quality water. The groundwater head with respect to mean sea level versus time plot drawn for 13 sample observation wells (Figure 3.5) is given in the Figure 3.6. As it can be seen from the figure, there is no drastic head level change over the years between 2004-2012. All in all, therefore, it was concluded that the head distribution in the Güzelyurt Aquifer can be approximated by steady-state conditions.

Doing calibration in a steady-state condition is easier than transient conditions, since the storage term becomes zero. One of the disadvantages of the steady-state modeling is the limited estimation of some aquifer parameters such as specific yield. Therefore, in the present steady state calibration the only parameter estimated is the hydraulic conductivity. It has successfully done a robust parameter estimation for the hydraulic conductivity distribution in unconfined aquifer of Güzelyurt. Moreover, the steady-state calibration can be a part of transient calibration where the estimated hydraulic conductivity values can be used to run the model for calibrating other unknown parameters (Hashemi et al., 2012).

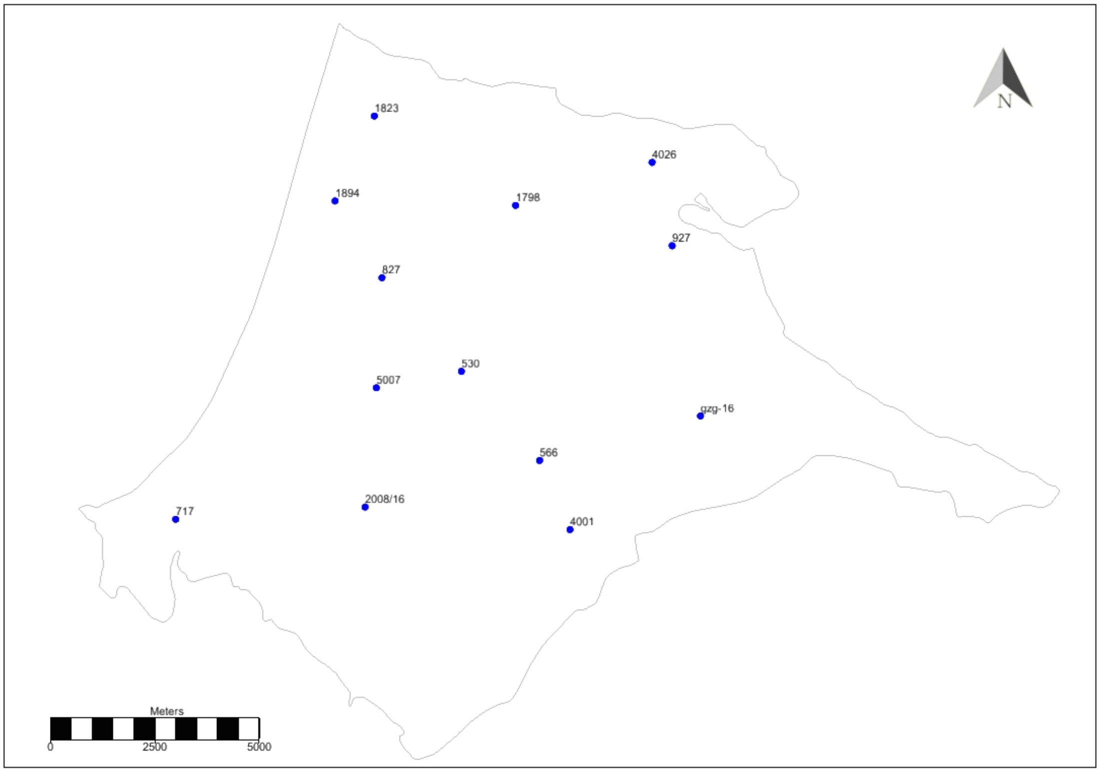

Figure 3.5. The sample observation wells

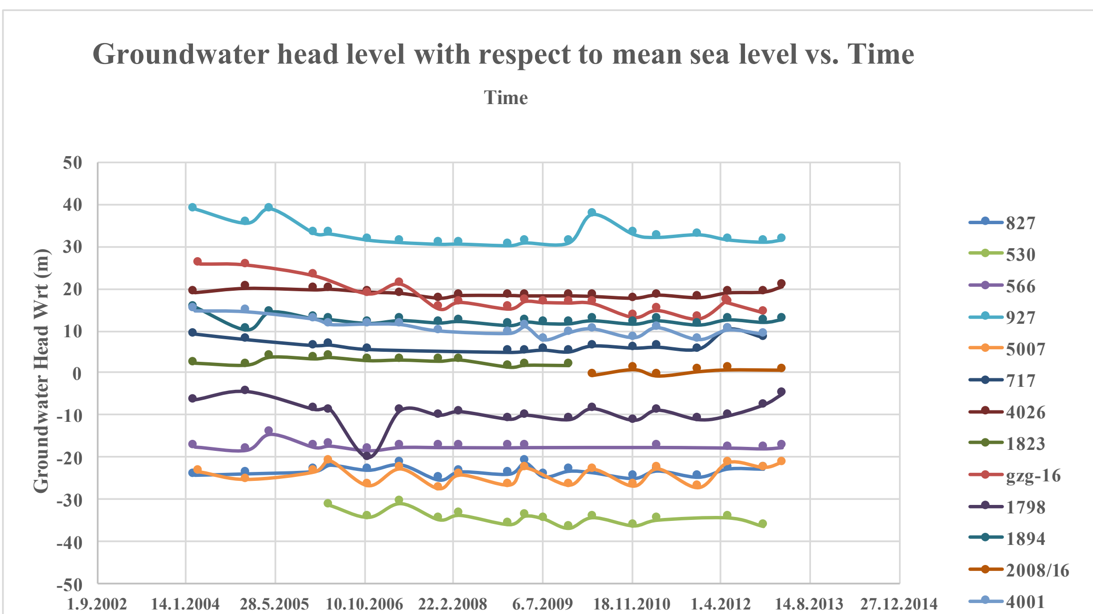

Figure 3.6. Groundwater head level change in a sample set of observation wells

In the steady-state models, flow through the unsaturated zone is treated implicitly such that spatially non-uniform and time-averaged net infiltration to the aquifer is assumed to occur at a constant rate. Moreover, the irrigational extractions are kept constant during the simulations (Ackerman et al., 2010).

The average of observed heads measured in 2013 was taken as the observed head and used in the steady-state calibration. The recharge value due to rainfall was taken as a fraction of the average annual precipitation, of 285 mm. Additionally, the inflow due to streams and derivation channel (21.8 MCM of water, given in Table 2.1.) have been added to the recharge value so that the mentioned amount of water was assumed to be infiltrating from the whole surface of the aquifer.

The pilot point automated PEST calibration tool in GMS was used to optimize the resultant head distribution by changing the hydraulic conductivity in each pilot point except the points where hydraulic conductivity measurement is available. In steady state calibration, a total of 90 pilot points distributed all across the aquifer have been used. The PEST runs have been repeated several times by manual parameter adjustments, until an acceptable match between measured and predicted head has been obtained under the pre-defined recharge conditions. The resultant head and the hydraulic conductivity distributions can be seen in Figures 3.7 and 3.8, respectively. The observed and predicted groundwater head values for a sample set of 10 wells are given in Table 3.5. The locations of the observation wells are shown in Figure 3.7.

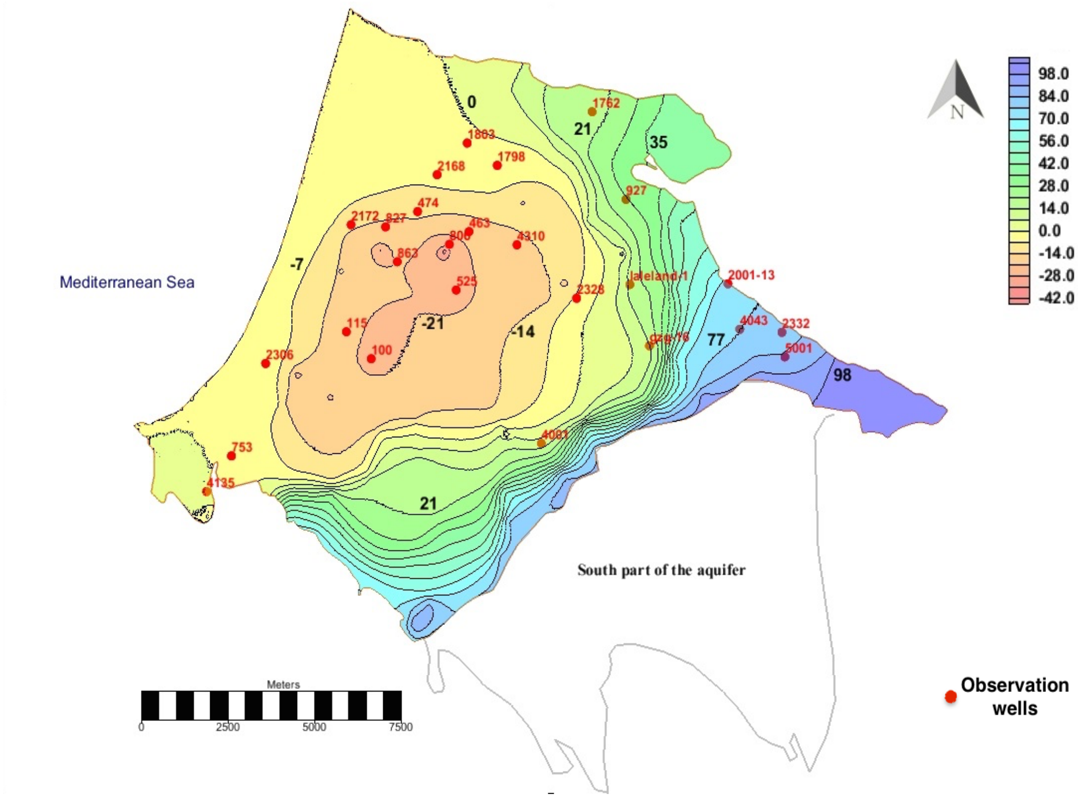

Figure 3.7. The predicted head contours (in meters) of the Güzelyurt Aquifer at the end of the steady-state calibration process & the observation wells of 2013

Table 3.5. Observed and predicted head values in 10 sample wells

WELL ID	Observed (m)	Predicted (m)
2168	-1.898	-4.323
2172	-15.333	-12.294
4001	8.635	7.4866
863	-20.631	-20.8266
gzg-16	14.645	15.5228
4310	-13.566	-14.876
927	31.765	27.79622
5001	81.885	83.388
laleland-1	16.046	15.662
2328	-7.438	-6.97

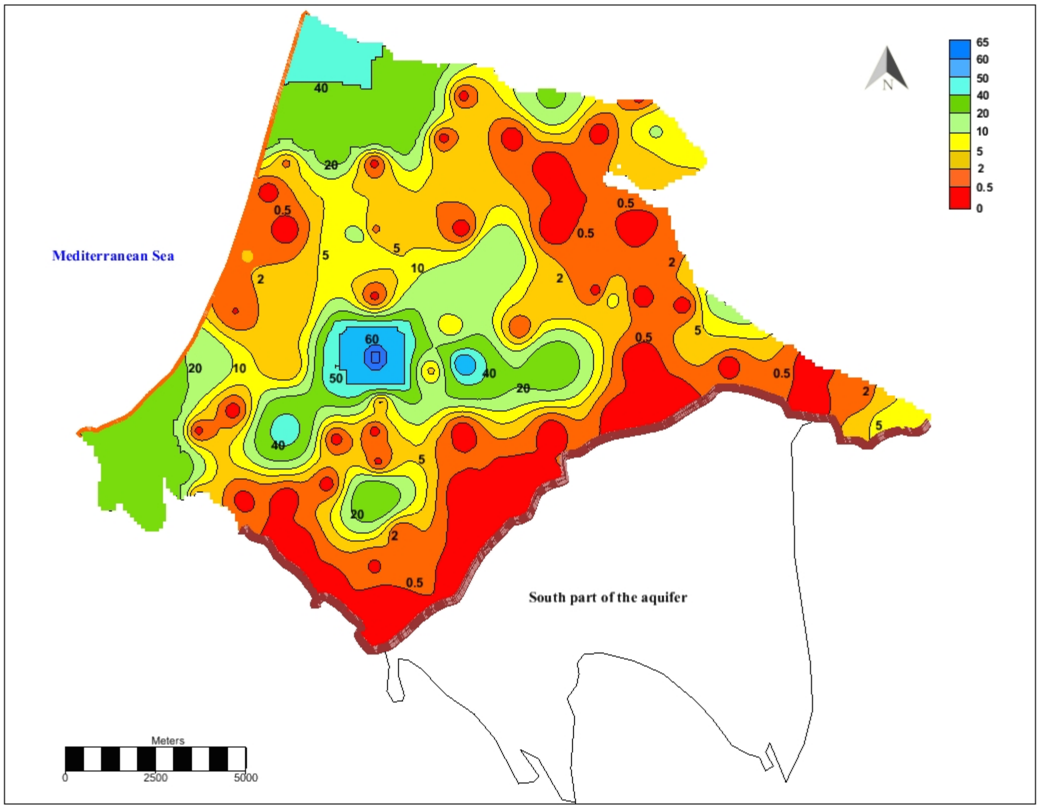

Figure 3.8. Hydraulic conductivity (m/d) distribution determined by steady-state automated PEST and hand calibration

While determining the hydraulic conductivity range which is used by PEST tool to find the optimal value, the measured hydraulic conductivity data that was gathered from the field studies (Table 3.4) were considered. It can be seen from Figure 3.8 that the conductivity values range between 0.005 and 65 m/d. The behavior of the aquifer observed in each trial run showed that the system needs hydraulic conductivity values which are bigger than 45 m/d (the maximum value of Table 3.4). Therefore, the initial range was extended.

The estimated hydraulic conductivity distribution has showed that the areas shown with reddish colors (Figure 3.8) are relatively less permeable. When compared with the detailed (ungrouped) lithological data along the boreholes located at the mentioned areas, the low conductivity values were found reasonable. In the areas near the north and the west part of the coast line, comparably higher conductivity values are seen. Because there is not enough borehole and observed head data in these parts, they are the results of interpolation. Additionally, the highest conductivity values are located around the center. It was observed from the boreholes located that in this region the aquifer material is highly dominated by high permeable gravel materials despite the presence of some lenses of low permeability materials Low permeable materials are localized in a small volume so that it does not affect the overall average conductivity.

When the measured hydraulic head contours are analyzed (Figure 3.9), it is seen that in an area from the coastline to the middle inlands, the space between contours are wider. This means that in that area the hydraulic conductivity values expected to be higher. Therefore, this information justifies the higher hydraulic conductivity zone at the middle of the present calibration result given in Figure 3.8.

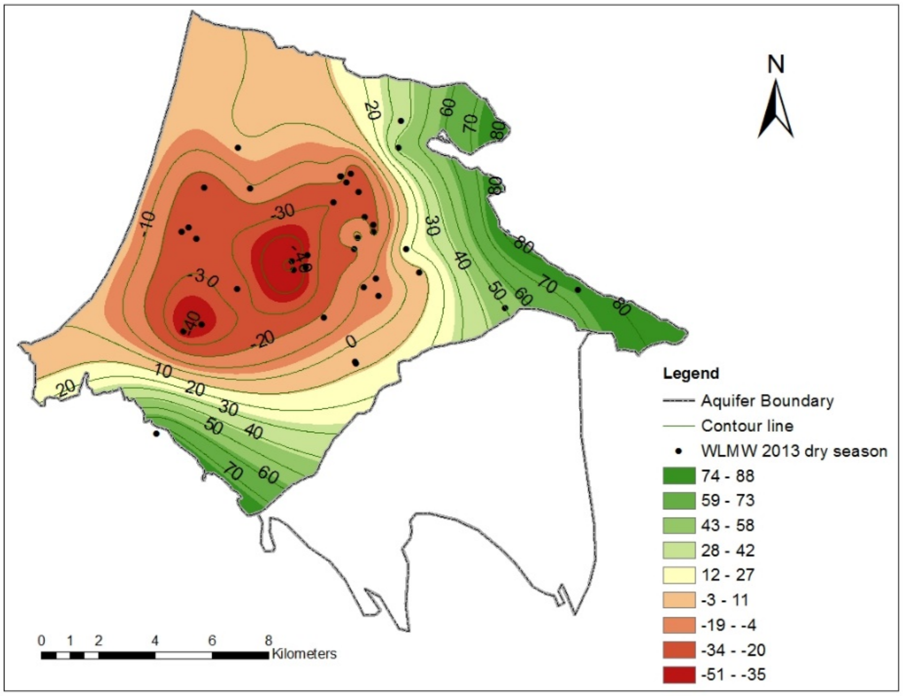

Figure 3.9. The groundwater level contour map indicating the status of 2013, dry season (March) (Fanta, 2015)

For the estimation of calibration error, the Root Mean Squared Error (RMSE) and Coefficient of Determination (R^2) measures were used (Eqn 3.4 and 3.5). The outputs and the computed versus observed head values plot were shown with Figure 3.10. The R^2 value is closer to 1 and the RMSE is small which reveals that the model fits to the observed groundwater levels well.

$$\text{RMSE} = \sqrt{\left[\frac{1}{n}\sum_{i=1}^{n}(h_o - h_c)_i^2\right]} \qquad \textbf{\textit{(Eqn. 3.4)}}$$

$$R^2 = \frac{SS_{yy} - SSE}{SS_{yy}} = 1 - \frac{SSE}{SS_{yy}}$$

$$SS_{yy} = \sum_{i=1}^{n}\left(h_o - \bar{h}_o\right)_i^2 \qquad \textbf{\textit{(Eqn. 3.5)}}$$

$$SSE = \sum_{i=1}^{n}(h_o - h_c)_i^2$$

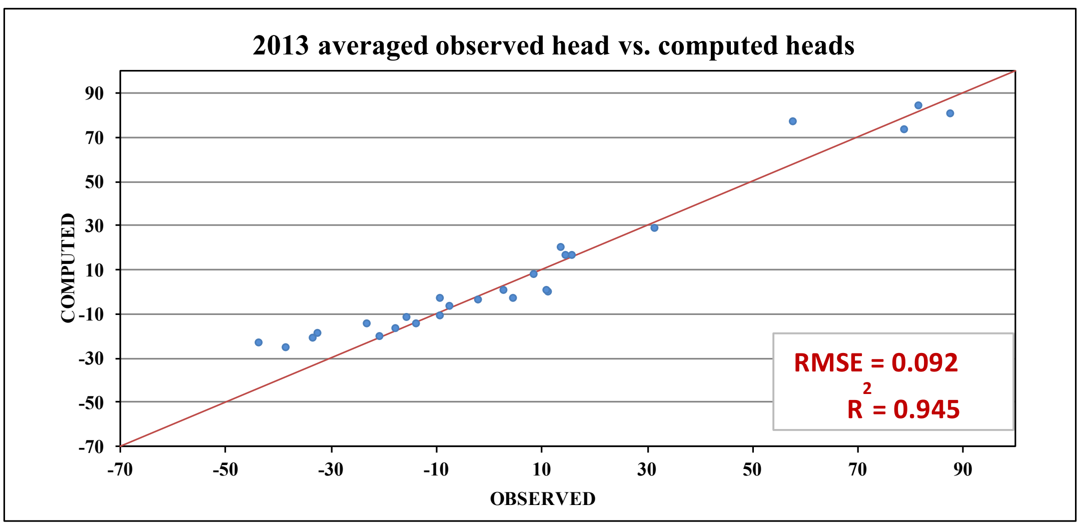

Figure 3.10. Comparison of predicted head values with the corresponding measured head values for steady-state calibration

3.2.2. Transient Calibration and Validation

A transient groundwater flow model represents a dynamic system with changes in inflows, outflows, and aquifer storage. In transient models, the irrigational extractions may change seasonally and should be represented with stress periods.

In transient models, the simulation time is divided into discrete interims named stress periods and time steps. The stress periods indicate the time intervals where the specified inflows or out flows are constant. These flows can differ from one stress period to the next. Time steps which are the smaller intervals covered in the stress periods represents the times at which the user wants the software to calculate heads and flows (Ackerman et al., 2010).

In this study, the observed head data recorded between years 2009-2013 were used in the transient simulations. For the transient calibration, this set of data was divided into two parts; data between 2009-2011 was used to calibrate the GHB conductance and the specific yield parameter manually, and 2011-2013 was used as a validation dataset. A total of 21 stress periods starting from April 01, 2009 were determined for the calibration process by considering the monthly recharge data. On the other hand, a total of 36 stress periods starting from January 01, 2011 were assigned to the transient validation run. The number of time steps in each stress period were taken as 10. Table 3.6 shows the stress period dialog for the transient calibration as it is assigned in the GMS software.

Table 3.6. Transient Calibration Stress Periods

	Start	Length	Num. of Time Steps	Multiplier
1	01.04.2009	30	10	1
2	01.05.2009	31	10	1
3	01.06.2009	30	10	1
4	01.07.2009	31	10	1
5	01.08.2009	31	10	1
6	01.09.2009	30	10	1
7	01.10.2009	31	10	1
8	01.11.2009	30	10	1
9	01.12.2009	31	10	1
10	01.01.2010	31	10	1
11	01.02.2010	28	10	1
12	01.03.2010	31	10	1
13	01.04.2010	30	10	1
14	01.05.2010	31	10	1
15	01.06.2010	30	10	1
16	01.07.2010	31	10	1
17	01.08.2010	31	10	1
18	01.09.2010	30	10	1
19	01.10.2010	31	10	1
20	01.11.2010	30	10	1
21	01.12.2010	31	10	1
END	01.01.2011			

For the initial heads, the distribution of measured water level data for April, 2009 was used to start the transient calibration run (Figure 3.13. (a)). In each stress period the sources and sinks were attributed according to the dry and wet seasons. With this approach, for the dry season, all the irrigation and drinking wells were considered to be active, in the wet season, only the drinking wells were kept active assuming that in the wet months there will be no irrigational pumping throughout the aquifer due to the rainfall feeding the crops.

As used in the steady-state calibration analysis, both the precipitation (infiltrated amount) and the water infiltrating from streams and derivation channel (Table 2.1.)

were used to recharge the aquifer. The monthly precipitation data used in the simulation runs belong to Güzelyurt meteorological Station. Recharge from precipitation was assumed to be 25% of the monthly precipitation, as suggested by (DSI, 2003). The streams and derivation channels were assumed to be recharging the aquifer only during the wet season. Therefore, the total amount for two of these sources as given in Table 2.1, was divided accordingly to the stress periods. At the end, the infiltrating water coming from rainfall and the mentioned additional recharge were summed up and input to the model in the form of transient dataset (Figure 3.12.).

With the set up of the numerical model, several forward runs have been made. In each simulation, the conductance parameter for the General Head Boundary or the specific yield parameter of the aquifer (assigned as uniform value throughout the aquifer) was changed manually to achieve a good fit between the resultant groundwater head data and the water level observations. The locations of the observation wells of which groundwater levels have been measured in different months during the measurement period between 2009-2013 were shown in Figure 3.11. Additionally, the conductance values were adjusted to obtain a reasonable inflow value from the southern part of the aquifer. Fanta (2015) has proposed that approximately 5 MCM of water is contributing to the aquifer from south. It was assumed that the incoming water coming from the formation boundary which was also represented with a General Head boundary condition, is much lower than the inflow through the country boarder. Therefore, the total water coming from general head boundaries were calibrated to get closer to 5 MCM.

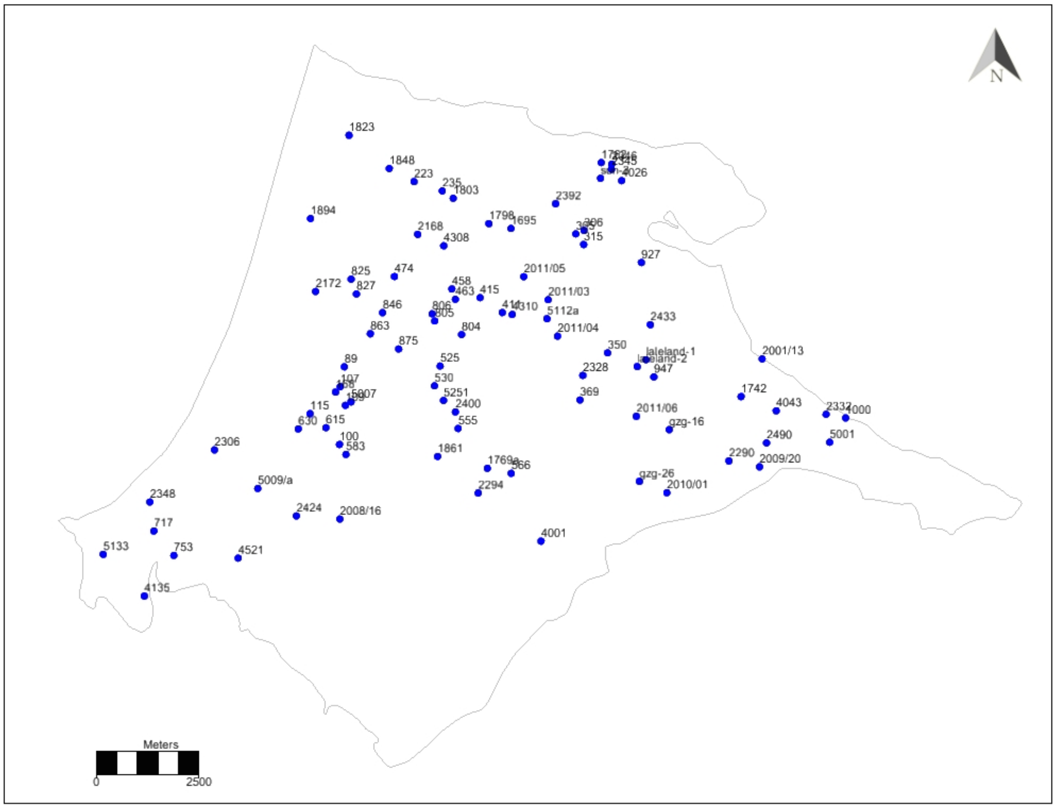

Figure 3.11. The location of the observation wells used in the transient runs (measurements between 2009-2013)

After the completion of the calibration, the groundwater head contours of each time step were drawn by the software. They are shown with the Figures 3.13. And in Table 3.7, observed and computed head values of a sample observation well set (Figure 3.13) have been given. Moreover, as it was done in the steady state calibration, the statistical error calculations were made. The results and the calibration plot is given in Figure 3.15. Since the R^2 value is close to 1 and the RMSE is small, the errors are in an acceptable range.

Finally, the conductance values in the cells of general head boundaries have been approximated to range between $8.7*10^{-6}$ and 0.086 m^2/d, with an average of 0.03

m^2/d. The net inflow entering from the general head boundaries were read as 4.7 MCM in the output water budget prepared in the software. This value was found reliable since it is close to 5 MCM which is the calibration target for the general head boundary.

Anderson et al. (2002) stated that the specific yield for different sized sand and gravel ranges from 0.1 to 0.4. They also claimed that given this narrow range, it is common to select a value within this range and then test the effect of the changes to the model. According to this information, a set of specific yield values were tried in different simulations where all the other parameters were kept constant and as a result, the best head distribution case was achieved with a specific yield value of 0.4

After successfully completing the calibration, with another observation data set (2011-2013), the accuracy of the model was validated. The resultant head contours and errors were given in Figure 3.14. Additionally, in Table 3.8, the same sample observation well set with their observed and computed head values have been demonstrated.

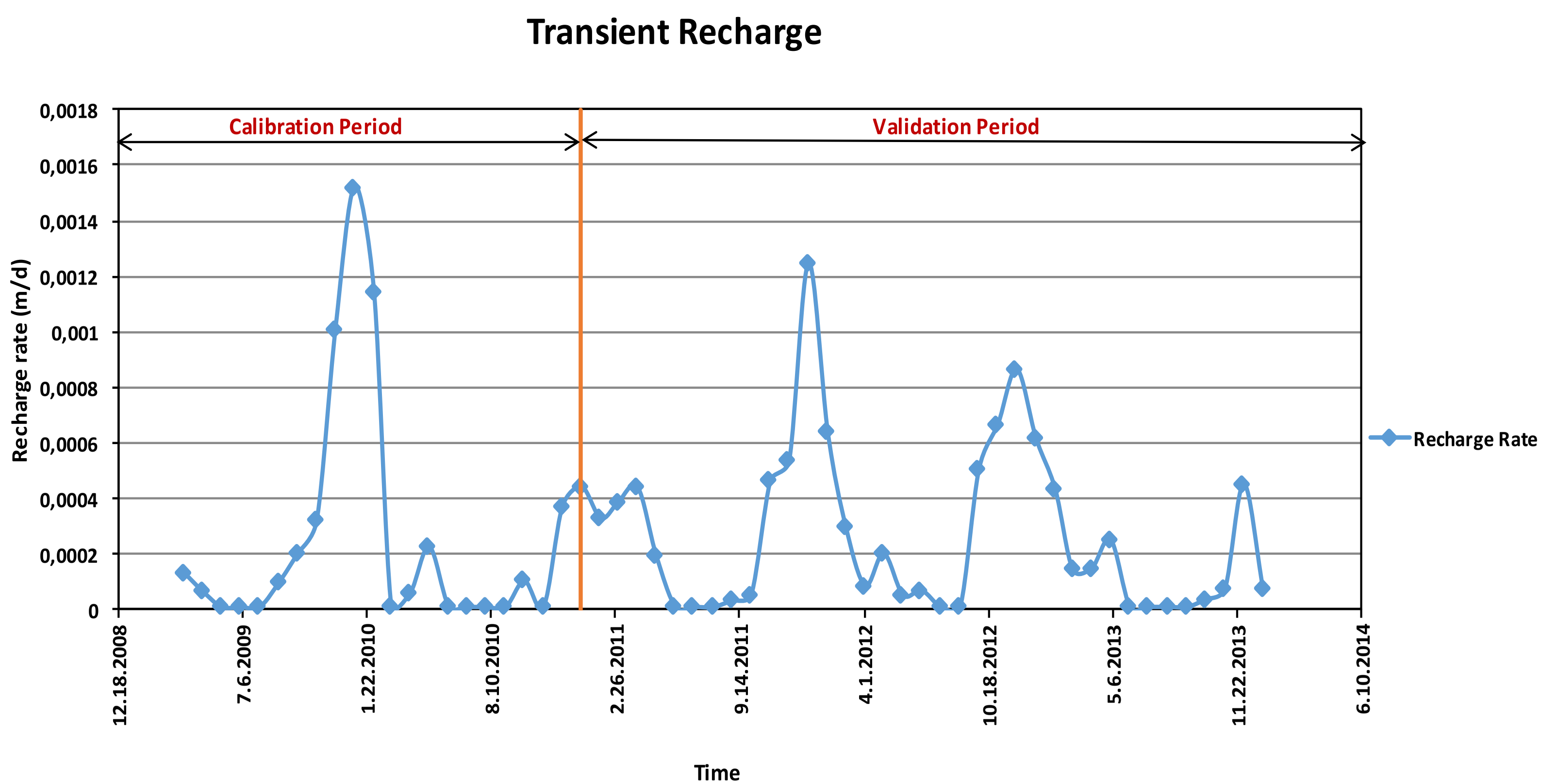

Figure 3.12. Recharge Rate changing with time (showing the dataset for both calibration and validation periods)

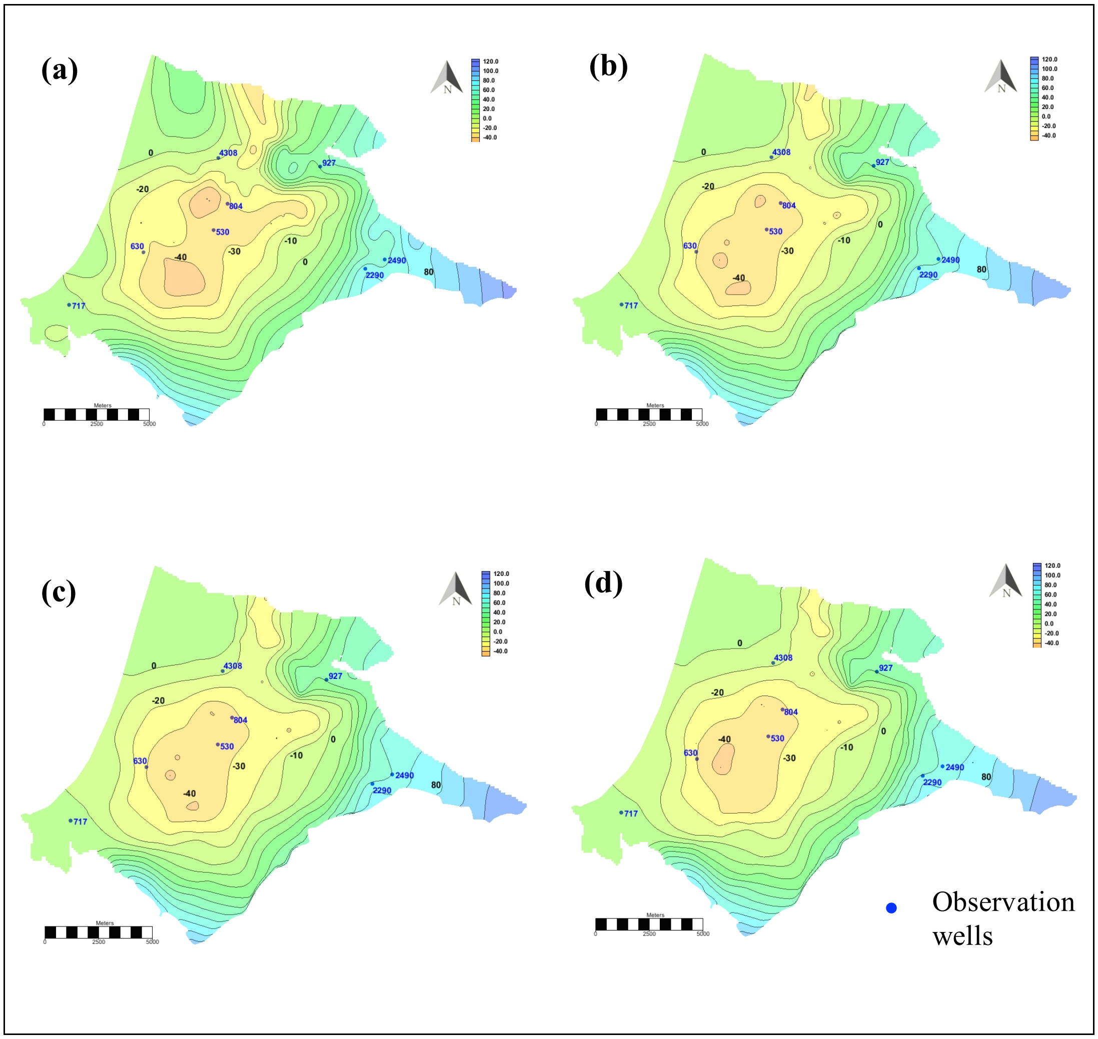

Figure 3.13. Groundwater head contours drawn after the completion of calibration (a) April 2009, (b) December 2009, (c) April 2010, (d) December 2010

Table 3.7. Observed and predicted head values in 8 sample wells

	April 2009		*December 2009*		*April 2010*		*December 2010*	
Well ID	***Observed (m)***	***Predicted (m)***	***Observed (m)***	***Predicted (m)***	***Observed (m)***	***Predicted (m)***	***Observed (m)***	***Predicted (m)***
530	*-33.79*	*-34.07*	*-36.68*	*-34.74*	*-34.15*	*-34.34*	*-36.1*	*-34.05*
630	*-27.94*	*-27.78*	*-30.64*	*-28.79*	*-27.95*	*-28.85*	*-31.21*	*-29.17*
804	*-30.26*	*-30.91*	*-33.47*	*-32.99*	*-30.48*	*-31.96*	*-37.7*	*-31.06*
927	*30.9*	*30.56*	*30.87*	*30.76*	*37.52*	*30.77*	*32.87*	*30.23*
4308	*-9.2*	*-9.11*	*-10.2*	*-8.07*	*-8.95*	*-7.82*	*-10.16*	*-8.39*
717	*5.04*	*4.8*	*4.94*	*1.16*	*6.33*	*0.95*	*5.83*	*0.60*
2490	*57.09*	*57.28*	*50.25*	*59.10*	*55.37*	*60.18*	*46.23*	*61.10*
2290	*65.11*	*63.04*	*60.46*	*61.68*	*62.06*	*60.97*	*56.89*	*62.11*

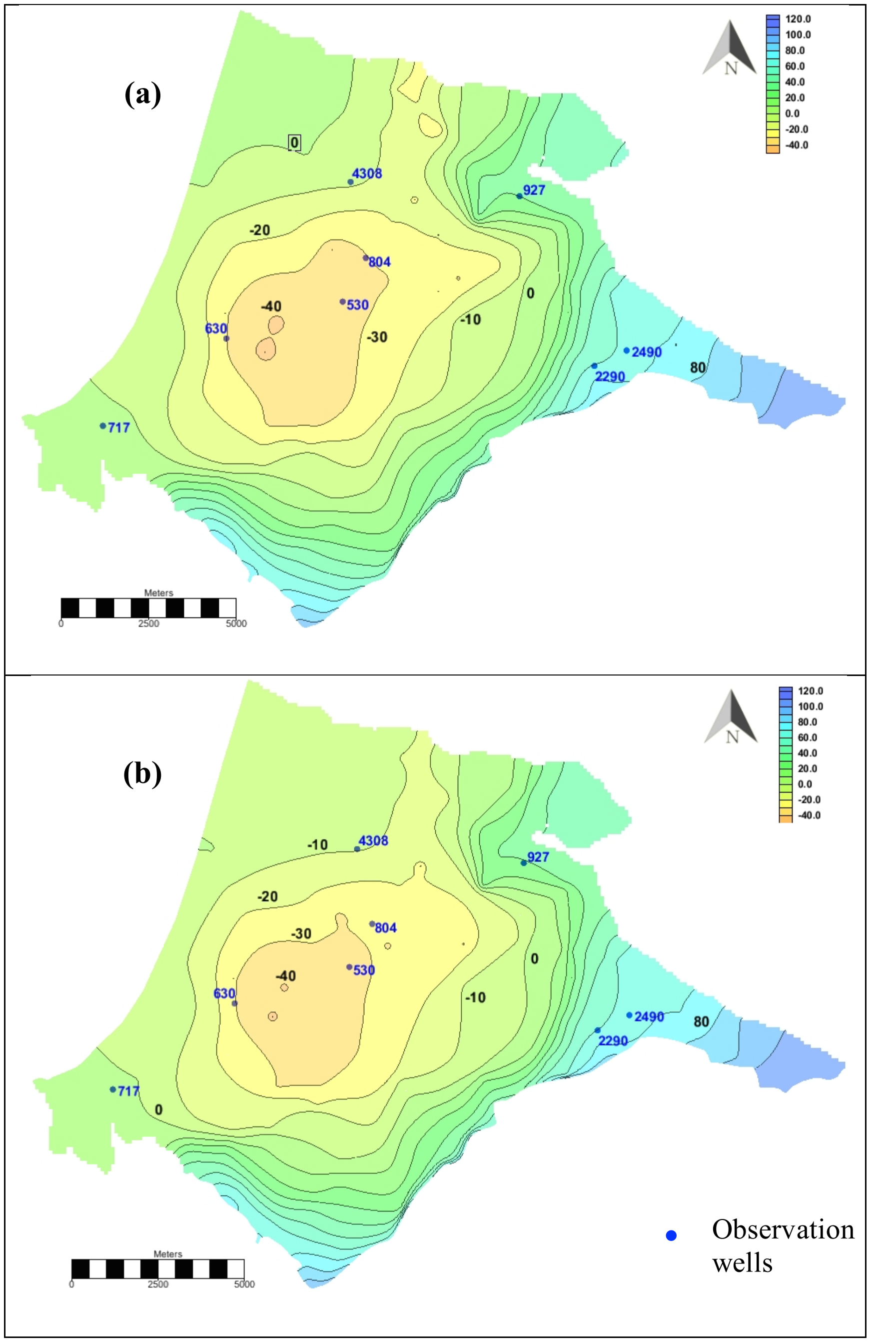

Figure 3.14. Groundwater head contours drawn for validation (a) April, (b) March 2013

Table 3.8. Observed and predicted head values in 8 sample wells

	April 2011		March 2013	
Well ID	**Observed (m)**	**Predicted (m)**	**Observed (m)**	**Predicted (m)**
530	-34.74	-33.68	NA	-32.34
630	-28.18	-29.11	-23.62	-30.55
804	-27.85	-30.46	NA	-28.35
927	32.19	29.99	31.58	28.72
4308	-6.76	-8.61	-5.68	-9.61
717	6.04	0.63	NA	0.29
2490	56.88	61.12	NA	62.6
2290	61.36	59.89	66.83	60.19

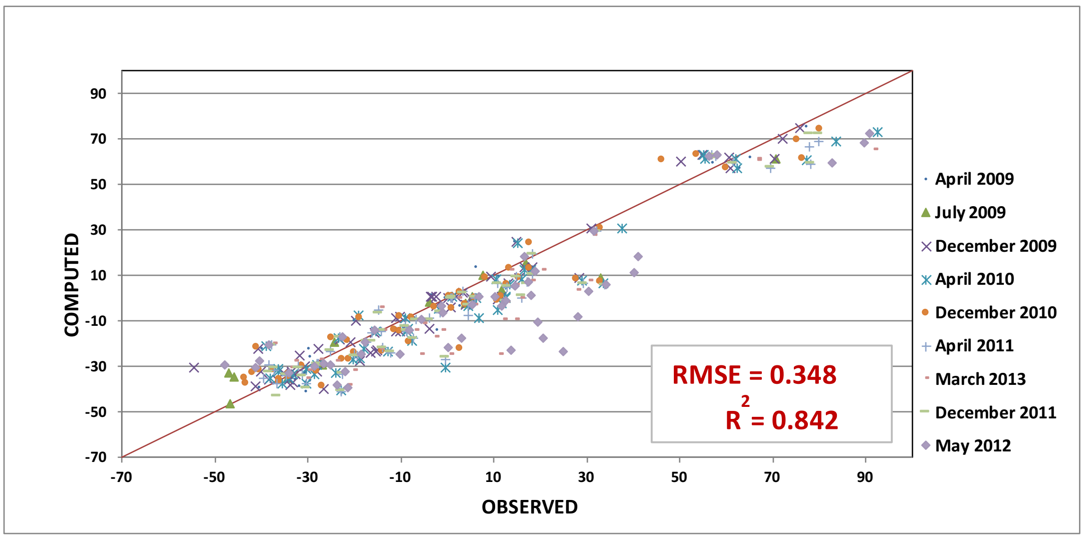

Figure 3.15. The computed versus observed head values covering both results of calibration and the validation

3.3. Simulations for Güzelyurt Aquifer Response

In this step of the study, the previously calibrated model was used to simulate different scenarios representing the hydraulic behavior of the aquifer. The overall aim of these simulations is to roughly predict the time required for the aquifer to reach the natural conditions that the aquifer had prior to being subjected to overexploitation. The questions answered in the mentioned simulations are as follows:

- If only drinking water supply wells are actively pumped, how long would it take for the aquifer to reach its natural state?
- If a portion of the excess water coming from Turkey via the TRNC Supply Project would have been artificially recharged to the aquifer through Güzelyurt Dam, how long would it take the aquifer to reach its natural condition?
- If a portion of the excess water coming from Turkey via the TRNC Supply Project would have been artificially recharged to the aquifer through Güzelyurt Dam and injection wells, how long would it take the aquifer to reach its natural condition?

The artificial recharge technique is a reliable and effective alternative in groundwater recharge. This method is being applied for almost 200 years by different countries for several different purposes such as replenishment of overexploited aquifer, reduction of salinity in groundwater and decrease in seawater intrusion around the coastal areas (Siddiqui, 2016).

There are various ways to apply artificial recharge. Three of them are direct surface recharge or surface spreading technique (shallow infiltration basin), direct subsurface recharge (injection wells) or the combination of surface-subsurface methods. The surface spreading technique is the most common and the simplest one which aims to increase the contact area and residence time of the surface water on top of the soil to augment the infiltration. The percolation of water through the soil depends on several factors including vertical hydraulic conductivity of the soil, different chemical and biological influences. The surface spreading method works best when the aquifer being fed is unconfined, permeable and has enough thickness to provide storage. On the other hand, the artificial recharge through injection wells method is applied when an aquifer is seriously de-saturated due to overexploitation of groundwater and need to be replenished. The wells inserted are similar to boreholes but they are used to add water to the aquifer by the gravity or under pressure. It is possible to conduct injection well recharge in the coastal areas where salt water intrusion problem exists, to stop/push the entrance of seawater. In alluvial aquifers, the injection wells can be constructed to normal gravel packed pumping well where an injection pipe with opening to the aquifer may be enough (CGWB, 2007).

There are advantages and disadvantages of each method over the other. With well injection, the land requirement and the water loss due to evaporation are minimal compared to the infiltration basin option. The infiltration basins are more prone to water loss due to evaporation which eventually decrease the net amount of water supplied to the aquifer. The injection wells can provide high rate of inflow through the unsaturated zone and it uses the advantage of horizontal hydraulic conductivity by eliminating the vertical flow limitations. But in the infiltration basins, the water should surpass the vertical distances where hydraulic conductivity variance may seriously decrease the infiltration rate. On the other hand, the wells have a higher risk of clogging compared to the infiltration basins because the infiltration rates around the well holes are much higher than the surface infiltration. Moreover, they are comparably costlier since the construction of recharge well requires specialized techniques and it is necessary to get operational and maintenance support to prevent well from clogging. However, it is easier to construct, operate and maintain the infiltration basins. Moreover, the remediation of possible clogging in the infiltration basins is much simpler than as in the wells (CGWB, 2000; Mohammedjemal, 2006).

As it can be clearly understood that each method has its own pros and cons. In order to benefit from their individual advantages both option may be used at the same time to achieve an optimum recharge – cost relation (CGWB, 2007). In this part of the study, first the natural condition estimation has been implemented by conducting a steady-state run with using the source & sink values used in the steady state calibration, the calibrated hydraulic conductivity distribution, calibrated general head conductance and the specific yield. Then, the determined head distribution has been utilized in the follow-up future simulations as a comparison data for the time requirement to reach natural state. In the first simulation, the numerical model has been run under minimum stress condition where only drinking water extraction from wells were allowed. Secondly, by keeping all the variables and parameters same as in the previous run, a total of 28 MCM of water (out of 37 MCM provided by the TRNC Supply Project for irrigational purposes) has been used to recharge the aquifer by infiltration basin approach through the existing Güzelyurt Dam (Figure 3.16). In the last simulation, the same amount of water has been equally divided between the injection wells located around the depressed water table area at the center of the aquifer (Figure 3.16) and the Dam to increase the net recharge to the aquifer. For the application of areal recharge in the model, Recharge (RCH) package has been used. This package requires values of recharge rate (L/d). Therefore, the water to be recharged was divided by the bottom area of Güzelyurt Dam which is 480,000 m^2 (Water Development Department, 2009). For the injection well recharge, the WELL package in MODFLOW-USG has been used.

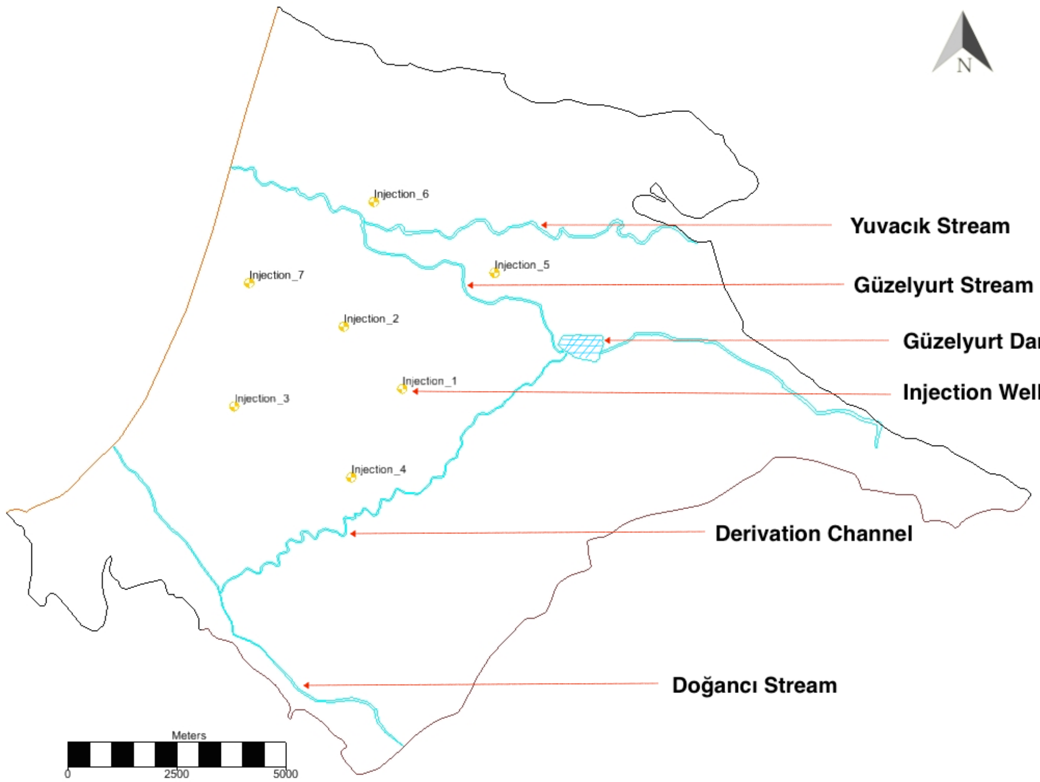

Figure 3.16. The location of the Güzelyurt Dam, modeled injection wells and the existing streams

All simulation scenarios explained in the sections 3.3.2, 3.3.3 and 3.3.4 have been designed to predict the hydraulic response of the aquifer under the present natural recharge status has been preserved. In this regard, the time period between 2014 and 2020 have been divided into 13 stress periods where each year contains dry and wet periods represented by dry and wet months. The time period after 2020 (2021-2095) has been divided into 13 stress periods such that the simulation years increase with the increments of 1, 2, 5 and 10 years (See Table 3.9). Until the final determination of the stress periods, the model has been run with higher number of stress periods and time steps to be sure if the same results were sustained relative to the final scheme where there are less stress periods and time steps. In the first 13 stress period, the total recharge coming form rainfall, streams and derivation channel have been divided to the periods according to the dry and wet months' average. In the remaining 13 stress periods where the period durations are minimum 1 year, the natural annual average recharge was used. The stress period dialog of the future simulations explained above is given in the Table 3.9. The measured head distribution of December 2013 has been taken as the initial conditions to start the simulations. The artificial recharge applications have been started from the beginning of the simulation period (2013, assumed that it was the present time) in order to achieve more accurate prediction, because 2013 is the last year of groundwater level observations.

The predictive modeling scenarios explained below were not attempts to predict the real future. Rather, these scenarios were aimed to predict the hydraulic behavior of the aquifer under hypothetical modeled conditions. In reality, the actual future conditions will unavoidably differ from the modeled conditions owing to changes in climate, land use, and other factors.

Table 3.9. The stress periods dialog for the future prediction simulations

	No	Start	Length	# of Time Steps	Multiplier
Starting Heads	1	01.12.2013	90.0	1	1.0
Periods based on Wet and Dry months	2	01.03.2014	214.0	1	1.0
	3	01.10.2014	243.0	1	1.0
	4	01.06.2015	153.0	1	1.0
	5	01.11.2015	152.0	1	1.0
	6	01.04.2016	214.0	1	1.0
	7	01.11.2016	151.0	1	1.0
	8	01.04.2017	214.0	1	1.0
	9	01.11.2017	151.0	1	1.0
	10	01.04.2018	214.0	1	1.0
	11	01.11.2018	151.0	1	1.0
	12	01.04.2019	214.0	1	1.0
	13	01.11.2019	152.0	1	1.0
	14	01.04.2020	214.0	1	1.0
Periods based on annual average recharge conditions	15	01.11.2020	365.0	1	1.0
	16	01.11.2021	365.0	1	1.0
	17	01.11.2022	365.0	1	1.0
	18	01.11.2023	731.0	10	1.0
	19	01.11.2025	1826.0	10	1.0
	20	01.11.2030	1826.0	10	1.0
	21	01.11.2035	3653.0	1	1.0
	22	01.11.2045	3652.0	1	1.0
	23	01.11.2055	3653.0	1	1.0
	24	01.11.2065	3652.0	1	1.0
	25	01.11.2075	3653.0	10	1.0
	26	01.11.2085	3652.0	10	1.0
	27	01.11.2095			

3.3.1. Steady-state Natural Conditions Simulation

Zhou et al. (2011) stated that if it is possible, a groundwater balance indicating the pre-development period should be determined initially as a reference for pumped conditions. M. Ergil et al., (1993) stated that the depression in the water table in the Güzelyurt Aquifer has started to appear since 1963 because of the increase in groundwater extractions. The contour map showing the groundwater levels in 1950 is given in Figure 3.17.

In this study, the future predictions are all based on achieving a pre-estimated natural condition. In this part of the study, after the completion of calibration, a steady-state simulation has been implemented with the calibrated hydraulic parameters and the annual average recharge values but without groundwater pumping. The resultant groundwater head contours of the simulation are shown in Figure 3.18.

In the Island of Cyprus, the active water pumping applications have started by the end of 19th century. These were put one step further with the establishment of borehole drilling in the island in 1920. During 1950s, this practice was considerably increased the number of boreholes drilled around the island which in turn resulted in intensified exploitation of groundwater resources (Cyprus Geological Survey Department, 2016). Based on this information, the groundwater head contours seen in Figure 3.17 shows that the decrease in water table had already started before 1950s due to earlier pumping applications. Therefore, it does not represent the actual natural conditions. In Figure 3.17, the 10m head contour is approximately 4km away from the coastline to the inland while in Figure 3.18 it is 500 m inside. This situation well explains that the predicted steady-state head distribution given in Figure 3.18 is reliable and it can be taken as the estimated approximate natural condition for the aquifer.

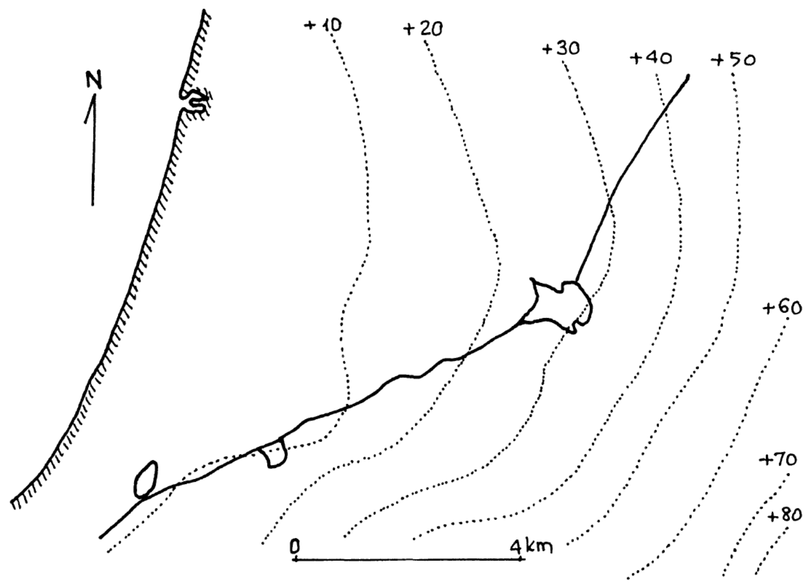

Figure 3.17. The water table contours in 1950 (M. Ergil et al., 1993)

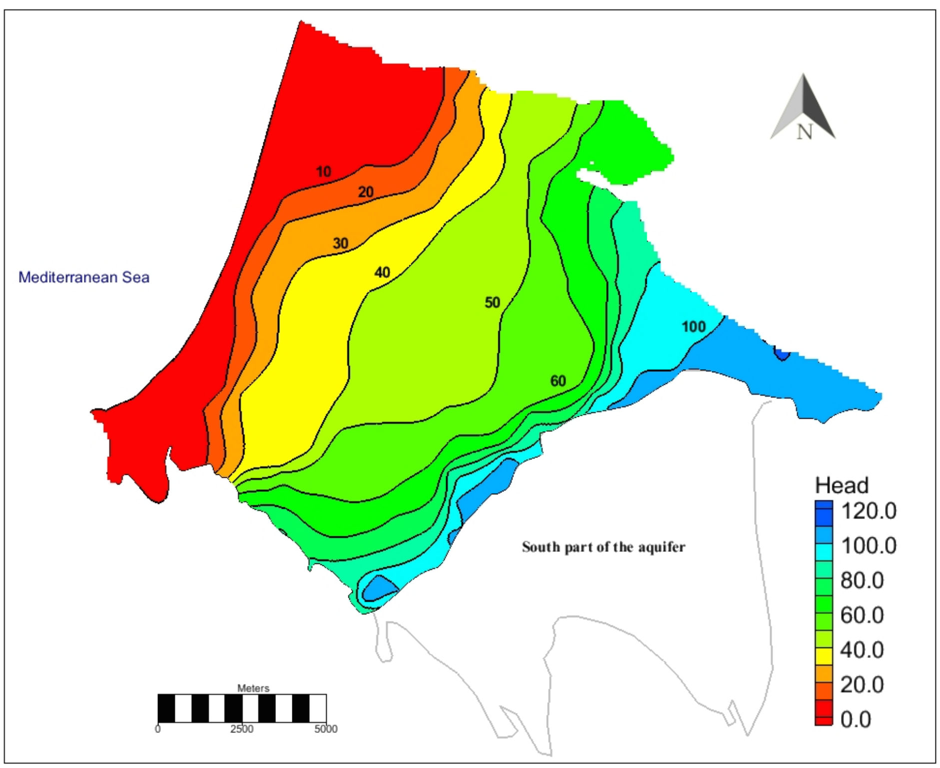

Figure 3.18. The modeled natural state of the Güzelyurt Aquifer

3.3.2. SCENARIO 1: Minimum Stress

In this case, all the stress due to irrigational wells have been stopped and starting from 2013 December, a long term simulation has been done. The results of this part of the study, has a role in the determination of the effectiveness of artificial recharge. In artificial recharge scenarios, the time to reach the steady-state conditions, i.e. the achievement of pre-pumping natural conditions has been taken as a measure for the effectiveness of artificial recharge scenarios. The earlier to reach natural conditions, the better the effectiveness of the recharge scenario. As it can be seen from the Figures 3.19 and 20, the depression zone is disappearing in time and after about 14 years in 2028 the "zero" head contour approaches to the coast. After approximately 73 years in 2087, the aquifer achieves the natural conditions and reaches the steady-state.

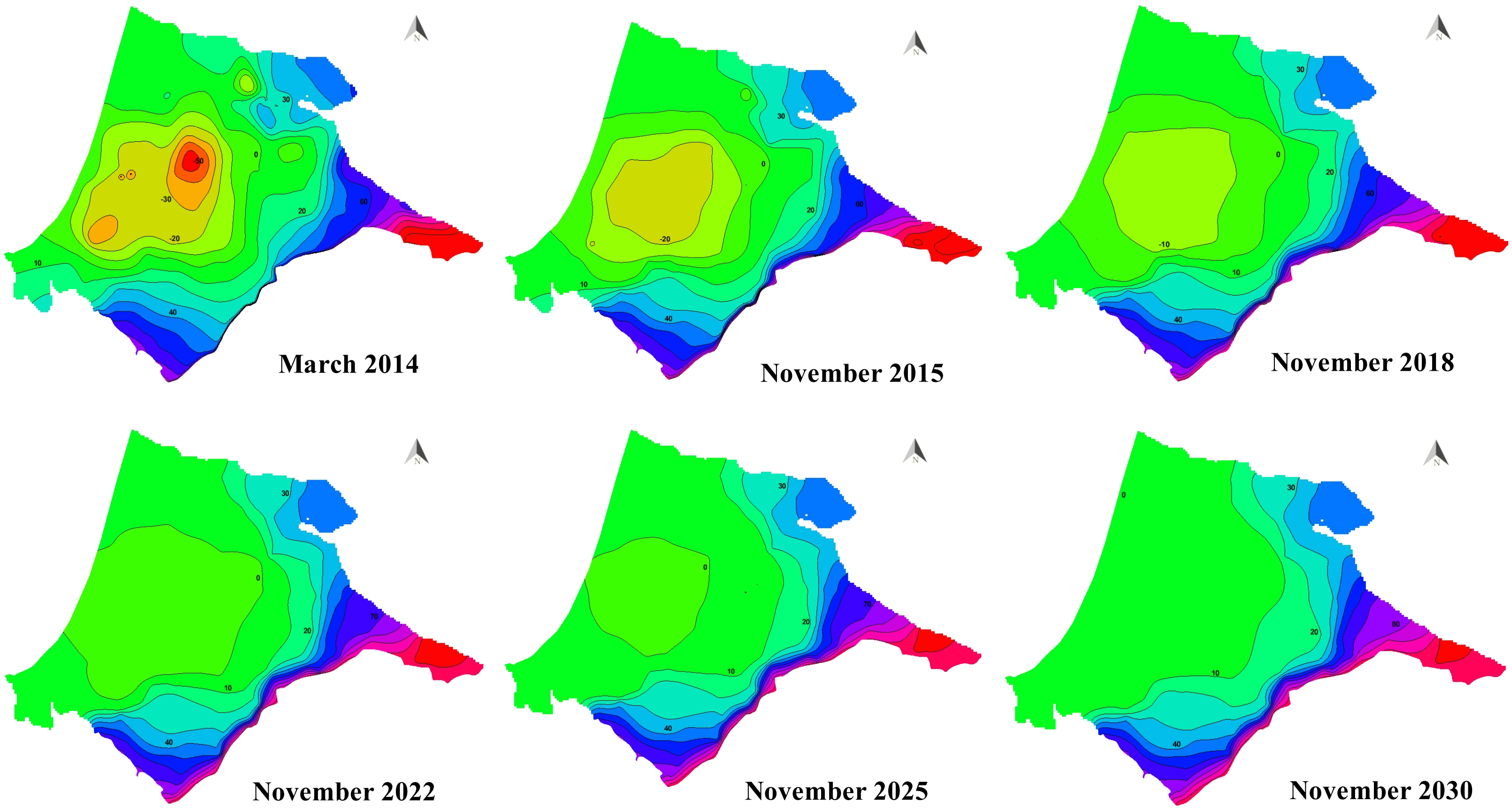

Figure 3.19. The groundwater head contours changing with time (Scenario 1)

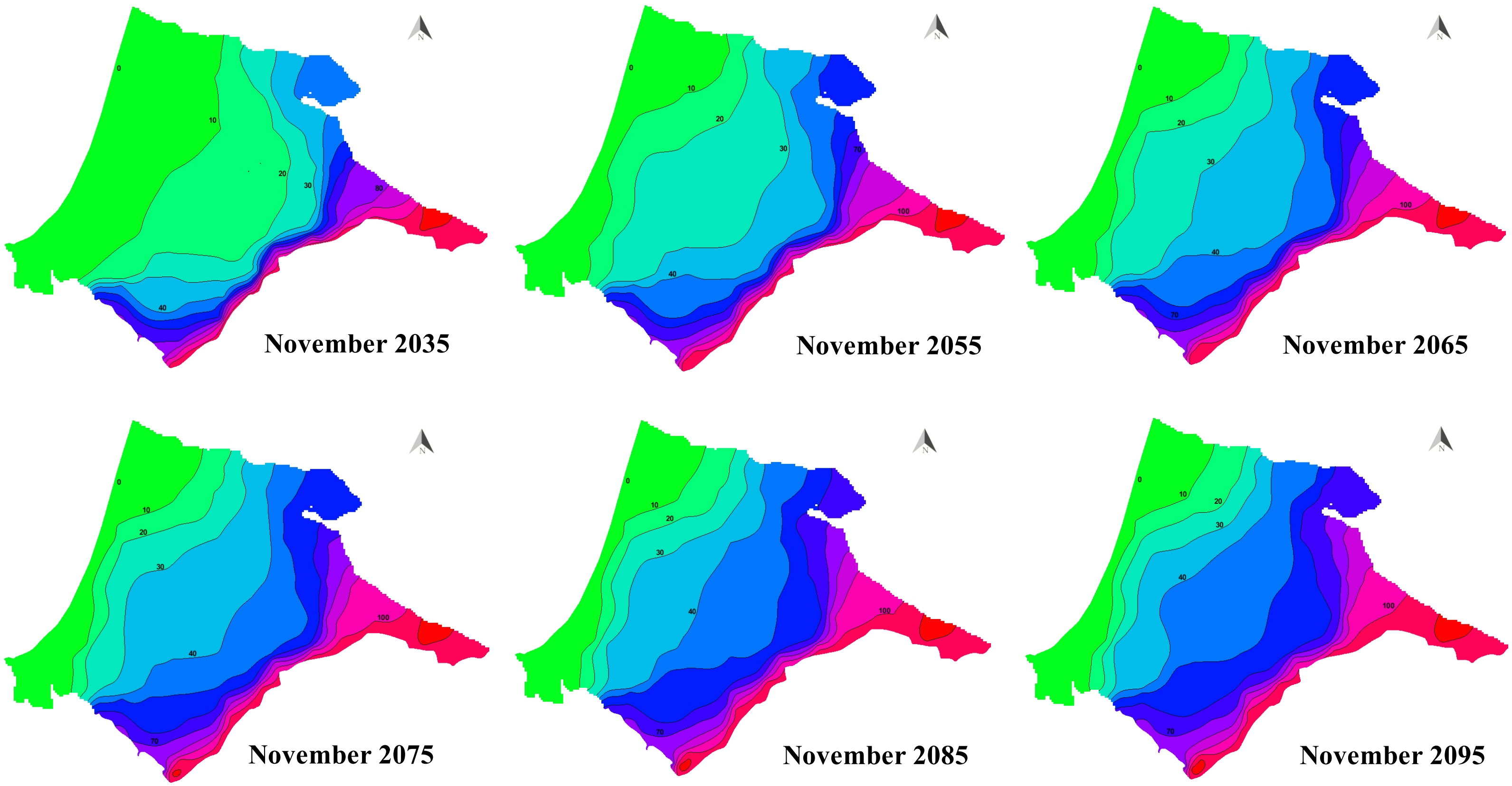

Figure 3.20. The groundwater head contours changing with time (Scenario 1, continued)

3.3.3. SCENARIO 2: Artificial Recharge by Güzelyurt Dam

In this second case, again all the stress due to irrigational wells have been stopped. Annually, 7 MCM of water has been fed through Güzelyurt Dam for about 61 years continuously and starting from December 2013, 82 years long simulation has been performed.

The siltation is a serious problem in the Güzelyurt Dam. This study assumes that the silt deposition at the bottom of the dam had been cleaned prior to the recharge applications

If the evaporation and other losses are assumed to be 75% as indicated by field observations, the actual amount that is taken from the TRNC Supply Project will be 7 MCM/ 0.25 = 28 MCM which corresponds to 76% of the project water allocated for irrigation.

As it can be seen from the Figures 3.21 and 22, the depression zone is disappearing in time and after about 13 years in 2027 the “zero” head contour reaches to the coast. After approximately 56 years in 2070, the aquifer achieves the natural conditions and reaches the steady-state.

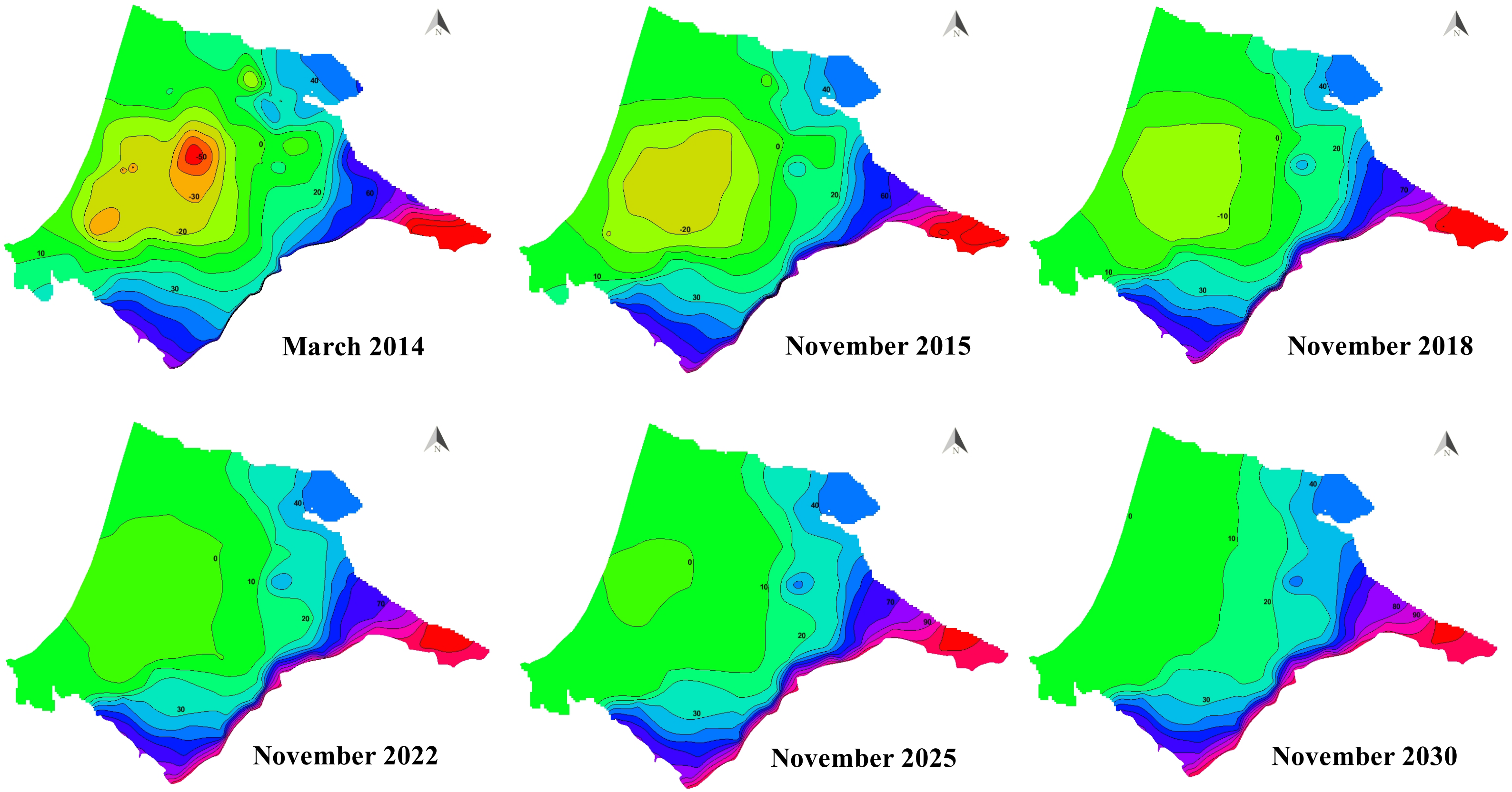

Figure 3.21. *The groundwater head contours changing with time (Scenario 2)*

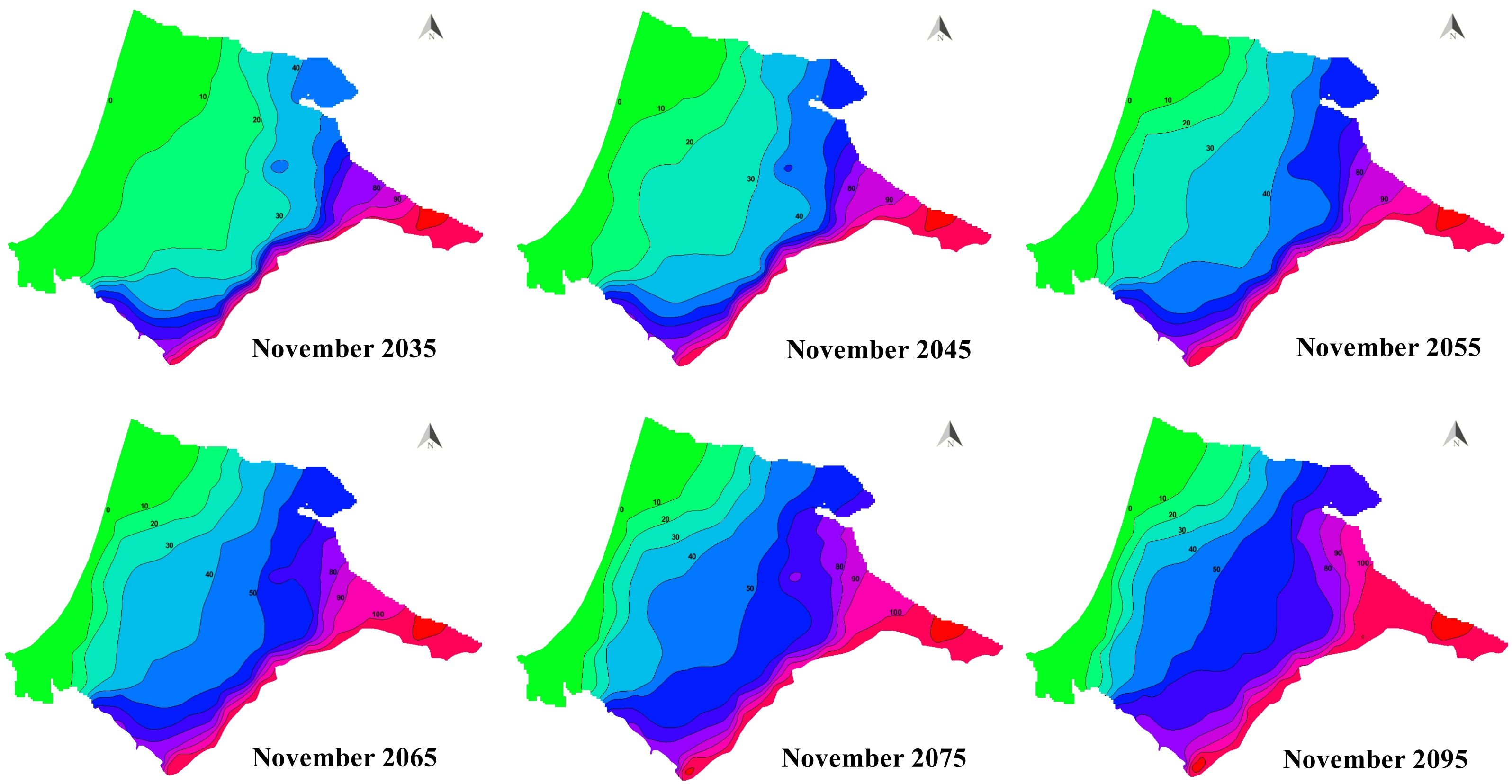

Figure 3.22. The groundwater head contours changing with time (Scenario 2, continued)

3.3.4. SCENARIO 3: Artificial Recharge by the Combination of Güzelyurt Dam and Injection Wells

In this third and the last predictive simulation of this study, again all the stress due to irrigational wells have been stopped. Annually, 5 MCM and 8 MCM of water have been simultaneously fed through Güzelyurt Dam and injection wells located in the highly depressed areas of the aquifer, respectively. It was assumed that recharge has lasted for about 61 years continuously starting from December 2013 and a 82 years long simulation has been performed.

If the evaporation and other losses are assumed to be 75% (DSI, 2003), the actual amount that is taken from the TRNC Supply Project and to be recharged through infiltration basin will be 5 MCM/ 0.25 = 20 MCM which corresponds to 54% of the separated project water for irrigation.

Due to the evaporation loss in the method of recharge with infiltration basin (Güzelyurt Dam), the limited amount of incoming water could be wasted. Therefore, an additional recharge was conducted through injection wells which were randomly placed within the zone of depression. The total of 8 MCM of water has been allocated equally between each well. Consequently, a total of 28 MCM of water supplied by TRNC Supply Project has been allocated for groundwater recharge. This total amount is equal to the amount of water in Scenario B where only Dam recharge was applied.

As it can be seen from the Figures 3.23 and 24, the depression zone is disappearing in time and after about 11 years in 2025 the "zero" head contour approaches to the coast. After approximately 48 years in 2062, the aquifer reaches the natural conditions and reaches the steady-state.

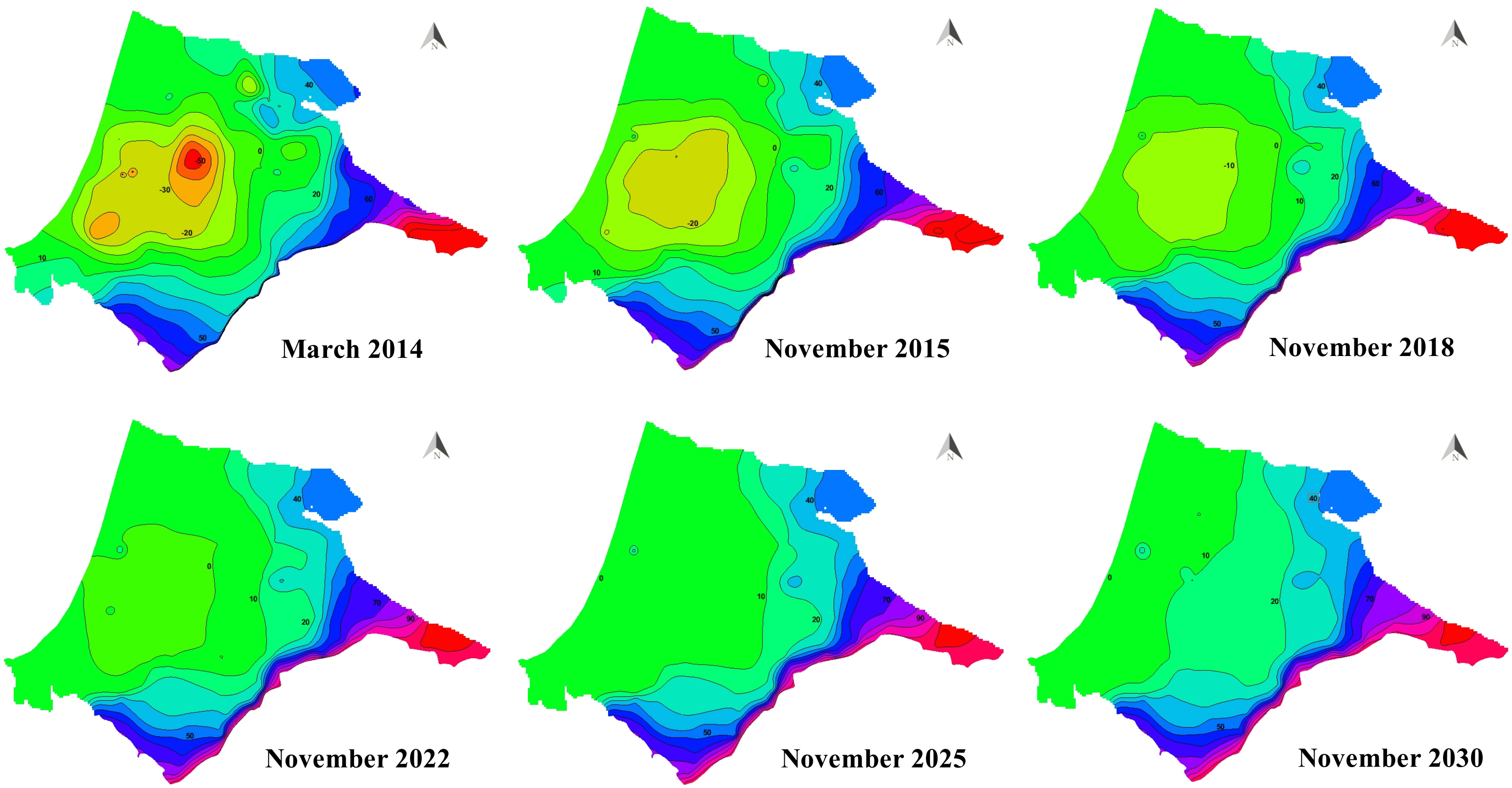

Figure 3.23. The groundwater head contours changing with time (Scenario 3)

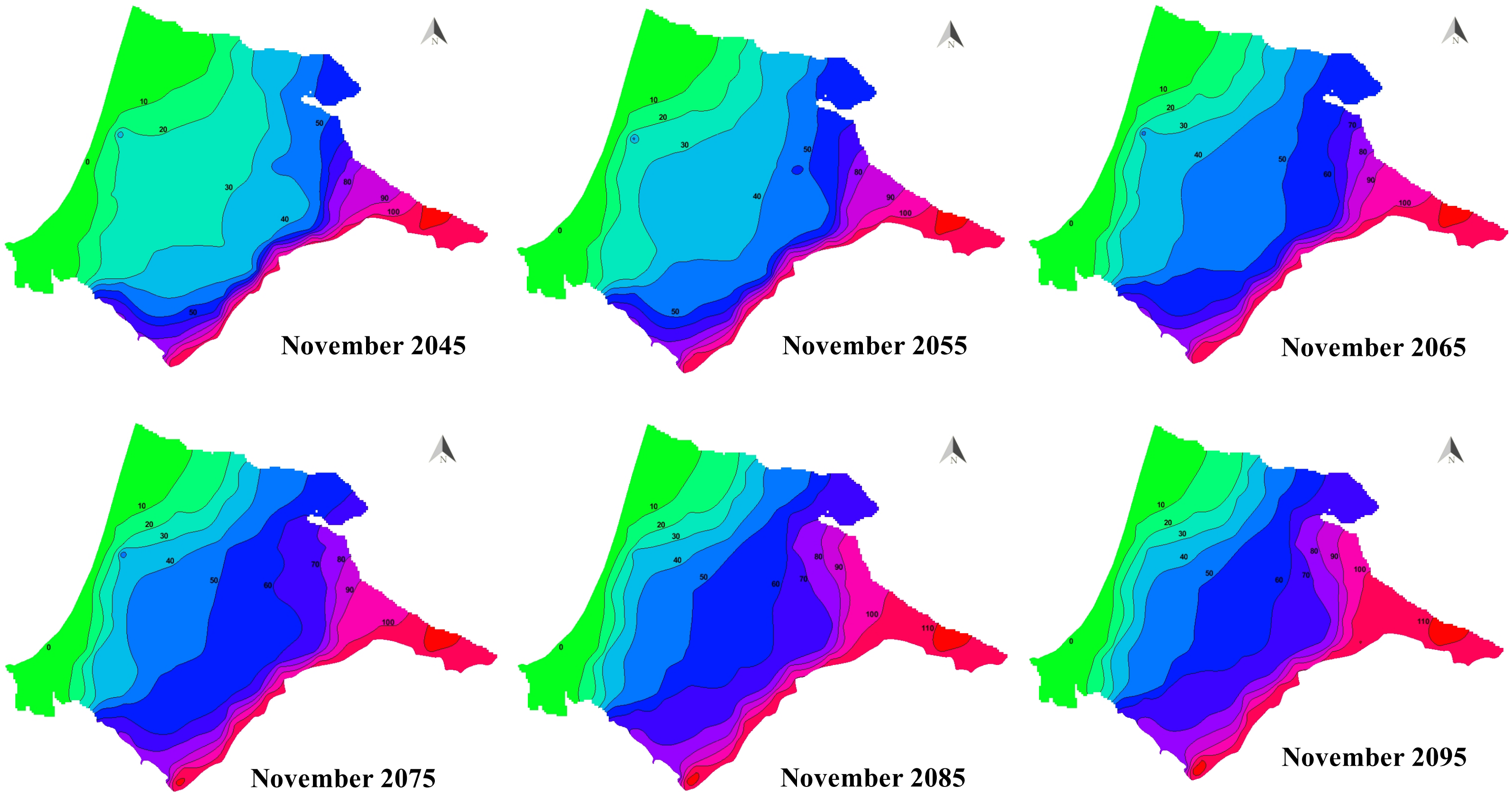

Figure 3.24. The groundwater head contours changing with time (Scenario 3, continued)

As a result of the simulation scenarios, it has been observed that after about 14, 13 and 11 years in 2028, 2027 and 2025, the “zero” contour reaches to the sea for scenarios named 1, 2 and 3, respectively. Furthermore, after approximately 73, 56 and 48 years in 2087, 2070 and 2062 the aquifer comes closer to the natural conditions and reaches the steady-state for scenarios numbered 1, 2 and 3, respectively.

CHAPTER 4

CONCLUSIONS AND RECOMMENDATIONS

4.1. Summary and Conclusions

A numerical simulation model has been developed for the Güzelyurt Aquifer located in the western coast of Turkish Republic of Northern Cyprus. The study aimed to predict the hydraulic behavior of the aquifer under natural and artificial recharge/discharge conditions. The available hydrological, hydrogeological and meteorological data have been processed and analyzed to develop a conceptual model of the system which consists of geometry, material distributions, boundary conditions, sources/sink and the hydraulic parameters. Subsequently, the conceptualized system has been transformed into a numerical unstructured grid system. The system was designed to have single layer with 39658 cells such that they differ in size from 100m x 100m to 10 m x 10 m.

After set up of the model, it has been calibrated under both steady-state and transient conditions to find the unknown parameters which are necessary to make a reliable prediction on the behavior of the aquifer. At the first hand, in steady-state calibration analysis, the hydraulic conductivity distribution has been estimated by using pilot point approach with Parameter Estimation algorithm called PEST (Doherty, 1998) available in GMS software. In order to start and maintain the calibration/optimization process by PEST, a range of hydraulic conductivity values have been introduced to the software. This range has been determined according to the average hydraulic conductivity values obtained by field pumping test analysis. In this manner, the drawdown data collected for 4 pumping wells with their 8 observation wells have been analyzed in Aquifer Test Pro software. For the determination of the parameters in each observation well, Theis with Jacob Correction method which is suitable for unconfined anisotropic aquifers has been applied such that the drawdown data have been corrected by a defined formula (Eqn.2.3) and then fitted to the Theis curve.

Additionally, a transient calibration study for the general head boundary conductance values and for the specific yield parameter has been performed during the years between 2009-2011 by comparing with the measured groundwater level data of same years. Moreover, the available head data of the period between 2011 and 2013 have been used to validate the reliability of the calibrated model for predictive simulation runs.

Finally, when the model become ready for predictive simulations, three scenarios have been run and the major findings have been presented below. As a base case scenario for the purpose of comparison, a steady-state simulation of the calibrated model, without application of any stress due to water extractions has been used. The resultant head contours have been compared with the conditions determined for 1950 and it has been seen that the predicted base head distribution may represent the natural conditions, in other words, the status of the aquifer when the artificial discharge activities had not affected the water balance yet.

In the first scenario, 82 years-long period has been simulated under no stress conditions, except drinking wells are pumped out water during the simulations. In the second and the third cases, again for the same duration, a 61 years long artificial recharge through Güzelyurt Dam and injection wells has been simulated considering only Dam recharge and both Dam and injection wells are combined, respectively.

The most important findings of this study can be listed as follows:

- The aquifer material thickness varies between 60 m and 165 m from the east to the coast and between 110 m and 175 m from the south to the north. The localized silt-clay lenses are distributed in the subsurface. Especially, they are intensely seen just south of the high hydraulic conductivity zone at the central area and just near the coast. Since they are not continuously distributed, the aquifer can be modeled as a single layer system.

- By relying on the available observed groundwater level data of the Güzelyurt Aquifer, the northeast and a part of the southwest formation boundaries have been modeled with no-flow condition. Due to the observed head contours lying parallel to the remaining part of the southwest formation boundary, this line has been assigned with general head boundary condition. The country boundary that divides the aquifer into two parts (South and North), has also been modeled with general head boundary package to account for the continuity of flow through the aquifer.

- The lack of sufficient data regarding the number and location of actively used pumping wells as well as the lack of data on pumping schedule has been the main source of uncertainty in terms of modeling in this study.

- The locations of the pumping wells, especially the ones used for irrigation, have been approximated by considering the agricultural land boundaries and the areas where the depression is at its highest as seen in the measured head distribution maps. This approach seemed reliable since the depression zone in the resultant contour map obtained from simulations with the calibrated model is considerably closer to the one observed in the measured groundwater head distribution.

- The pumping test data carried out in 4 wells to estimate the transmissivity and in turn, the hydraulic conductivity parameter range of the aquifer has been analyzed. The resultant hydraulic conductivity values have a range between 5.5-25 m/d which corresponds to the transmisivity range of 293 to1150 m^2/d. Gathering all the hydraulic conductivity values estimated and the ones reported by DSI (2003), it was found that the overall hydraulic conductivity values ranged from 0.5 to 46 m/d.

- The available groundwater level monitoring data has shown that the aquifer system has approached the steady-state conditions under the existing recharge and stress conditions.

- As a result of the steady-state calibration study, the observed and the computed head values have shown a good fit. The RMSE and R^2 values have been estimated as 0.092 m and 0.945, respectively.

- In the steady-state calibration analysis, the resultant hydraulic conductivity range between 0.05 to 65 m/d was taken. The final range of calibrated hydraulic conductivity values was found reliable since the aquifer is composed of mostly sand-gravel and comparably less amounts of silt and clay. The locations of the lower hydraulic conductivity values have matched nicely with the actual material distribution. Moreover, the higher hydraulic conductivity values were observed in the part of the aquifer where the measured groundwater head contours show wider spacing. Therefore, these values have been also found to be reliable.

- As a result of the transient calibration, the conductance values in the cells of general head boundaries have been estimated to range between $8.7*10^{-6}$ and 0.086 m^2/d, with an average of 0.03 m^2/d. In addition, a uniform specific yield value of 0.4 for the entire aquifer has been estimated by calibration. The observation data of 2011 to 2013, have been used to validate the calibrated model. The resultant plot covering both the calibration and the validation data has demonstrated a well fit between the observed and measured head values. The RMSE and R^2 values have been estimated as 0.348 m and 0.842, respectively.

- ❖ The zero head was initially (in 2013) reaching 8.7 km from the coast towards the inland and the depression zone (zone of negative head values) was covering an area of approximately 61 km^2 which is 34% of the total area. As a result of the scenarios, the zero head contour has been pushed back to coastal line and the depression zone generated by excessive pumping has been disappeared in an average of 12 years, for all three cases (1, 2 and 3).

- ❖ The results of the simulation scenarios have showed that the time required to reach natural state has dramatically decreased with the use of artificial recharge. Although the same amount of water has been utilized from the TRNC supply project in both artificial recharge scenarios (2 and 3), the natural steady-state conditions have been reached 8 years earlier in scenario 2. This is due to the fact that the recharge of the aquifer through dam was not effective since significant amount of the 28 MCM water subjected to evaporative losses.

- ❖ At least %76 of the water allocated for irrigation by the TRNC Supply Project was found to be sufficient to achieve an effective recovery of the aquifer water balance. Although, %76 (28 MCM) has been used to recharge the aquifer with the duration of and that there is no serious artificial discharge from the aquifer, in other words, there is no irrigational water extraction, this amount has not been enough to return the aquifer back to its natural conditions in a near future (according to the simulation results). Therefore, this study has shown that the full recovery of the aquifer (i.e. its return to pre-pumping conditions) will not be possible even after very long time.

- The most promising outcome of this study is that seawater intrusion can be stopped in a not-so-distant future via artificial recharge applications.

- The weakness of this study is that due to the data limitations, especially in the southern part of the aquifer, the results carry an un-quantified uncertainty. Moreover, prediction of the aquifer behavior by modeling flow of water without considering the density effect of seawater may have limited the accuracy of the future predictions.

4.2. Recommendations for Future Work

The numerical results of the groundwater flow model of the Güzelyurt Aquifer carry an un-quantified uncertainty due to the limited amount of data including lack of evenly distributed boreholes and hydraulic properties of the aquifer, lack of detailed recharge/discharge characteristics and lack of information about the aquifer in South Cyprus. Although it is possible to estimate the model prediction uncertainty, it was not conducted as a part of this study. Model uncertainty will develop when the conditions are monitored in the future and these observations are compared with model predictions. Therefore, a continuous monitoring of hydrological/hydrogeological conditions in the aquifer carries a great importance. For practical purposes, it is prudent to keep up a versatile approach whereby management strategies can change if observations vary from forecasts. Water administrators ought to be watchful for local oddities coming about because of geologic multifaceted nature. Model error and uncertainty can be diminished later on by further improvements and gathering of additional reliable calibration data.

The application of artificial recharge through Güzelyurt Dam can only be possible if the silt deposited at the bottom of the dam lake is cleaned periodically. The authorities should be aware of the importance of taking preventive maintenance measures while operation of the artificial recharge activities by either infiltration basin or the injection wells. In this study, the predictive modeling scenarios simulated explained were not attempts to predict the real future. Rather, these scenarios were aimed to predict the hydraulic behavior of the aquifer under hypothetical modeled conditions. In reality, the actual future conditions will unavoidably differ from the modeled conditions owing to changes in climate, land use, and other factors. This numerical model has become successful in approximating the answers of the aquifer to different kinds of stresses and will shed a light on the determination of future management strategies. But, to have a final decision on which artificial recharge application can be applicable both physically and financially, more detailed studies should be implemented by counting on realistic future climate scenarios, economic growth factors, water demand and population projections, cost-benefit analysis, the adverse effects that might occur in the nearby environment due to artificial recharge (such as inundation of basement buildings when the recharge site is close to residential areas) etc. It is possible to estimate upper limits of recharge quantities through each artificial recharge structure based on studies carried out in different hydrogeological set-ups.

Implementation of a seawater intrusion modeling study in the future by using numerical tools such as SEAWAT will enable inclusion of density differences in the prediction of hydraulic behavior of the Güzelyurt Aquifer. The combined modeling of flow and the density effects might offer more realistic results regarding the saltwater push towards the coastal area. Thus, the outcomes of such study, combined with the ones found in this thesis, may greatly contribute to the decision making process in the determination of management strategies.

For optimal management of the aquifer, extractions of groundwater from wells over the study area should be controlled by laws and regulations. Stopping the sea water intrusion may be possible if proper artificial recharge applications are applied together with controlling extractions. To lower the irrigational pumping in the area, the treated wastewater effluents can be used to irrigate the agricultural lands and the awareness on the application of drip irrigation can be applied. And for the strategies to be taken in the near future, it should be noted that the water transferred from Turkey to TRNC with the Water Supply Project should be carefully managed to be able to achieve optimum benefit for the sake of the Aquifer.

The other important issue in the preparation of good management plans of Güzelyurt Aquifer, is the agreement of the both North and the South sides of the Island on data sharing. If academic relations can be set aiming to investigate the area as a whole, the outputs of the future studies can greatly improve, such that more reliable strategies may come up.

4.2.1. Future Data Need

The additional data requirements for the improvement of this study and for the future work have been given with the following statements:

- Collection of up-to-date data on active groundwater pumping wells (irrigational and drinking), their locations and the pumping schedules.

- Additional borehole drillings in the areas where no information is available as shown in Figure 4.1.

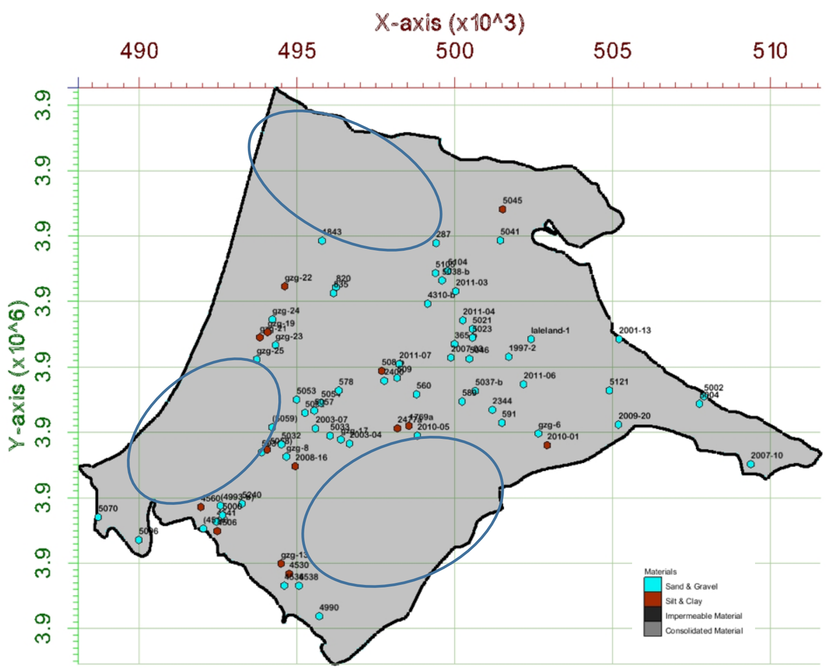

Figure 4.1. The areas where borehole log information is not available.

❖ Additional pumping tests to estimate the hydraulic parameters in the areas where the tests have not been implemented. The areas suggested for new pumping tests are shown in Figure 4.2.

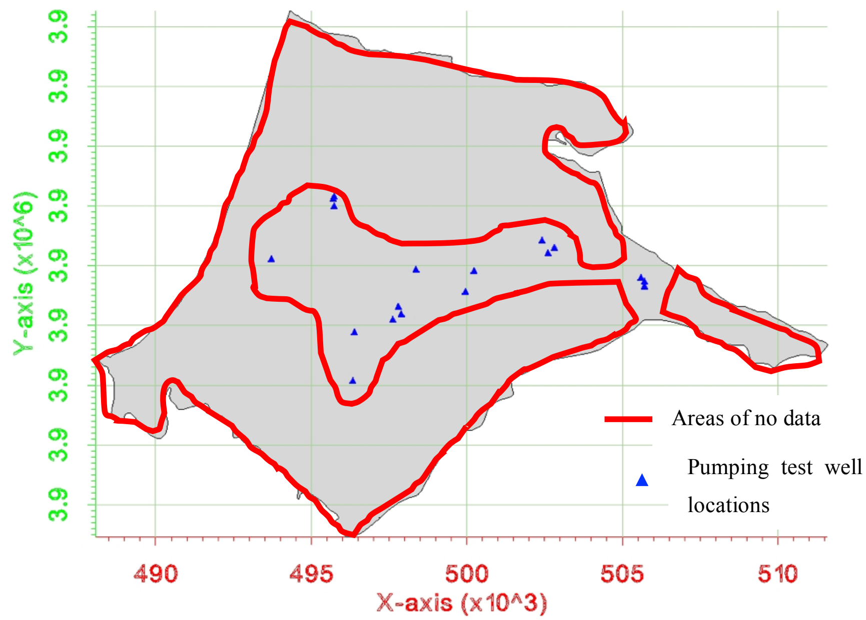

Figure 4.2. The areas suggested for new pumping test.

❖ Groundwater level monitoring should be continued. The number of water level observation wells has decreased by approximately 33% from 2009 to 2013 (the last available year of observations) due to water level fallen below the well bottom line and/or because of siltation. Figure 4.3 shows the observation well locations of 2013. As shown in the figure, there are parts that water level has not been measured.

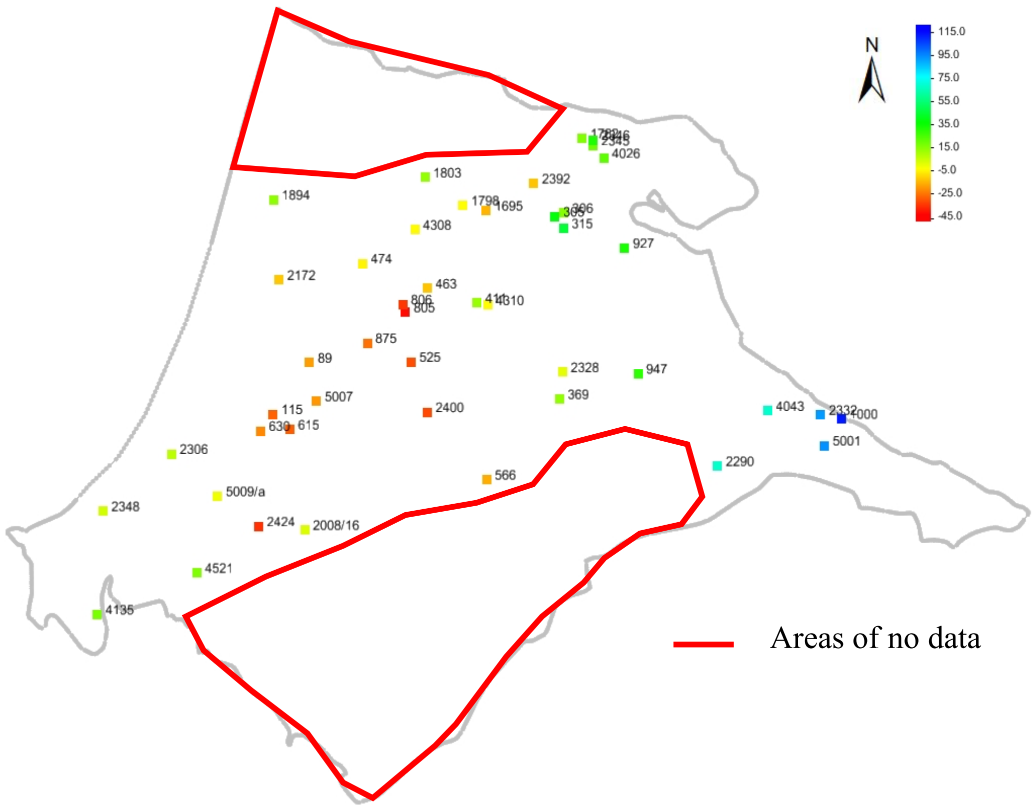

Figure 4.3. Water level observation wells of 2013 and the areas of no data

- Borehole lithological data, groundwater level measurements and active groundwater pumping information for the other part of the aquifer located in Southern Cyprus.

- More up-to-date water budget information regarding the Güzelyurt Aquifer's recharge and discharge status, including the southern part of the aquifer.

- Reliable and up-to-date salinity measurements to be used in saltwater modeling studies recommended as a future work.

REFERENCES

Ackerman, D. J., Rousseau, J. P., Rattray, G. W., & Fisher, J. C. (2010). *Steady-State and Transient Models of Groundwater Flow and Advective Transport, Eastern Snake River Plain Aquifer, Idaho National Laboratory and Vicinity, Idaho*. Virginia.

Agboola, P., & Egelioglu, F. (2011). Water Scarcity and Solar Desalination Systems in the Eastern Mediterranean Region: A Case of Northern Cyprus. In *Proceedings of the ASME 2011 5th International Conference on Energy Sustainability*. Washington DC.

Alfarrah, N., & Walraevens, K. (2018). Groundwater Overexploitation and Seawater Intrusion in Coastal Areas of Arid and Semi-Arid Regions. *Water*, *10*(2), 143. http://doi.org/10.3390/w10020143

Anderson, M. P., & Woessner, W. W. (2002). *Applied Groundwater Modeling Simulation to Flow and Advective Transport*. *Academic Press*. San Diego, USA: Elsevier.

ASTM. (2014). *Standard Guide for Conceptualization and Characterization of Groundwater Systems*.

Baalousha, H. (2008). Fundamentals of Groundwater Modeling. *Groundwater: Modelling, Management and Contamination*, *Chapter 4*, 113–130.

Barazzuoli, P., Nocchi, M., Rigati, R., & Salleolini, M. (2008). A conceptual and numerical model for groundwater management: A case study on a coastal aquifer in southern Tuscany, Italy. *Hydrogeology Journal*, *16*(8), 1557–1576.

http://doi.org/10.1007/s10040-008-0324-z

Barnett, B., Townley, L. R., Post, V., Evans, R. E., Hunt, R. J., Peeters, L., … Boronkay, A. (2012). *Australian groundwater modelling guidelines*. *Waterlines Report Series*.

Burdon, D. J. (1951). *Groundwater in the island of Cyprus*.

CGWB. (2000). *Guide on artificial recharge to groundwater*. New Delhi.

CGWB. (2007). *Manual on Artificial Recharge of Groundwater*. New Delhi.

Cinar, B., & Aksu, H. (n.d.). The Turkish Republic of Northern Cyprus Water Supply Project. Retrieved May 26, 2018, from http://en.dsi.gov.tr/docs/projeler/sunum_ trnc-water-supply-project-pdf.pdf?sfvrsn=2

Cyprus Geological Survey Department. (2016). *Groundwater Resources of Cyprus*. Lefkosia. Retrieved from http://www.moa.gov.cy/moa/gsd/gsd.nsf/All/D28597CA5471E4CFC22580E5002F89D4/$file/GROUNDWATER%20RESOURCES%20OF%20CYPRUS_low.pdf?OpenElement

Doherty, J. (1998). PEST: Model-independent parameter estimation. Brisbane, Australia.

DSI. (1975). *Guzelyurt Hidroloji Calismasi, Teknik Rapor*. Ankara.

DSI. (1976). *Guzelyurt Yeralti Su Tuketimi, Teknik Rapor*. Ankara.

DSI. (2003). *KKTC Su Master Plani, Cilt I & II*. Ankara.

Elkiran, G. (2004). The Water Budget Analysis of Girne Region , North Cyprus, (October), 6–8.

Elkiran, G., & Ergil, M. (2006). The assessment of a water budget of North Cyprus. *Building and Environment*, *41*(12), 1671–1677. http://doi.org/10.1016/j.buildenv.2005.06.014

Elkiran, G., & Turkman, A. (2008). Salinity Problems in Northern Cyprus and Desalination Applications. In M. Morell, C. Popovska, & O. Morell (Eds.), *BALWOIS Conference*. Ohrid, Macedonia.

Ergil, M. E. (2000). The salination problem of the Guzelyurt aquifer, Cyprus. *Water Research*, *34*(4), 1201–1214. http://doi.org/10.1016/S0043-1354(99)00253-5

Ergil, M., & Gunyakti, A. (1993). Saltwater Intrusiom Problems in Guzelyurt Aquifer. *Transactions on Ecelogy and the Environement*, *2*(1), 401–408.

Esca, S., & Venturini, L. (2006). Hydrogeological impact of wellpoint dewatering upon unconfined coastal aquifer of the municipality of Cervia (Ravenna – Italy). In *1st SWIM-SWICA Joint Saltwater Intrusion Conference* (pp. 71–78). Cagliari-Chia Laguna.

Fanta, D. B. (2015). *Conceptual Model Development for Guzelyurt Aquifer, North Cyprus*. Master's Thesis. Middle East Technical University.

Franke, O. L., Reilly, T. E., & Bennett, D. (1987). Definition of Boundary and Initial Conditions in the Analysis of Saturated Ground-water Flow Systems-an Introduction. In *Techniques of Water-Resources Investigations Survey of the United States Geological Survey*. Washington DC.

Gannett, M. W., Wagner, B. J., & Lite, K. E. (2012). *Groundwater Simulation and Management Models for the Upper Klamath Basin, Oregon and California*. Retrieved from https://pubs.usgs.gov/sir/2012/5062/section6.html

Gökçekuş, H. (2014). TRNC's Water Law and Policies. In *Presentation: International Integrated Water Management Symposium*. Istanbul. Retrieved from http://www.sesric.org/Presentations/Water_Management_Symposium/Turkey/TRNC.pdf

Gokmenoglu, O., Erduran, B., Özgür, C., & Tamgaç, Ö. F. (2002). *Kuzey Kıbrıs Türk Cumhuriyetinin Hidrojeolojisi*. Ankara.

Gozen, E., & Turkman, A. (2008). Water Scarcity Impacts On Northern Cyprus And Alternative Mitigation Strategies. *Environmental Problems of Central Asia and Their Economic, Social and Security Impacts*, 241–250. http://doi.org/10.1007/978-1-4020-8960-2_17

Gungor, A. P. (2016). International Water Transfer Project: Northern Cyprus Turkish Rebuplic Water Supply Project (TRNC). In *2nd World Irrigation Forum*. Chiang Mai.

Harbaugh, A. W. (2005). MODFLOW-2005 , The U . S . Geological Survey Modular Ground-Water Model — the Ground-Water Flow Process. In *Book 6. Modeling techniques*. Reston, VA.

Hashemi, H., Berndtsson, R., & Kompani-Zare, M. (2012). Steady-State Unconfined Aquifer Simulation of the Gareh-Bygone Plain, Iran. *The Open Hydrology Journal*, *6*(1), 58–67. http://doi.org/10.2174/1874378101206010058

Iacovides, I. (2011). Water Resources Allocation, *1*, 11–22. http://doi.org/10.1007/978-90-481-9825-2

Jacob, C. E. (1963). Determining the permeability of water-table aquifers. In R. Compiled by Bentall (Ed.), *Methods of Determining Permeability, Transmissibility, and Drawdown* (pp. 245–271). Washington: U.S. Geological Survey Water-Supply PAper.

Keir, G., Bulovic, N., & Mclntyre, N. (2018). Stochastic Modeling of Groundwater Extractions over a Data-Sparse Region of Australia. *Groundwater*. Retrieved from https://doi.org/10.1111/gwat.12658

Kresic, N. (2007). *Hydrogeology and Groundwater Modeling*. *Taylor & Francis Group* (Second Edi, Vol. 2). Boca Raton, FL, USA.

Liu, J. J., & Soni, B. K. (1998). 2D Groundwater Contaminant Transport Modeling by using the Finite Volume Method on an Unstructured Grid System. *Applied Mathematics and Computation*, *211*, 199–211. http://doi.org/0096-3003

Mansour, A. Y. S., Baba, A., Gunduz, O., Şimşek, C., Elçi, A., Murathan, A., & Sözbilir, H. (2017). Modeling of seawater intrusion in a coastal aquifer of Karaburun Peninsula, western Turkey. *Environmental Earth Sciences*, *76*(22). http://doi.org/10.1007/s12665-017-7124-5

McMahon, A., Heathcote, J., Carey, M., & Erskine, A. (2001). *Guide to Good Practice for the Development of Conceptual Models and the Selection and Application of Mathematical Models of Contaminant Transport Processes in the Subsurface*. *National Groundwater & Contaminated Land Centre*. Bristol: Environment Agency.

Mederer, J. (2009). *Water Resources and Dynamics of the Troodos Igneous Aquifer-system , Cyprus Balanced Groundwater Modelling*. Julius-Maximilians University of Würzburg.

Mohammedjemal, A. (2006). *Assessment of artificial groundwater recharge using greenhouses runoff (North East Naivasha, Kenya)*. *MSc Thesis*. International Institute for Geo-Information Science and Earth Observation.

MTA. (1997). *Guzelyurt Havzasinin Hidrojeolojisi*. Ankara.

Neuman, S. P. (1975). Analysis of pumping test data from anisotropic unconfined aquifers considering delayed gravity response. *Water Resources Research*, *11*(2), 329–342. http://doi.org/https://doi.org/10.1029/WR011i002p00329

Oude Essink, G. H. P. (2000). *Groundwater Modelling*. Utrecht University.

Panday, S., Langevin, C. D., Niswonger, R. G., Ibaraki, M., & Hughes, J. D. (2013). MODFLOW – USG Version 1: An Unstructured Grid Version of MODFLOW for Simulating Groundwater Flow and Tightly Coupled Processes Using a Control Volume Finite-Difference Formulation. *U.S. Geological Survey*, (Techniques and Methods 6-A45).

Qiu, S., Liang, X., Xiao, C., Huang, H., Fang, Z., & Lv, F. (2015). Numerical simulation of groundwater flow in a River Valley Basin in Jilin Urban Area, China. *Water (Switzerland)*, *7*(10), 5768–5787. http://doi.org/10.3390/w7105768

Schlumber Water Services. (2011). Visual MODFLOW Help.

Sen, Z. (2015). *Practical and Applied Hydrogeology*. *Practical and Applied Hydrogeology* (First). Istanbul: Elsevier.

Siddiqui, R. A. (2016). *Modeling Artificial Groundwater Recharge and Low-Head Hydroelectric Production: A Case Study of Southern Pakistan*. Colorado State University.

Sofroniou, A., & Bishop, S. (2014). Water scarcity in Cyprus: A review and call for integrated policy. *Water (Switzerland)*, *6*(10), 2898–2928. http://doi.org/10.3390/w6102898

Spitz, K., & Moreno, J. (1996). *A Practical Guide to Groundwater and Solute Transport Modeling*. New York: John Wiley & Sons, Inc.

TDKB. (2016). *KKTC Tarım Strateji Belgesi (2016-20)*. Retrieved from http://tdkb.gov.ct.tr/Portals/1072/BELGELER/Tarım-Strateji-Belgesi.pdf

TDKB. (2017). *Tarim master plani*. Retrieved from http://www.tarim.gov.ct.tr/Portals/1072/MasterPlan/Tarım Master Planı 2017_1.pdf

Theis, C. V. (1935). The relation between the lowering of the Piezometric surface and the rate and duration of discharge of a well using ground-water storage. *Eos, Transactions American Geophysical Union*, *16*(2), 519–524. http://doi.org/10.1029/TR016i002p00519

Thorp, W. L. (1961). *Cyprus-Suggestions for a Development Programme*. New York.

TRNC State Planning Organization. (2017). *Economic and Social Indicators*. Lefkosa. Retrieved from http://www.devplan.org/Ecosos/BOOK/SEG-2015.pdf

Türker, U., Alsalabi, B. S., & Rizza, T. (2013). Water table fluctuation analyses and associated empirical approach to predict spatial distribution of water table at Yeşilköy/AgiosAndronikos aquifer. *Environmental Earth Sciences*, *69*(1), 63–75. http://doi.org/10.1007/s12665-012-1934-2

UNDP. (1970). *Survey of Groundwater and Mineral Resources of Cyprus*. New York.

Waren, K. B., Bobst, A. L., Swierc, J. E., Madison, J. D., Water, G., & Program, I. (2013). Hydrologic Investigation of the North Hills Study Area Lewis and Clark County , Montana, (September). Retrieved from http://mbmg.mtech.edu/pdf-open-files/mbmg643_scratchgravelmodel.pdf

Water Development Department. (2009). *Dams of Cyprus*. Nicosia. Retrieved from http://www.moa.gov.cy/moa/wdd/Wdd.nsf/booklets_en/54BA140DDED88117

C2257640002971DA/$file/Page1_47(8MB).pdf

Waterloo Hydrogeologic. (2013). Understanding MODFLOW-USG: A Comparison between Structured MODFLOW and UnStructured MODFLOW. Retrieved June 2, 2018, from https://www.waterloohydrogeologic.com/2013/08/22/understanding-modflow-usg-a-comparison-between-structured-modflow-and-unstructured-modflow-1/

Weight, W. D. (2008). *Hydrogeology Field Manual* (Second). McGraw Hill. http://doi.org/10.1036/0071477497

Winston, R. B. (2018). USGS Online Guide to MODFLOW.

Yildiz, D., & Cakmak, C. (2014). *Peace River to Cyprus from Turkey, Intercountry Water Transfer*. Ankara.

Zhou, Y., & Li, W. (2011). A review of regional groundwater flow modeling. *Geoscience Frontiers*, *2*(2), 205–214. http://doi.org/10.1016/j.gsf.2011.03.003

APPENDIX A

THE HYDROGEOLOGICAL MAP DESCRIPTIONS

Table 4.1. Descriptions of the legend of hydrogeological map of Northern Cyprus given in Figure 2.4 (Grouping by Fanta (2015))

Material Unit IDs	Formation	Lithology	Descriptions	Grouped descriptrions
JKth	Hilarion limestone	Recrystallized limestone	Marl, Limestone, Mudstone	Base Material
Klm	Mallıdağ formation	Mudstone, Limestone	Marl, Limestone, Mudstone	Base Material
Kls	Selvilitepe breccia	Gravel	Gravel	Alluvial Material
KT	Lower Pillow Lavas	Pillow lava	Pillow lava, Tuff, Trachyandesite and Dacite	Base Material
Kta	Lower Pillow Lavas	Pillow lava	Pillow lava, Tuff, Trachyandesite and Dacite	Base Material
Ktaß	Host andesite and basalt dikes	Andesite and basalt dikes	Pillow lava, Tuff, Trachyandesite and Dacite	Base Material
Ktd	Diabase	Diabase dikes	Pillow lava, Tuff, Trachyandesite and Dacite	Base Material
KTl	Çınarlı volcanic	Pillow lava	Pillow lava, Tuff, Trachyandesite and Dacite	Base Material

Material Unit IDs	Formation	Lithology	Descriptions	Grouped descriptrions
KTlç	Çınarlı volcanic	Pillow lava	Pillow lava, Tuff, Trachyandesite and Dacite	Base Material
KTly	Tuff, trachyandesite, dacite	Tuff, trachyandesite, dacite	Pillow lava, Tuff, Trachyandesite and Dacite	Base Material
Kttg	Base group	Pillow lava and diabase dykes	Pillow lava, Tuff, Trachyandesite and Dacite	Base Material
Ktü	Upper pillow lavas	Pillow lava	Pillow lava, Tuff, Trachyandesite and Dacite	Base Material
Q1a	Marine terraces	Calcarenite	Sandstone and Calcarenite	Consolidated Material
Q1b	Terrestrial terraces	Gravel	Gravel	Alluvial Material
Q1bt	Flood deposits	Terra rossa soils, tufa and chalk	Marl, Limestone, Mudstone	Base Material
Q1by	Slope wash	Gravel	Gravel	Alluvial Material
Q2a	Marine terraces	Calcarenite	Sandstone and Calcarenite	Consolidated Material
Q2b	Terrestrial terraces	Limestone	Marl, Limestone, Mudstone	Base Material
Q3a	Marine terraces	Calcarenite	Sandstone and Calcarenite	Consolidated Material
Q3b	Terrestrial terraces	Gravel	Gravel	Alluvial Material
Q3d	Terrestrial terraces	Gravel	Gravel	Alluvial Material

Material Unit IDs	Formation	Lithology	Descriptions	Grouped descriptrions
Q4a	Marine terraces	Calcarenite	Sandstone and Calcarenite	Consolidated Material
Q6ba	River Sand & Gravel	Gravel-Sand Sequence	Gravel	Alluvial Material
Q6bt	Flood deposits	Terra rossa soils, tufa and chalk	Marl, Limestone, Mudstone	Base Material
Q6by	Slope wash	Gravel	Gravel	Alluvial Material
Q6h	Landslide masses	Turbidite sandstone and shale	Sandstone and Calcarenite	Consolidated Material
Q6tr	Travertine	Turbidite sandstone and shale	Sandstone and Calcarenite	Consolidated Material
Qh	Landslide masses	Turbidite sandstone and shale	Sandstone and Calcarenite	Consolidated Material
Qmb	Bostancı Gravel	Gravel	Gravel	Alluvial Material
Qmg	Gürpınar formation	Gravel, Calcarenite, Sandstone	Sandstone and Calcarenite	Consolidated Material
Qmgç	Gravel member	Gravel	Gravel	Alluvial Material
Ta	Ardahan formation	Sandstone, Siltstone, Gravel,	Sandstone and Calcarenite	Consolidated Material
Td	Kaynakköy formation	Dolomitic limestone	Marl, Limestone, Mudstone	Base Material
Tdb	Büyüktepe formation	Gravel	Gravel	Alluvial Material

Material Unit IDs	Formation	Lithology	Descriptions	Grouped descriptrions
Tdbe	Beylerbeyi formation	Turbidite sandstone and shale	Sandstone and Calcarenite	Consolidated Material
Tdd	Dağyolu formation	Sandstone, Shale, Marl	Marl, Limestone, Mudstone	Base Material
Tdg	Geçitköy formation	Limestone, Mudstone	Marl, Limestone, Mudstone	Base Material
Tdko	Kozan formation	Sandstone, Marl sequence	Marl, Limestone, Mudstone	Base Material
Tdm	Mermertepe gypsum	Gypsum	Marl, Limestone, Mudstone	Base Material
Tdt	Tirmen formation	Turbidite sandstone and calcarenite	Sandstone and Calcarenite	Consolidated Material
Tdy	Yılmazköy formation	Sandstone, Siltstone, Mudstone	Marl, Limestone, Mudstone	Base Material
Tdya	Yazılıtep formation	Chalk, Clayey limestone, Sandstone and Marl sequence	Marl, Limestone, Mudstone	Base Material
Tk	Kantara formation	Gravelly Sandstone, Gravel	Sandstone and Calcarenite	Consolidated Material
Tly	Yamaçköy formation	Clayey limestone volcanic sequence, Limestone, Chert	Marl, Limestone, Mudstone	Base Material
Tmç	Çamlıbel marl	Gray Marl, Sandstone	Marl, Limestone, Mudstone	Base Material

Material Unit IDs	Formation	Lithology	Descriptions	Grouped descriptrions
Tmçç	Gravel member	Gravel	Gravel	Alluvial Material
Tml	Lefkoşa sandstone	Sandstone	Sandstone and Calcarenite	Consolidated Material
Tmt	Taşpınar formation	Sandstone, Marl, Gravel sequence	Sandstone and Calcarenite	Consolidated Material
TRtk	Kaynakköy formation	Dolomitic limestone	Marl, Limestone, Mudstone	Base Material
Ttk	Kaynakköy formation	Dolomitic limestone	Marl, Limestone, Mudstone	Base Material
Ty	Kaynakköy formation	Clayey limestone volcanic sequence, Limestone, Chert	Marl, Limestone, Mudstone	Base Material
Tya	Akiltepe formation	Sandstone, Marl, Chalk	Marl, Limestone, Mudstone	Base Material
Tyl	Lefke limestone	Reef limestone	Marl, Limestone, Mudstone	Base Material

APPENDIX B

THE RESULTS OF PUMPING TEST DATA ANALYSES

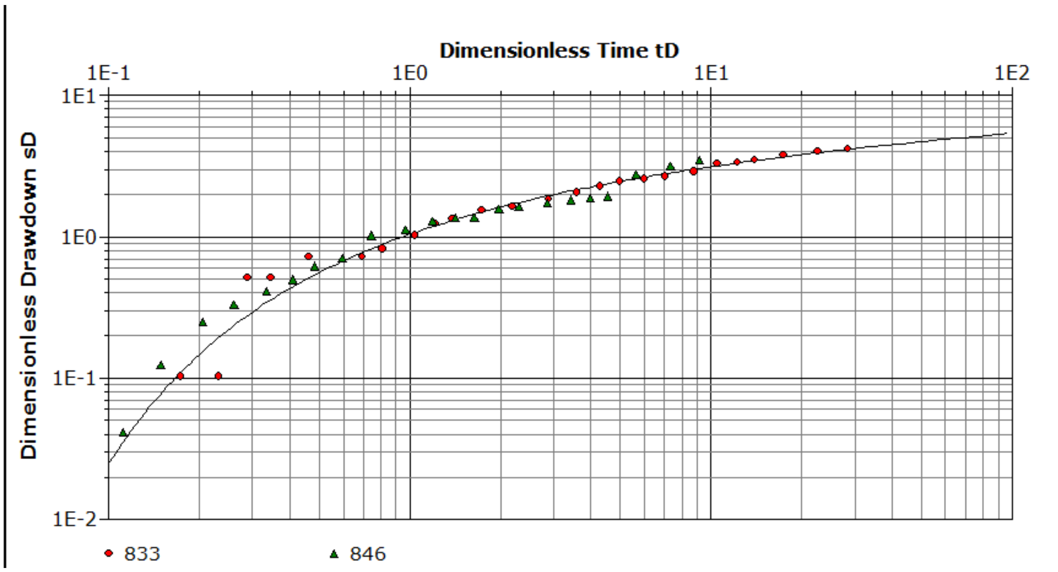

Figure 4.4. Theis with Jacob Correction type curve fit for observation wells numbered with 833 and 846

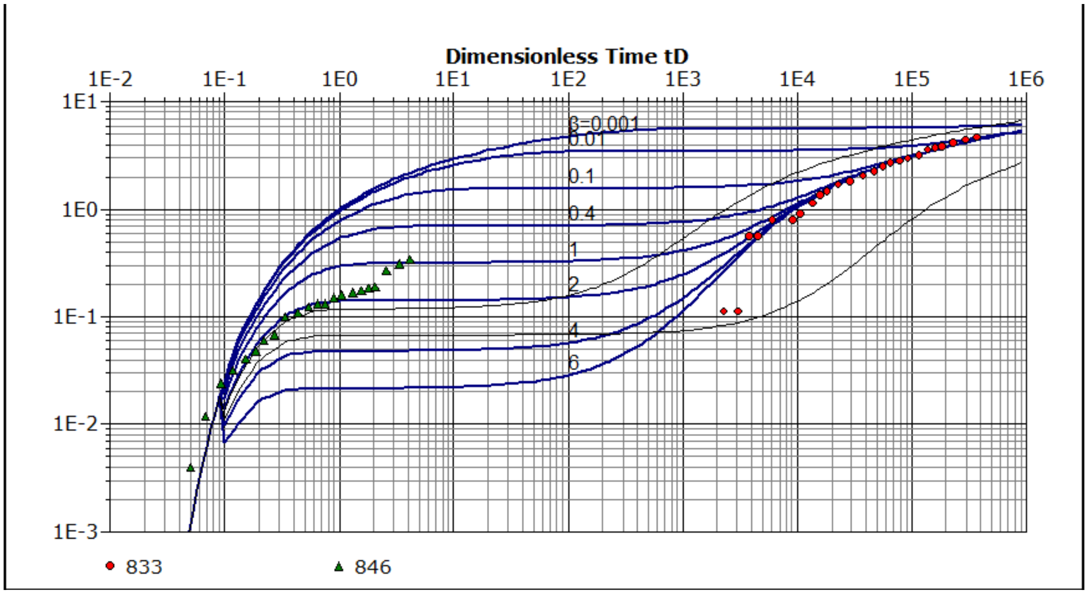

Figure 4.5. Neuman method type curve fit for observation wells numbered with 833 and 846

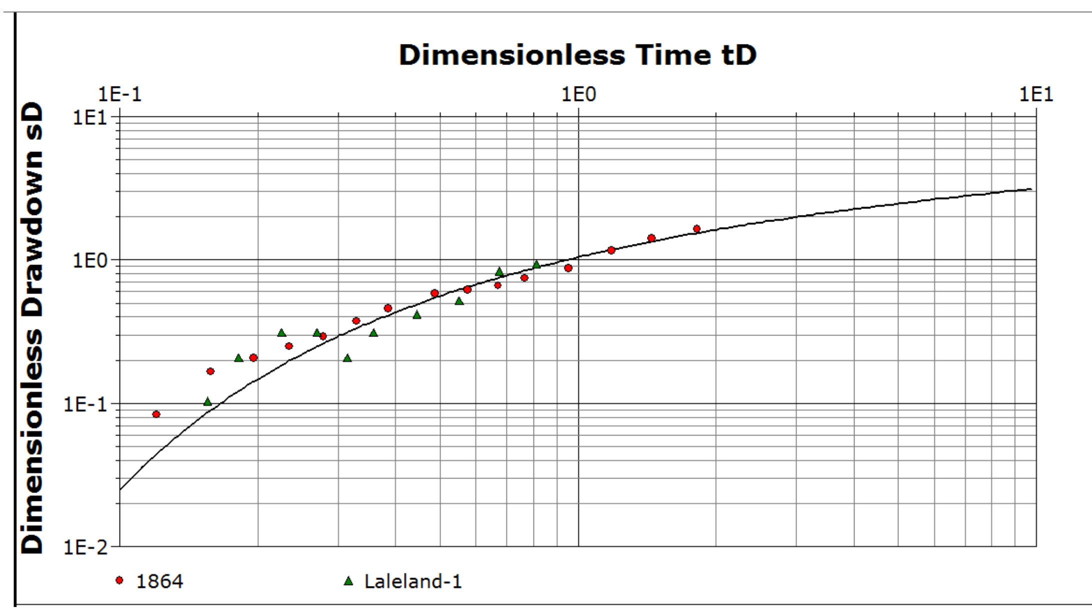

Figure 4.6. Theis with Jacob Correction type curve fit for observation wells numbered with 1864 and Laleland-1

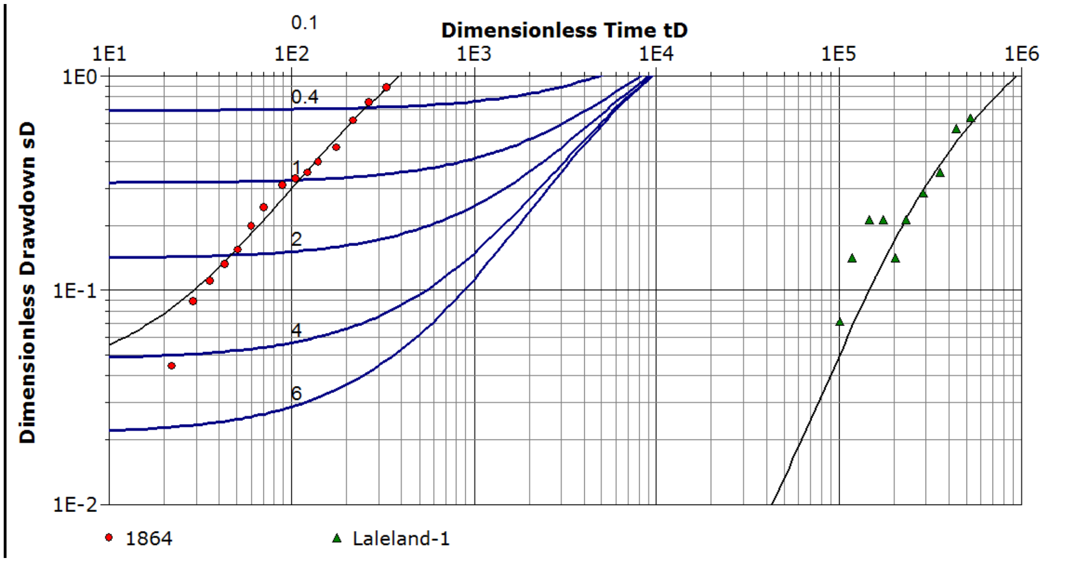

Figure 4.7. Neuman method type curve fit for observation wells numbered with 1864 and Laleland-1

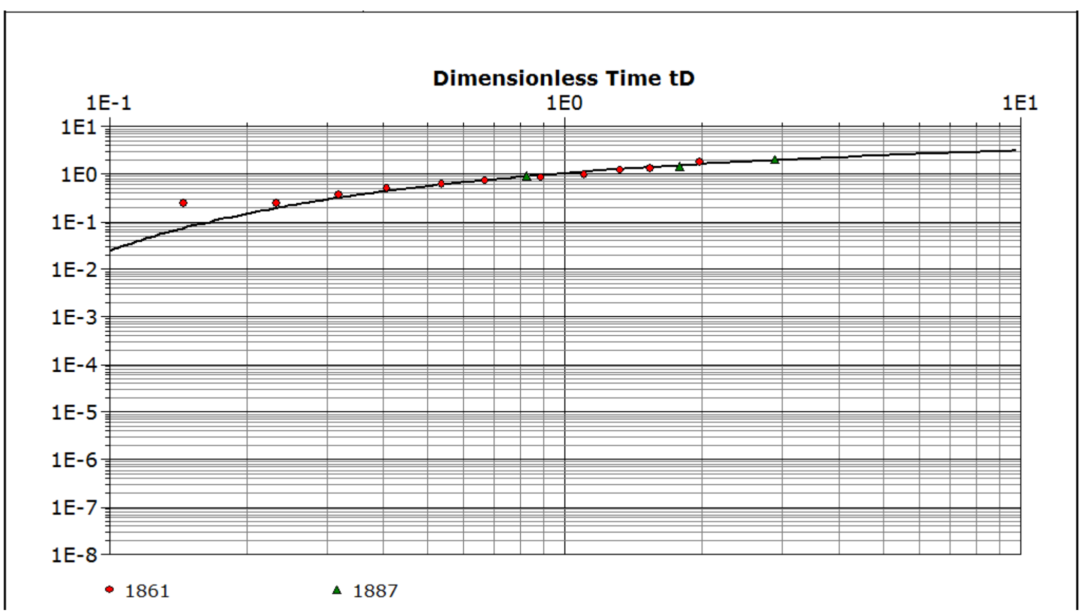

Figure 4.8. Theis with Jacob Correction type curve fit for observation wells numbered with 1861 and 1887

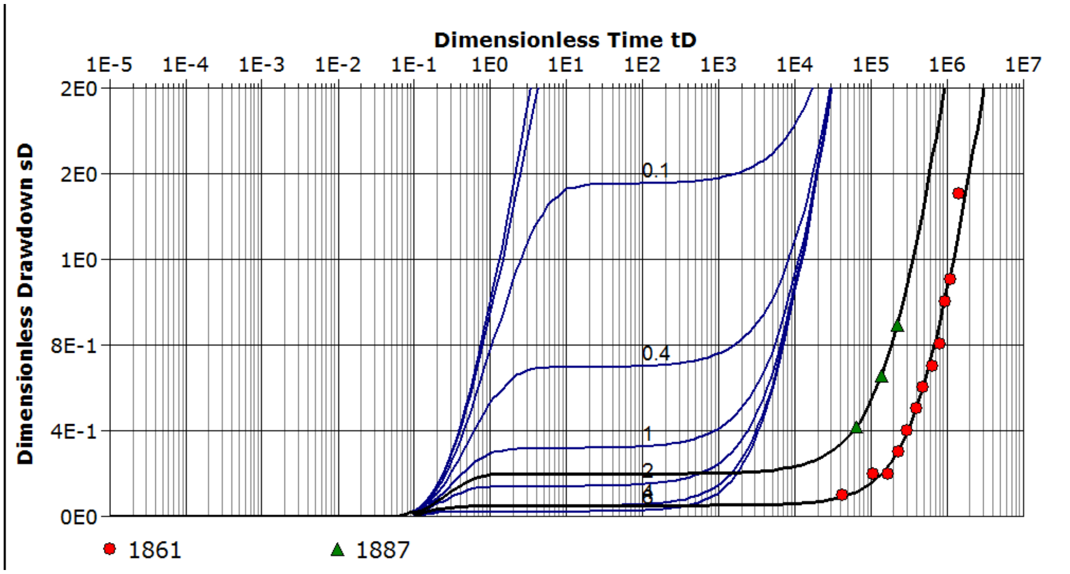

Figure 4.9. Neuman method type curve fit for observation wells numbered with 1861 and 1887

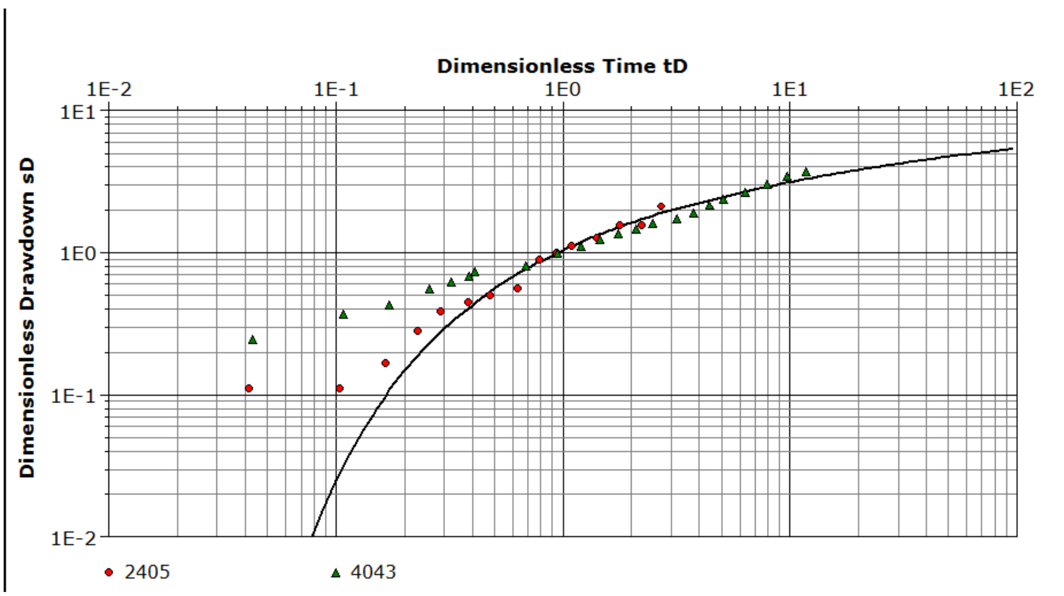

Figure 4.10. Theis with Jacob Correction type curve fit for observation wells numbered with 2405 and 4043

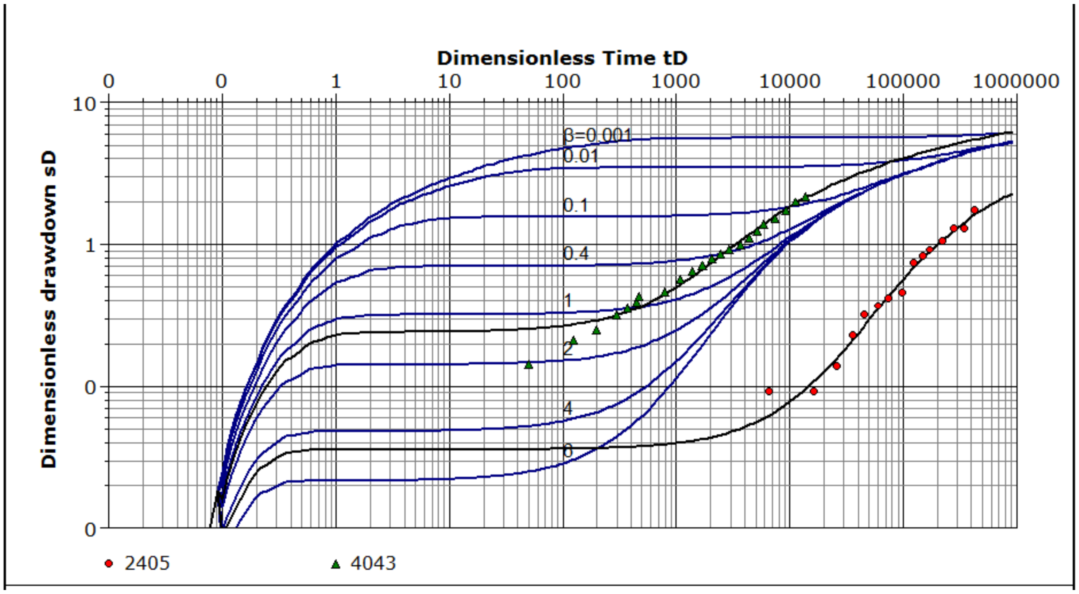

Figure 4.11. Neuman method type curve fit for observation wells numbered with 2405 and 4043